THERMAL PERFORMANCE OF ROOF MATERIALS AND CONFIGURATIONS SUITABLE FOR RESIDENTIAL BUILDINGS IN IBADAN, NIGERIA

By

Joel Babawale TAIWO

(SI: 210327)

B.Sc., M.Arch. (Ife)

MNIA, REG. ARC. (ARCON)

A Ph.D. Thesis in the Civil Engineering Department

Faculty of Technology

In partial fulfilment of the Degree of

DOCTOR OF PHILOSOPHY

of the

UNIVERSITY OF IBADAN

AUGUST, 2023

CERTIFICATION

I certify that this work was carried out by Joel Babawale **TAIWO** (Matric No.: 210327) in the Department of Civil Engineering, Faculty of Technology, University of Ibadan, Ibadan, Nigeria.

……..

Supervisor & Head
B. I. O Dahunsi
B.Sc (Ife), M.Sc., Ph.D (Ibadan), MNSE, MASCE, REG. ENGR. (COREN)
Professor, Department of Civil Engineering, Faculty of Technology
University of Ibadan, Ibadan, Nigeria.

DEDICATION

To the Alpha and Omega, the beginning, and the end, the first and the last. Revelation 22: 13.

ACKNOWLEDGEMENTS

I thank Almighty God to whom all knowledge and blessings comes, the source and the origin of my strength. Unto Him that can do exceeding, abundantly above all that we ask or think, glory be to His name. “Ephesians 3:20 (kjv).

My deep appreciation goes to my supervisor, Professor B. I. O Dahunsi, for his direction, sacrifice, ideas, understanding, valuable contribution, mentoring and patience in reading and correcting my write up at various stages of the work despite his busy schedule.
I acknowledge Dr J. O. Labiran, the indefatigable mentor, who made himself a ready help in time of need. He has always been there for me. I say thank you for your counselling and mentorship.

To my adopted aunty Mrs Omolara Olaiya, who spent her money to buy the data logger for this work, I say thank you ma. Also, to a dear Brother Dr Segun M. Ojetunde, my pastor and his wife, Pastor Alabi, and Dr Alabi, I sincerely express my unreserve appreciation for all your prayers and encouragement, may the Almighty God bless you and your ministry. Special thanks to my PGC, Dr Akintayo, you are indeed a mother in Israel, thank you so much. To my able formal PGC Dr S. O. Adesogan, you are a true father. I also say thank you to Dr W. O. Ajagbe, for your love and concern throughout this program. My thankfulness also goes to all the postgraduate lecturers in the department, Prof O. A. Agbede, Prof Coker, Prof G. M. Ayininunola, and Dr Achi. They were all interested in the research work. To the members of staffs in the department, you are all awesome, you supported me from beginning to the end, God shall reward your labour of love.

Finally, I want to thank my family for their help. Thank you to my wife Toyin, my children, Jewel, Juliet, and Joel, for supporting me during my career journey with your prayers and counsel. I would be extremely ungrateful if I didn't thank my parents, Late E. O. Taiwo and Mrs. E. A. Taiwo, for their parental guidance and support. I want to thank my brothers and sisters for their support.

ABSTRACT

Heat influx through roofs is the leading cause of internal temperature imbalance problems in buildings. Roofing materials and configurations are key in regulating heat infiltration into buildings. There is a dearth of information on their synergistic contribution to the control of internal temperature imbalance. This study was designed to investigate the thermal performance of selected roofing sheets and underlays, under different configurations in residential buildings in Ibadan.

Plywood-Lined Aluminium Roof (PLAR) and Selected Roofing Materials (SRM) [Stone Coated Sheets (SCS) and Aluminium Roofing Sheets (ARS)], were tested using ice and steam apparatus for 5 and 7 minutes, based on UNE EN standard. These and Selected Ceiling Materials (SCM) [Polyvinyl Chloride Ceiling (PVC), Asbestos (ASB), Plaster of Paris (POP), Gypsum (GYP) and Plywood Ceiling Board (PCB)], were tested using fabricated conductivity apparatus, for Thermal Conductivity (TC) (W/mK), Thermal Resistivity (TR) (mk/w), Thermal Diffusivity (TD) (m^2/s), Specific Heat Capacity (SHC) (J/kgK), and Thermal Absorptivity (TA) (J), based on ASTM standards. Forty-five prototype buildings were constructed using a factorial combination of three roofing sheets, five ceiling underlays, and three angular configurations. Optimum Comfortability Roof (OCR) for the buildings were obtained using multichannel data logger between 9 am to 10 pm at 30 minutes interval for six months. Data were analysed using descriptive statistics and ANOVA at $\alpha_{0.05}$.

The TC; 135.60-150.62 (TC_{PLAR}), 83.680-97.069 (TC_{SCS}), and 76.149-123.43 (TC_{ARS}); indicated PLAR was a suitable heat conductor. The TR; 0.0066-0.0074 (TR_{PLAR}), 0.0103-0.0119 (TR_{SCS}), and 0.0081-0.0131 (TR_{ARS}), implied PLAR has poor heat resistance. The SHC; 3.726-4.739 (SHC_{PLAR}), 3.164-8.887 (SHC_{SCS}), and 2.180-7.082 x 10^3 (SHC_{ARS}), indicated the heat storage potential of PLAR. The TD; 1.066-1.507 (TD_{PLAR}), 1.390-3.095 (TD_{SCS}), and 1.021-2.643 x 10^{-7} (TD_{ARS}); implied heat diffuses slowly through PLAR. The TA; 392.66-398.09 (TA_{PLAR}), 425.18-491.07 (TA_{SCS}), and 327.73-380.55 (TA_{ARS}), indicated that PLAR possessed good heat absorption. Similarly, TC for underlays; 0.191 (TC_{PVC}), 0.125 (TC_{ASB}), 0.184 (TC_{POP}), 0.228 (TC_{GYP}), and 0.283 (TC_{PCB}), indicated that PCB was an insulator. The SHC; 1.654 (SHC_{PVC}), 2.050 (SHC_{ASB}), 1.596 (SHC_{POP}), 2.070 (SHC_{GYP}), and 2.850 x 10^3 (SHC_{PCB}), showing that PCB had a better storage capacity. The TD; 1.360 (TD_{PVC}), 0.399 (TD_{ASB}), 1.266 (TD_{POP}), 1.410 (TD_{GYP}) and 0.456 x 10^{-7} (TD_{PCB}), showed that PCB diffused heat slowly. Also, TA; 319.00 (TA_{PVC}), 338.24 (TA_{ASB}), 336.93 (TA_{POP}), 334.24 (TA_{GYP}), and 353.43 (TA_{PCB}), suggested higher TA in PCB. The temperature of the SCM decreased with increase in the angle of configuration. The average temperature at 30, 45, and 60°, for 6 pm and 10 pm were; PLAR (37.04-29.74, 35.5-28.66, 31.02-28.64°), SCS (37.14-26.28, 35.18-26.38, 37.28-28.06°), and ARS (36.97-29.7, 38.72-30.16, 37.82-29.58°), respectively, implied that between 45° and 60° gave OCR ranged 22 - 29°, with the highest coefficient of correlation (R^2 = 0.95, 0.70, 0.90) obtained. A significant difference between the OCR of SRM and SCM was observed.

Plywood-lined Aluminium, stone-coated and Aluminium roofs configured between angles 45° and 60° offered acceptable thermal performance with the plaster of paris or polyvinyl chloride as roof configurations in Ibadan.

Keywords: Thermophysical properties, Thermal conductivity, Specific heat capacity, Thermal diffusivity, Plywood-lined Aluminium roof.

Word count: 486

TABLE OF CONTENTS

LIST OF TABLES

LIST OF FIGURES

LIST OF PLATES

APPENDIXES

Figure **Page**

CHAPTER ONE
INTRODUCTION

1.1 Background to the Study

People of all ages aim for a conducive and welcoming home. Humanity and shelter are two interrelated concepts. Therefore, every designer is extremely concerned with the sustainability and comfortability of the building parts, particularly the roofing components, to ensure internal thermal comfort. Sustainability and comfortability of a building affect body system in terms of psychology, physiology, emotion, and metabolism. However, due to physiological and psychological, is difficult to satisfy everyone in a space because of the variations in human metabolic rate (Coopeer, 2004).

Some schools of thought believed that the roof and its components were expected to provide sustainable accommodation and a conducive thermal atmosphere to the interior part of the building. Considering this, Elewa, Afolalu, and Fayomi (2019) affirmed that the strength of a good roofing sheet lies in its ability to withstand external forces.

To provide sufficient and be self-sustaining internal comfort of a building, particularly in a tropical environment, the roof covering, and the underlay (ceiling) must be thermally compactible to drop the internal ambient temperature to between 22 and 29 °C. As a result, the comfortability of the roofing materials and matching underlays used use in tropical regions must be sustainable. Therefore, for optimal comfort and productive work, individual needs buildings with a desirable indoor environment, which depends on the type of roof-to-ceiling materials used to resist weather conditions year-round (German, 2010). The reflectivity, absorption, conductivity, or heat emission characteristics of the roof directly affect the level of comfort that a certain material will offer for the interior space(s). According to Adesogan (2012), a roof is the most expose part of a building. Also, Ariyadasa, Muthurathne, and Adikary (2015), considered roof as an essential component of a structure that protects the occupants from environmental hazards. Therefore, protecting the building's

components and its occupants from the damaging effects of weather is the primary function of roofing. The absence of a roof in a building makes it an incomplete project, thus choosing the right roofing materials should be a priority before any project is started.

Historically, before the development of the railway system in the nineteenth century, roofing for building coverings was typically made from locally accessible materials (Barry, 2015). Prominent among such materials is Thatch, which is widely accessible roofing material in the southwest. Thatch roofs served as efficient insulators, delaying the flow of heat energy or the transfer of heat (German, 2010) and ensuring all-day internal comfort. Since Thatch was readily available, providing peace and coolness to the interior area, thatch material was mostly used by local builders to construct the roofs of mud structures. At the period, Thatch was used exclusively without underlay, but when used in conjunction with underlay, the roof space can serve as storage purposes. However, the beginning of the nineteenth century brought forth technological advancement and invention, which snowballed into the plethora of brands of roofing materials that are available in the construction sector today. Different roofing materials, such as galvanized roofing sheet, metal roofing sheet, long-span Aluminium roofing sheet, and eventually stone-coated roofing sheet, were introduced because of the invention (Barry, 2015).

By way of definition, a roof is the top of the structure that provides protection from the environmental conditions like rain and sun which could damage other building component. The roof has a variety of purposes, one of which is to make sure that the interior is comfortable for the occupant. Since a building's roof is the most exposed structure to heat and has a little chance of being shaded, the performance of the roof and the interior comfort of a building depend on each other (Kruger, Harimi, Kurian, and Ideris, 2005). When the interior of the building becomes too hot or uncomfortable for the inhabitant, the building is is said to have issue because the normal body core temperature is thought to be between 34°C and 37°C (ISO 7730, 2002). More so, it could as well be regarded as issue when such a roof is no longer ensuring balance between external and the interior temperature or providing shelter for occupants and other building’s elements (Stathopoulos, 2006).

A structure without a working roof is comparable to half-baked bread, which is challenging to consume yet challenging to discard. Such is the case with a structure devoid of a weatherproof roof. Numerous studies on the roof's performance have been conducted up to this point by various academics both domestically and abroad. One of the most important factors in obtaining indoor thermal comfort in tropical structures is the thermal performance of the roof. Therefore, a variety of factors that have an impact on both external and internal roof structures determine a roof's thermal efficiency in this region of the country (the southwest). According to reports, a building's thermal design is dependent on the local climate and the materials used in its construction (Al-Sanea, 2002).

Environmental condition of Ibadan as a study area is characterized by repeated wetting, drying, and a variety of solar variables, as well as ongoing exposure to wind and rain. The combination of these and numerous other elements defines the roofing kinds and materials that are anticipated to satisfy people while still offering a level of comfort that is fair. The temperature difference between the heat flow into the space and the solar reflection radiation recorded outdoors is often caused by the amount of heat penetration through the roof. Measuring the heat flow across the roof will reveal this. Therefore, ensuring favourable indoor climatic conditions in structures is a crucial duty for every designer.

A report by Ettah *et al*. (2016), hinted at the possibility that homes with tropical roofs let in more heat internally. Therefore, during daylight hours, the roof is the component of the structure that is most exposed to solar radiation. As a result, Ibadan is a tropical city where the sun's angle of incidence is always high, direct, and hotter during the hottest part of the day. Due to the nature of the roofing configuration over them, most buildings in the tropical region became inhospitable and non-conductive, which led to a metabolic imbalance since the heat produced is not comparable to the heat lost in the body (Pavlou, 2009).

The development of modern architecture and construction in Nigeria, particularly in the southwest, has given rise to a variety of roof design patterns and material usages in the community (Thirumaran and Mathew, 2017). There is a search for thermal comfort in residential buildings because of the rise in temperature and rising energy costs (Al-Sanea,

2002). Rooting pattern popularly practiced in this region particularly Ibadan include zinc roofing, also known as metal roofing, Aluminium roofing, and the recently developed stone-coated roofing sheet. Therefore, this study developed natural means of providing thermal comfort and lowering reliance on mechanical or energy-intensive cooling systems by providing possible combinations of roofing and ceiling materials optimum comfortability roof within the space.

1.2 Statement of the problem

Because roof is the most exposed component of the building, most of the heat influx into the indoor space are being trapped under the roof. Roofing not only plays a significant role in providing shelter for human settlement. Evidently, roofs play a significant role in the construction of an energy-efficient structure. Report by Thirumaran and Mathew (2017) concluded that buildings use between 50 and 70% of the energy produced globally and that a higher proportion of occupants are not satisfied with their thermal environment (Schlavon, Hoyt, and Piccioli, 2014). Additionally, there is a trend toward an increase in the yearly mean temperature from 0.2 to 0.5 °C (Egbinola and Amobichukwu, 2013). These factors worked together to produce and bring excessive heat into the building's interior space(s). Because of this, both living and non-living occupants find the interior space(s) difficult to live in. A bigger proportion of the building's interior heat is infiltrated through the roof.

Even though the construction industry has recently adopted many technological advancements and innovations, particularly in the roof design, the interior space(s) still struggle with a high level of discomfort for the occupant. Most building roofs allegedly underperformed in their thermal responsibilities due to bad design, inferior materials or poor execution, a problem with the orientation of the building, and improper configurations of the roofing components. Many efforts had to be made in this direction since the quantity of heat that enters the building percolates through the roofing materials.

Even though the interior space(s) continue to suffer with a high level of discomfort for the occupant, the construction industry has recently incorporated many technological developments and innovations, particularly in the roof design. Most building roofs are said to have failed to meet their thermal obligations because of poor design, substandard

materials or poor workmanship, an issue with the building's orientation, and inappropriate arrangements of the roofing materials. Since the amount of heat that enters the structure percolates via the roofing materials, significant effort was required in this direction.

However, these efforts were largely ineffective since many aspects of nature can never be modified or altered. One of these is the angle of incidence of the sun's rays to the earth, which is typically direct, higher, and harsher at the peak of the day and constant on the roofs regardless of the orientation and position of the building. As designers, we must create artificial (scientifically-proof) roof configurations that are both cost-effective and protective of the interior space to maintain a climatic balance between human metabolism and the indoor environmental weather condition. Be aware that a beautiful structure without a useful roof configuration will be unsafe for human living. When a roof fails, the entire structure fails. To uncover strategies to improve and decrease the level of heat infiltration into the building through suitable roof layouts, this research was needed.

1.3 Aim and Objectives

This was to investigate the thermal performance of selected roofing sheets and underlays, under different roof configurations in residential buildings in Ibadan. Based on the above aim of the research, the following objectives provided the roadmap for which the research shall be undertaken. The specific objectives were to:

i. measure and compare the thermo-physical properties (Thermal Conductivity TC, Thermal Resistivity TR, Thermal Diffusivity TD, the Specific Heat Capacity SHC and Thermal Absorptivity) of the Selected Sample Materials SSM, within Ibadan.
ii. evaluate the lagging effect of plywood-lined Aluminium roof PLAR, on the thermal performance of roof.
iii. determine appropriate optimum comfortability roof (OCR) configuration suitable for minimum comfort in this zone; and
iv. develop predictive models for different roof configurations that will ensure thermal comfort in tropical buildings.

1.4 Justification

Recent personal field research and observation revealed that the impact of climate and environmental conditions on roofing materials used in building construction is not given much thought, especially about the choice of roofing materials to be employed. This study was conducted with the goal of achieving the following. These factors had previously raised the energy consumption for heating and cooling in buildings, which appeared to have damaged the comfort, health, and effectiveness of the roofs.

i. Because there is currently no real data for any roof configurations in Nigeria, this work will offer prognostic information for suitable roof layouts.
ii. If the claim made by (Egbinola and Amobichukwu, 2013) that the annual mean temperature in Ibadan has increased geometrically is correct, then a climatically responsive roof layout is urgently needed to limit heat transfer from the roof into the inside of the building.
iii. Since most structures require electricity for internal cooling, it is necessary to promote an environmentally friendly inside atmosphere through optimal roof construction.

Therefore, a roof is considered to have failed when any aspect of its behavior seems to jeopardize the security and comfort that it was designed to offer (Adesogan, 2018).

1.5 Scope of the study

The study covered available roofing and underlay ceiling materials in the Ibadan city builders' market. Laboratory and a field test were conducted were conducted on the Selected Roofing Sheets SRS which include Stone Coated Sheets SCS and Aluminium Roofing Sheet ARS, as well as Plywood-Lined Aluminium Roof (PLAR). Likewise, the Underlay Ceiling Products UCP include plywood ceiling board PCB, plaster of Paris POP ceiling, plaster of Paris ceiling, gypsum GYP ceiling, and polyvinyl chloride PVC ceiling.

The field study was conducted from October to March, during the dry season, on 45 prototype models utilising a factorial combination of three roofing sheets, five ceiling underlays, and three angular configurations of 30, 45, and 60°. The chemical characteristics

of the materials, the effect of fenestration size or quantity, roof color, or roof shape were not included in the study.

CHAPTER TWO

LITERATURE REVIEW

2.1 Preamble

According to Agboola and Zango (2014), traditional buildings in Nigeria today have demonstrated a full sensitivity to the environment, indigenous technology, and socioeconomic context to which they belong. The origin of these many traditional building bodies is related to the local builders' availability to natural resources as well as their shared cultural, religious, and taboo beliefs. The beginning of colonialism in Nigeria changed the traditional way of life and culture of Nigerians, resulting in a tenuous link between traditional and modern architecture in Nigeria.

The early human being lives in caves as necessity to safeguard them from weather elements and to protect them from the effects of inclement weather. Some lived in valleys where shelter from winds was significant and under trees for protection against the blazing sun, (Adesogan, 2018). In the seventeenth and late eighteenth century the form of roof materials common to most buildings in the country was dictated by the availability of local materials used as roof coverings. Thatch was common roof covering in the southwest region of Nigeria. Thatched roofs provide shield against heat, sunlight, cold and wind. The local builders use weaved long straight stalks of water and marsh plants with reeds, properly dried, and bound together. This is formerly arranged up the slopes of the pitched roofs as thatch. It was proved that ‘thatch roof’ proficiently drains rainwater, eliminates wind, and perform as an active insulator to heat transfer, a double advantage that no other roof covering provides. This is a perfect example of the traditional method of insulating the interior building space from harsh weather.

However, the usage of common roofing materials, tile, and slate, spread to every region of the world in the nineteenth century because of the development of a vast railway system (Barry, 2015).

2.2 The study area

According to the National bureau of statistics (NBS, 2011), Oyo state by land mass has a hectare of about 2,650,000 (26,500square kilometer), with acres of 6,519,000 (10,351.56 square miles). Ibadan is 645 kilometers from Abuja, the federal capital of Nigeria. The climate of Ibadan is depicted by strong latitudinal zones, which often alternate between the wet and dry seasons. The rainfall in this area is being control by two air masses, one, the air coming from the Atlantic Ocean and two, the dry continental air coming south from the African landmass, (Kale, 2013). This region falls within warm humid climate, (Lawal, Akinpade, and Makinde, 2017).

The quantity of rainfall and sunshine each year dictate the fluctuations in heat that may be expected, which in turn determines the percentages of heat that enters homes through the roof. Beginning in February or early March and lasting until approximately July, when the amount of rain is at its highest, is the rainy season. Rain normally stops in August before starting up again in September and lasting through late November. The weather is typically reasonable from early October until the middle of December, after which there is a spike in temperature that lasts until late February or early March.

Tables 2.1a, 2.1b, 2.2a, and 2.2b revealed a trend in the annual rainfall and increased in the minimum and maximum temperature between 2005 until 2009, also the mean radiation and relative humidity between 2006 until 2010, respectively for southwest Nigeria, (Kale, 2013).

Table 2.1a: Annual Rainfall in southwest 2005-2009

STATE (CAPITAL)	2005	2006	2007	2008	2009
EKITI (ADO-EKITI)	114.6	109.7	-	-	-
OGUN (ABEOKUTA)	924.2	1142.1			
ONDO (AKURE)	1,317.7	1,381.0	1,405.7	1,466.1	1,309.6
OSUN (OSOGBO)	1,130.2	1,469.7	1,421.7	1,597.6	1,277.7
OYO (IBADAN)	1,192.0	1,260.2	1,218.8	889.4	1,702.1

Source: NBS (2011)

Table 2.1b: Annual Mean Minimum Temperature in southwest 2005-2009

STATE (CAPITAL)	2005	2006	2007	2008	2009
EKITI (ADO-EKITI)	-	-	-	-	-
OGUN (ABEOKUTA)	24.2	24.3	24.5	23.1	23.6
ONDO (AKURE)	22.0	20.6	20.5	21.8	-
OSUN (OSOGBO)	21.9	21.0	19.4	21.3	21.8
OYO (IBADAN)	23.0	23.3	24.7	20.8	23.2

Source: NBS (2011)

Table 2.2a: Annual Mean Maximum Temperature in southwest 2005-2009

STATE (CAPITAL)	2005	2006	2007	2008	2009
EKITI (ADO-EKITI)	-	-	-	-	-
OGUN (ABEOKUTA)	33.7	32.9	33.6	33.3	33.6
ONDO (AKURE)	31.1	33.5	31.6	31.3	31.0
OSUN (OSOGBO)	31.1	31.7	33.4	32.1	31.4
OYO (IBADAN)	31.8	31.6	35.8	31.2	31.7

Source: NBS (2011)

Table 2.2b: Annual Mean Radiation in southwest 2006-2010

STATE (CAPITAL)	2005	2006	2007	2008	2009
EKITI (ADO-EKITI)	18.0	18.0	18.3	18.1	18.4
OGUN (ABEOKUTA)	18.0	17.7	18.8	18.6	17.9
ONDO (AKURE)	19.8	19.0	18.9	19.3	19.5
OSUN (OSOGBO)	18.0	18.3	17.9	18.3	18.2
OYO (IBADAN)	18.4	18.3	18.5	17.9	18.2

Source: NBS (2011)

According to Abam et al. (2016), map 2.1 generally shows the three categories of solar radiation in Nigeria: the northern region, the middle belt region, and the southern region. According to reports, each zone has a minimum of 5 to 6 hours of sunshine per day. Table 2.4 shows the annual mean radiation for the southwest.

The summary of the solar radiation in Nigeria was depicted similarly on map 2.1. The claim made by (Egbinola and Amobichukwu, 2013) that there was a trend increase in yearly mean temperature from 0.2 ℃ to 0.5 ℃ was supported by this. According to Eruola (2013), over the past 10 years, the mean maximum temperature has increased by around 0.5 ℃, ranging from 30.5 ℃ to 32.5 ℃. In essence, this means that as the amount of solar radiation reaching the globe increases, temperatures are rising.

2.3 The Roof

Elewa *et al*. (2019, define roof as the most exposed element of building to solar radiation, with hardly a possibility to be shaded. Prakash and Ravikumar, (2015) also asserted that roof structure cannot reduce the entry of solar radiation effectively, however, with the adequate roof configurations this can be achieved, resulting in a good thermal comfort. A roof, as the sensitive part of a building, provide barrier against sun and rain, exclusive of which the components of the building be damaged, (Adesogan, 2018).

2.4 Type of Roofs

1. The flat roofs
2. The Pitched roofs

2.4.1 The flat roofs

The Flat roof is a roof structure which its angle of slope is below 10°, to the horizontal (Barry, 2015). This can be used in domestic garages, stores, high rise office buildings and shopping centres. This can be constructed using timber system, steel system and reinforced concrete system.

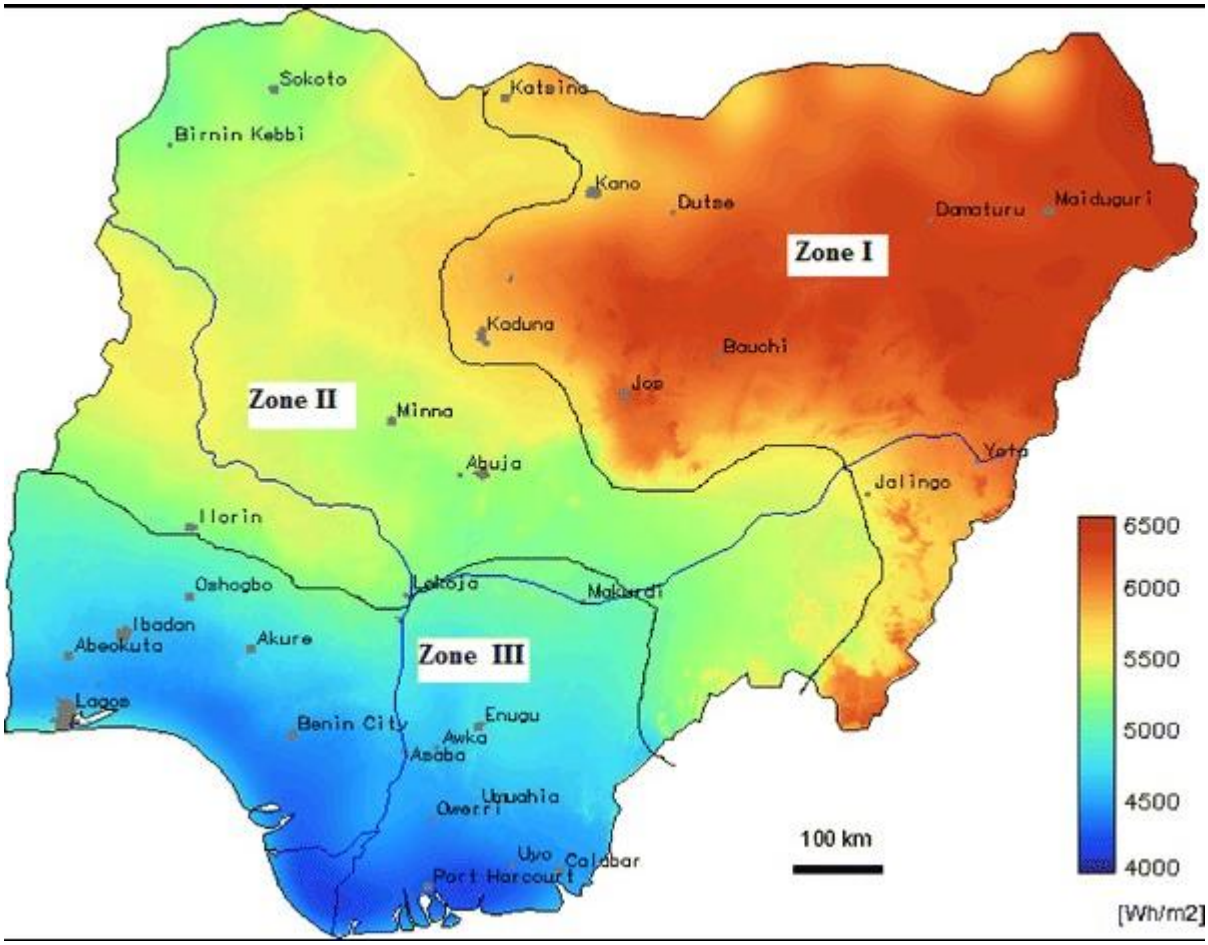

Figure 2.1: Nigeria map showing solar radiation of each zone

Source: Abam *et.al* (2016)

Traditionally, flat roofs used a tar and gravel-based surface, but care must be taken to prevent pooling of water from penetration through the roof. Flat roofs are sensitive to human traffic because they can produce cracks or punctures in the surface (except the reinforced concrete slab) and lead to leaks.

2.4.2 The pitched roofs

This can be high pitched (25 ℃-70 ℃) or low-pitched roofs (slope between 10 ℃-24 ℃). Adesogan (2018) explained that a roof is said to be pitch when the slope is more than 10 ℃ to the horizontal, which includes, lean-to roof, gable roof and hipped roofs.

2.5 Functional requirement of a roof

Among other things, roof is required to perform the functions of resisting the passage of heat, sound, weather, provide strength and stability, be durable and free from day-to-day maintenance and be fireproof, (Barry, 2015). But according to Condron (2007) some factors contributed to the dysfunctional or premature failure of the roofing systems. This includes bad design, poor workmanship, substandard or unsuitable construction materials and questionable methods of construction. Highlighted that in instances when the design is good with excellent workmanship, the untimely compromise and failure of the roofing system may still occur due to misuse or abuse of the roofing system in the form of accidental damage caused by building users or building maintenance personnel.

2.5.1 Strength and stability of roof

This is a life span measurement of roof and the ability of the roof component retain their strength, chemical and physical properties, appearance, and resistance to all forms of failure, (Warseck, 2003 and Roberts, 2006). The strength and stability of a roof depends on the way or formation of the carcass, the types of material the roof is made from, whether timber or steel. Meanwhile, walls or beams give the strength or support to a flat roof. Meanwhile the strength of pitched roof is gotten from the stability of its triangular frames at mid-span. The roof carcass should be stable and strong to act as self-support weight and in addition support the live loads from snow, wind, and human traffic during maintenance, (Adesogan, 2018).

2.5.2 Resistance to weather of roof

The roof resistance to weather is a function of obstruction to the flow of heat energy, therefore, roof weather resistant is the ability of the roof to conduct heat away from the space, (Ochang et.al 2018). A roof excludes rain as result of the materials from which it is covered and should offer effective resistance to weather both the outer covering and the interior, to withstand the inclement factors within environment. A good roof should be able to normalise to a lowest minimum the solar infiltration into a building, through the installation of insulation materials, (Adesogan, 2018).

2.5.3 Durability of roof

Hyde (2000) believed that the roof surface facing the sky should provide a defense against sun and precipitation. The durability of roof usually depends on the ability of the roof covering to exclude rain, snow and destructive action of frost and temperature fluctuations. Roof covering should prevent permeation of water into the roof structure which will result or encourage decay of timber, deterioration of steel by corrosive action or disintegration of concrete. Therefore, roof durability is very important, as the functionality of static elements and movable elements in building depends on. The corrugated galvanized iron sheet also durable, light, corrugated and easy to transport for use on site, (Romero, Romero, Romero, 2017).

2.5.4 Fire safety of roof

Barry, (1984), asserted the ideal rating for roof resistance to fire, which should be within 0.5 to 6 hours. No doubt the fire standard stipulate that every building element should provide a safe escape for the occupants to the outside of building. The roof as an element of a building is expected to limit the spread of fire across from part of the building to another. The roof is also expected to be fire rated by delay the fire from being ignited until after the occupants have escaped.

2.5.5 Resistance to heat passage of roof materials

Barry (2000) noted that the materials use for roof assemblies and coverings for roofs are poor insulators against the transference of heat. This call for the integration of materials with good insulating properties, such as lightweight boards, mat, or loose fill to provide lagging against excessive loss or gain of heat. He gave the thermal coefficient of insulating roof materials for dwelling to be within the maximum of 0.25 w/m^2 °C. Where the expected standard for thermal coefficient of a roof configuration (including the ceiling), is given to be 0.35 w/m^2 ºC. Therefore, this information has assisted in the selection of various roofing materials based on the function is expected to perform in construction (Michels, Lamberts, and Guths, 2008). Due to the high conductivity of heat through metal roofing, which causes thermal discomfort in homes (Kruger, Harimi, Harimi, Kurian, and Ideris, 2005), this information has been useful.

Nick Sabino, 2016, submitted that the type of metal install determines the rate of thermal movement and temperature that escapes to the base of the metal. The ambient temperature outside will be different from the temperature of the metal, depending on the direct solar radiation at the time. Therefore, the fundamental requirements of buildings roof are to offer safety to the dwellers who live and work within them from hash weather because damage of this can lead to heat stroke and dehydration couple with other illnesses, (Romero, Romero, and Romero, 2017).

2.5.6 Resistance to heat passage using insulation materials

Peoples quest for thermal comfort has increase many more demands for thermal insulation in residential buildings, (Al-Sanea, 2002). Thermal insulation plays a major role in reducing the influence of heat admitted and transmitted by metal roofing materials (Kruger, Harimi, Harimi, Kurian and Ideris, 2005). The impact of solar radiation causes the temperature at roof surface to reach their maximum level, therefore, the radiant temperature from roof into air space warm the ceiling and then causes the greatest discomfort and increases the physiological stress induced by heat, Gruger *et.al* (2005). Gruger et.al (2005), further explained the impact of using insulation above the ceiling or just under the roof, which may reduce efficiently the energy use, which causes reduction on the money spend on basic

(utility bills) needs in residential buildings under active cooling system. Examples of such insulator include fiberglass, which serves to minimise conduction and convention, thereby decreasing the temperature on the ceiling. He stressed that fiberglass is much efficient in reducing ceiling temperature in comparison to foil-Aluminium. This is due to the low emissivity of metal roofing, which can considerably minimize the emitted radiation into attic before reaching the foil-Aluminium. This tend to gain temperature difference of 3°c. Harimi *et..al* (2005), also allured to role of fibre glass in minimising conduction and convection, thereby causing the temperature on the ceiling to decrease, whereas, the principal function of reflective insulator, is to act as barrier to reflect radiant heat rays and acts also as vapour barriers. A well-insulated roof gives and aided durable roof and help to control the climate of the building, (Romero, Romero, and Romero, 2017).

2.5.7 Resistance to heat passage using green roof

Morau (2011), suggested the environmental benefits of green roofs in buildings, one, its ability to ensure the consumption on energy is reduce and two, to boost the internal comfort during the spring and summer seasons, in location, where the climatology is characterized by high temperature and irradiance values during the day. He stressed that the introduction of systematic air conditioning systems into the building, with their high cost expended on energy, has become the standard alternative used to natural cooling. Green roof provides protection for buildings against solar radiation and temperature fluctuations and by reducing building's energy consumption by direct shading, (Morau, Libelle, and Garde, 2012). The performance of green roof was explored by assessing its effect on temperature fluctuations and heat fluxes during the summer season. This was done by the determination of major parameters including U-value, R-value, and k-value, demonstrated the green roof' thermal and energetic behavior and helped to highlight Sedum plant benefits.

2.5.8 Resistance to heat passage using cool roof

Miller (2006) studied cool roofs with the attic strategies by using combined experiment and analytical study of their thermal performance. Cool roofs with coloured were used as defense against penetrating effect of heat into the conditioned space. However, in

conclusion he stressed that, radiant barriers, above-sheathing ventilation, low-emittance (low-e) surfaces in an inclined air space above the roof deck, insulation, and conventional and advanced thermal masses are all thinkable candidates that can improve cool roof and attic performance.

2.6 Thermal performance

Al-senea, (2002) defined thermal performance as a function of many factors, which includes external climatic factors and the choice of building construction materials. Such material like roof, which could offer comfortable internal ambient to his occupant by acting as barrier to the influx of heat through solar radiation.

2.6.1 Thermal performance in building

According to Markus and Morris (1980) thermal conditions impact the body system in many ways, causes body level arousal, vigilance, fatigue, attention, and boredom. The adaptation of man to different climatic condition under special environmental situation determine his quality of life, (Lawal and Ojo, 2011). The thermal building behavior is controlled by the extent of thermal measure provided within the building roof and the existing outdoor conditions. Therefore, building design in hot areas, must aim at minimizing heat gain indoors and maximizing evaporative cooling of the occupants of the spaces to achieve thermal comfort. Therefore, the relationship between thermal performance and efficiency of buildings should be measured through climate responsive design. Noted that, site building orientation and the impact of climate for design regarding thermal efficiency has further potential for reducing active energy, which is the operational energy of the building, (Lawal and Ojo, 2011). Life cycle costing for entire project is new computation building method employed due to growing concern for passive energy utilisation for provision of thermal comfort, Lawal (2008) and (Lawal, Akinpade, and Makinde, 2017).

2.6.2 Thermal comfort in building

ISO 7730: expresses thermal comfort as a condition of mind which expresses satisfaction with the thermal environment. Fanger (2004) defines thermal comfort as a point where the person is in thermal equilibrium with the environment. To maintain this equilibrium most

designers have adopted mechanical means rather than natural comfort. Building therefore, is a construction that protects people from the environmental conditions and provides healthy and comfortable indoor conditions with the possible use of systems, Pavlou, (2009). Pavlou highlighted two basics important of thermal comfort in building which are having the “right temperature and air freshness. Meanwhile Lawal (2011), believed that human beings partake in various activities within building enclosures. These activities can only be performed best when the environmental conditions are favorable. Prakash *et al*. (2015) deduced that the cause of poor thermal comfort in buildings is as a result solar radiation which rises the indoor temperature. Therefore, Saberi *et al (2016)* believed that the main goal of building design is to provide a comfortable space for living. Evidence now shown that building consume 50% to 70% of the total energy generated globally (Thirumaran and Mathew, 2017). Hence, thermal comfort helps substantially in human performance at both mental and physical levels. The efficiency at any given tasks would indicate the level of influence generated by the impulses caused by the varied environmental parameters.

2.7 Thermal performance of roof

Thirumaran and Mathew (2017), expressed that the thermal performance of roof is one of the most important aspects to achieve indoor thermal comfort in tropical buildings. He noted that the key element to determine the thermal performance is the heat transfer across the roof and its measurement. The material of roofing is an important parameter to determine the thermal performance. Heat transfer across the building roof system is a very important research topic that bears large consequences on energy consumption and conservation in buildings. This measuring technique utilises the capacity of thermocouple to measure the temperature difference between two places which are in contact with two different junctions of thermocouple.

2.8 Thermal parameters to determine roof performance

Some parameters determined the effectiveness of any Roofing materials, thereby resulting in their performance in the building interior. Namely are the diffusivity, resistivity, emissivity, absorptivity, conductivity, and the specific heat capacity.

2.8.1 Transmittance value

Opoko (1998) express this as the ability of a building enclosing elements to conduct heat from one side of the wall to the other and it represented with U-value. The U-value, according to Ezeilo (1998), determined in the tropics, varies with the type of enclosing building elements. For the roof, it depends on materials used, thickness of materials and space, vapour barrier, temperature and surface texture, and ranges from 0.08-3.22 w/m² ºC. For glazed materials, it ranges from 2.2-8.74 w/m² ºC.

Madhumathi, 2012, explained that the most widely used parameters for roof thermal evaluation are the thermal resistance, u and its reciprocal the thermal resistance R. It is considered as the smaller U (the bigger R); better the thermal performance it depends on the quantities such as time lag and decrement factor which characterize the periodic changes in heat flow across the roof section. Since, heat flow lags temperature differences. These effects are most noticeable in roof systems. Summarily, Table 2.3 shown the mean values for emmissivities, absorptivities and reflectivities of various building materials surfaces, (Vanstraaten, 1987).

Table 2.3: Average emmissivities, absorptivities and reflectivities

SURFACE	EMMISSIVITIES	ABSORPTIVITIES	REFLECTIVITIES
Aluminum, bright	0.05	0.02	0.08
Asbestos cement, new	0.95	0.60	0.04
Asbestos cement, aged	0.95	0.75	0.25
Asphalt pavement	0.95	0.90	0.10
Brass and Copper, dull	0.20	0.60	0.40
Brass and Copper, polished	0.02	0.30	0.70
Brick, light buff	0.90	0.60	0.40
Brick, red rough	0.90	0.70	0.30
Cement, white Portland	0.90	0.40	0.60
Concrete, uncoloured	0.90	0.65	0.35
Glass	0.90	-	-
Marble white	0.95	0.45	0.55
Plant aluminum	0.55	0.50	0.50
Paint, white	0.90	0.30	0.70
Paint, brown red, green	0.90	0.70	0.30
Paint black	0.90	0.90	0.10
Paper white	0.90	0.30	0.70
Slake dark	0.90	0.90	0.10
Steel, galvanized, new	0.25	0.55	0.45
Tiles, red clay	0.90	0.70	0.30
Tiles, black concrete	0.90	0.90	0.10
Tiles, uncoloured concrete	0.90	0.65	0.35

Source: Vansraaten, 1987

2.8.2 Thermal reflectivity of roofing materials

All roofing materials have high or low albedo capacity rate. Akridge and James (1998) believed that dark and impervious roofs have the capacity to store heat because of their low albedo (low reflectivity) compared to high albedo materials. They concluded that a light-coloured roof reduces building energy use. Meanwhile, according to (Bisam *et al.* 2017) the usage rate of low albedo materials is still higher than the usage of high albedo materials in most residential buildings and urban form in many cities. The reasons being that desired for low cost of such materials, lack of experience of the decision makers, and lack of awareness about the importance of using high-reflectivity materials on the thermal behaviour of building and energy needed.

Meanwhile, Akbari and Konopacki (2015) allured to the fact that increasing the overall albedo of roofs is an attractive way to reduce the net radiative heat gains through the roof and hence, reduce building cooling loads. Therefore, to change the albedo of any roofing material, the rooftops of buildings may be coated or covered with a new material.

Bisam *et al.* (2017) established the fact that many previous studies confirm that high albedo and high emissivity roof materials (white color material, or another material with another color after changing their chemical composition) can play an important role in enhancing the thermal behaviour of a roof, indoor/outdoor air temperature, and energy consumption. He suggested that the appropriate rooftop albedo value is 0.8 for all types of building. Suggested that for maximum and excellent roof performance, the roof parameter such as thermal emittance or thermal emissivity is very important factor which work together with surface albedo effecting rooftop temperature and then give the best-performing construction materials for surface temperature, cooling load, air temperature reduction and has both high albedo and high emittance. Apparently, almost all the previous studies related to the high-reflectance roof have shown that high-albedo materials can influence greatly the surface temperature through shed heat by reradiation regardless of percentage of temperature reduction that is provided by high albedo rooftop. Therefore, good building design requires some thought in the selection and use of materials, hence, reflective building materials stand to benefit the occupants and the environment.

The materials with high solar reflectivity can offer better thermal performance than materials with lower reflectivity by way of lower cooling energy costs and/or improved thermal comfort. Highlighted that many building materials are designed to be highly reflective. Noting that the main benefits being that highly solar reflective materials do not absorb as much heat as less reflective materials and therefore stay cooler. Generally, the use of highly solar reflective materials will result in a building with greater thermal efficiency (which can improve occupant comfort and improve effectiveness of cooling systems). The laws of physics dictate that metallic materials (materials with low thermal emittance) get hot under the sun. Dark roofs are heated by the summer sun and thus raise the summertime cooling demand of buildings. For highly absorptive roofs, the difference between the surface and ambient air temperatures may be as high as 50 °C (90 °F), while for less absorptive (high albedo) roofs, such as white coatings, the difference is only about 10 °C. Generally, building materials are design to reflect heat, highly reflective materials are low or poor absorptive heat materials, (Blue scope, 2021).

2.8.3 Thermal emissivity of roofing materials

Chudley and Greeno (2004) expresses emissivity as the heat transfer across and from surfaces by radiant heat emission and absorption effects. Theoretically, the higher the emissivity (the rate at which heat is been repel) the higher the radiative heat transfer from the roof to the sky. Abkari and konopacki (2015) explained that thermal emissivity is another property of the roof surface that affects the building heating and cooling energy use. (Zbigniew, 2018), explained that appropriate choice of kind and color of roofing affects meaningfully the energy balance of a building. He further noted that the amount of energy transferred between the building's interior and its environment can be significantly reduced by application of the right roofing material with right reflectivity and emissivity of roofing outer layers. During the hottest hour of the days, high emissivity roofs are desirable since they maintain coolness and reduce heat gain through the roof. In the winter nights, during cold climates, low emissivity roofs are more desirable since they add a resistance to the heat loss through the roof.

Akbari further came up with the equation which related the absorptivity of temperature by the roofing material with the emissivity rate of such material. In conclusion he asserted that the surface temperature of a roof is a strong function of both absorptivity and emissivity. Therefore, for a roof surface exposed to the sun, the steady-state surface temperature is obtained by

$$(1 - a)\, I = \varepsilon\sigma\,(T_{s4} - T_{sky4}) + h_c(T_s - T_a) + U(T_s - T_{in}) \quad \ldots \quad 2.1$$

where, a = solar reflectivity = solar flux, Wm^{-2};ε = thermal emissivity; σ = Stefan Boltzmann constant ; $5.6685x10^{-8}$ $Wm^{-2}K^{-4}$; T_s = steady-state surface temperature, K; T_{sky} = sky apparent radiative temperature, K h_c = convective coefficient, $Wm^{-2}K^{-1}$;T_a = air temperature, K ;T_{in} = inside temperature, K ;U = overall roof heat transfer coefficient, $Wm^{-2}K^{-1}$.;r_c is the resistivity; $G_{s\beta}$ is total irradiance that reaches the roof surfaces

2.8.4 Thermal conductivity of roofing materials

A school of thought believed there is intense heat transfer to the internal environment, which may cause thermal discomfort to the inhabitants (Etuk *et al*., 2007), but one way to reduce the thermal discomfort is the use of radiant barrier which reduce the heat flux. The heat flow through any building depends on the thermal properties of the materials used in the building (Michels *et al*., 2008). Though heat is conducted in a solid phase through the energy transport by flow of electrons and through molecular vibration. But dark metal roofing sheets are heated during the hot hour of day (Akbari *et al.,* 2015) compared to the light metal roofing sheet, which has better reflective rate. Zhang *et al.* (2017) suggested that heat transfer during the summer period through the building envelopes constitutes the leading part of indoor cooling load in summer.

Building coated on the external walls with high reflectivity materials proves to be an effective way to decrease heat gains from solar radiation and save cooling energy consumption accordingly. Then, temperature of a roof with light coloured can be up to 35°C during hot sunny weather, cooler than roof with a dark-coloured, (Blue scope 2021). Therefore, thermal conductivity is defined as the rate of heat transfer through the unit thickness of a material per unit area per unit temperature difference. The unit of thermal conductivity is w/m^{-K}. The table 2.4 Shown various surface resistance for most envelop components used in building.

Table 2.4: External surface resistances (R_{so})

Surface	Exposure		
	Sheltered	**Normal**	**Severe**
Wall – high emissivity	0.080	0.055	0.030
Wall – low emissivity	0.110	0.070	0.030
Roof – high emissivity	0.070	0.045	0.020
Wall – low emissivity	0.090	0.050	0.020
Floor – high emissivity	0.070	0.040	0.020

Source: Chudley *et al* 2004

2.8.5 Thermal performance of materials testing standard

The types of techniques for measuring thermal conductivity are in two forms, namely steady state techniques and transient techniques. In overall, steady-state techniques is use for measurement when the temperature of the materials measured does not change with time. This makes signal analysis simple. The techniques are used for measuring a material during the process of heating up and it is not simple. The advantage is that measurements can be made quickly.

Standard References and Necessary Procedural Adjustments (SRNPA), expresses that, Thermal Conductivity (λ) is the ability of a substance to conduct heat. This denotes the quantity of heat per unit, time per unit area that can be conducted through a plate of unit thickness of a given material, the faces of the plate differing by one unit of temperature.

$$R = \frac{S}{\lambda} \qquad \ldots \qquad 2.2$$

For material with multi-layer, the thermal resistance equals to the sum of the thermal resistance of the single layers. The laboratory measurement is used homogeneous materials to determine their thermal conductivity. The physical principle on which the experimental measures are based is a sample placed in contact with two thermostated plates, the first cold, and the latter hot. The two elements, hot plate and the cold plate produce a steady state temperature difference between the two faces of the sample and a consequent heat flux from the hot face to the cold one. This methodological approach is described in various UNI EN ISO standards, as a function of the main characteristics of the materials and samples. The standards describe two main different methodologies of measurement. One, the measures of thermal flux from the hot plate to the cold one (the heat flow meter method), however, the second measures the constant temperature of the power supplied to the hot plate (the guarded hot plate method). UNI EN ISO 12667 are also used to determining thermal resistance and thermal conductivity of building materials. This is use for roofing materials with thickness less than or equal to 10 cm, by means of the guarded hot plate and heat flow meter methods. UNI EN ISO 12939 standard are also use for the thickness greater than 10 cm. Meanwhile, UNI EN ISO 12664 were used for determining thermal conductivity and thermal resistance of building materials for dry and moist. This is meant for products that

are characterised by low and medium thermal resistance using guarded hot plate and heat flow meter methods.

The ability of a material to transmit heat is measured by its thermal conductivity or k-value. The k-value of a material is defined as the quantity of heat transmitted under steady-state conditions through unit area of the material of unit thickness in unit time when unit temperature difference exists between its opposite surfaces. It is expressed in W/m K. Table 2.5 gives the conductivity, k-values of some commonly used building materials.

2.8.6 Thermal diffusivity of roofing materials

Kochanowski *et al.* (2014), described thermal diffusivity as a material parameter which describes the movement of the isothermal surface during the heat flow through the material. Thermal diffusivity α characterises a material in a complex way because it includes the heat conductivity λ, specific heat *c* and the mass density *ρ*, of the material.

$$\alpha = {}^{\lambda}/c\rho \qquad \ldots \qquad 2.3$$

Where, λ is the conductivity of material; c is the specific heat capacity; *ρ* is the density

The value of this quantity depends on the chemical composition of the material and its internal structure.

2.8.7 Thermal effusivity/absorptivity of roofing materials

The absorptivity capacity of a roofing material is its ability to absorb and release heat. Any materials with high effusivity capacity cannot hold heat long enough.

Table 2.5: Thermal conductivity and density for some materials

Material	Density (kg/m^2)	Thermal Conductivity (W/mK)
General Building Materials		
Clay brickwork (outer leaf)	1,700	0.77
Clay brickwork (inner leaf)	1,700	0.56
Concrete block (heavyweight)	2,000	1.33
Concrete block (medium weight)	1,400	0.57
Concrete block (autoclaved aerated)	700	0.20
Concrete block (autoclaved aerated)	500	0.15
Concrete block (hollow)	1800	0.835
Cast concrete, high density	2,400	2.00
Cast concrete, medium density	1,800	1.15
Aerated concrete slab	500	0.16
Concrete screed	1,200	0.41
Reinforced concrete (1% steel)	2,300	2.30
Reinforced concrete (2% steel)	2,400	2.50
Wall ties, stainless steel	7,900	17.00
Wall ties, galvanized steel	7,800	50.00
Mortar (protected)	1,750	0.88
Mortar (exposed)	1,750	0.94
External rendering (cement sand)	1,800	1.00
Plaster (gypsum lightweight)	600	0.18
Plaster (gypsum)	1,200	0.43
Plasterboard	900	0.25
Natural slate	2,500	2.20
Concrete tiles	2,100	1.50
Clay tiles	2,000	1.00
Fibre cement slates	1,800	0.45
Ceramic/porcelain tiles	2,300	1.30
Plastic tiles	1,000	0.20
Asphalt	2,100	0.70
Felt bitumen layers	1,100	0.23
Timber, softwood	500	0.13
Timber, hardwood	700	0.18
Wood wool slab	500	0.10
Wood-based panels (plywood, chipboard etc.)	500	0.13

Source: I.S EN ISO 10456: 2007

2.8.8 Thermal resistivity of roofing materials

The thermal resistivity of a material is the reciprocal of its thermal conductivity, it may be defined as the time required for one unit of heat to pass through unit area of a material of unit thickness when unit temperature difference exists between opposite faces

$$r = {}^{1}/\mathrm{k} \qquad \ldots \quad 2.4$$

It is expressed as m k/w; r is the resistivity; k is the conductivity

2.8.9 Thermal resistance of roofing materials

Thermal resistance of any material refers to the temperature difference across a substance when a unit heat energy flows through it in unit time. This was calculated by dividing the thickness of the material by the conductivity value of such material, (Chudley and Greeno, 2004). Tables 2.6a and 2.6b is the surface resistance value for the direction of heat flow in relation to material thickness.

$$R = {}^{L}/\lambda \qquad \ldots \quad 2.5$$

Where, R is the resistance in m^2k/w; L is the thickness of the material in 'm'; λ is the conductivity in w/mk.

Table 2.6a: Surface resistance value

Surface resistance m^2k/w	Direction of heat flow		
	Upwards	**Horizontal**	**Downwards**
R_{si}	0.10	0.13	0.17
R_{se}	0.04	0.04	0.04

Source: ISO 6946:2007

Table 2.6b: Surface resistance value for unventilated air layer

Thickness of air layer (mm)	Thermal resistance (m^2k/w) direction of heat flow		
	Upward	Horizontal	Downwards
0	0.00	0.00	0.00
5	0.11	0.11	0.11
7	0.13	0.13	0.13
10	0.15	0.15	0.15
15	0.16	0.17	0.17
25	0.16	0.18	0.19
50	0.16	0.18	0.21
100	0.16	0.18	0.22
300	0.16	0.18	0.23

Source: ISO 6946:2007

2.8.10 The specific heat capacity of roofing material

Jitka Mohelnikova (2006) explained that specific heat capacity as an important property of building materials is used for thermal evaluation of building constructions.

2.9 Thermal equipment used in laboratory measurements

In the laboratory, a variety of tools have been utilised to measure the thermophysical characteristics of building materials. This includes thermocouple and infrared thermography apparatus.

2.9.1 Thermal parameter using infrared thermography

Kochanowski, *et.al* (2014), explain the most cost effective and efficient tool for non-destructive assessment of conventional roofing systems. When handled by an experienced professional, the use of infrared thermography can play a key role in helping to quickly determine the location and general scope of moisture imprisonment hidden within the roofing system.

The introduction of moisture, whether in the free state or absorbed by the insulation, reduces the insulation's effectiveness, and increases its conductivity. During the summer months, under clear sky conditions, the moisture within the roof acts as a large thermal collector and heat sink. At sunset, the roof surface starts to cool rapidly, while the moisture laden insulation continues to emit heat to the membrane from below as it too slowly starts to cool. For many hours following sunset (this duration depends on several variables) the membrane sections above wet sections of insulation of a conventional roofing system will continue to emit heat and remain warmer than the surrounding roof membrane above dry insulation. Using an infrared camera to detect minute variations in the emission of heat of exposed surfaces and to convert this information into an electrical signal and color image, infrared thermography makes it possible to detect/predict the presence of moisture within the insulation of most conventional roofing systems.

2.9.2 Thermal parameter using thermocouple

The principle of thermocouple was used by (Thirumaran and Mathew, 2017) to determine the thermal conductivity of a sample material. Thermocouple being is a device used extensively for measuring temperature. A thermocouple is comprised of at least two metals joined together to form two junctions. One is connected to the body whose temperature is to be measured; this is the hot or measuring junction. The other junction is connected to a body of known temperature; this is the cold or reference junction. Therefore, the thermocouple measures unknown temperature of the body with reference to the known temperature of the alternative body.

2.10 The roofing materials and its performance

Performance of a roof is the ability of the roof to serve it primary purpose of protecting the dweller from the direct harsh solar radiation, winds, rain and ability to perform its structural stability. Roof cover provided the shelter needed from inclement weather, (Adesogan, 2018). Roof serves as a final shield over an enclosed space(s), be it solid or light materials to prevent harsh weather from penetrating into the interior space(s) thereby brings discomfort to the inhabitants. In the southwest part of Nigeria metal/Aluminium roofing sheet is a common roof building material in the society and such when use resulted in increased indoor heat and temperature due to its poor resistivity rate, causing discomfort for the occupants.

2.10.1 The roof colour, texture and thickness performance

Miller, Desiarlais, Parker, and Kringer, (2004) studied that colour in a roof goes a long way in reducing or minimizing surface temperature, he further submitted that roof with high solar reflectance and infrared emittance decreases heat gain and ultraviolent radiation received by roofs. He concluded that light colour roof have high solar reflectivity, buy less diffused. The colour, texture and thickness of such materials could affect their resistivity and absorptivity rate. Roofing materials are generally designed to absorb and insulate the interior part of the building from the inclement weather. They can be source locally and modernly produce in factories. Some of these roofing sheets are known to be a good thermal

conductor and has high absorptivity material, but very poor resistivity and diffusivity rate. According to Bludau *et.al* (2008), asserted that cool roof is usually made of bright surface to reflect the incident solar radiant, which in turn lowers the temperature during the daytime unlike the bituminous roof membrane. Generally, dark metal roofing sheet are heated during the hot hour of the day compared to the light metal roofing sheet, which has better reflective rate. The metallic materials (materials with low thermal emittance) get hot under the sun, so they can also lead to a higher heating energy use, (Akbari, *et al*. 2015). During the summer, the metallic roofing building is excessively hot and non-conducive, as in the winter period when the reverse is the case. Special attention is required in ameliorating or reducing the discomfort people encounter when under such intense condition. Essentially in this region with harsh weather condition, adequate solution should be provided to reduce the indoor temperature. Barozzi, Bellazzi, Maffe, and Pollastro, (2017) noted that cool roofs are manufactured specially to reflect a large amount of incident solar radiation.

2.10.2 The green roof performance

Generally vegetative roofs are very good heat reduction or absorption in temperate climates. Ayala *et.al* 2001, believes that green roof improves air quality, acoustic insulation and reduce solar intrusion through the roof into interior space(s). Floridis *et.al* (2002) assessed that green roof provide the needed cooling in a warm climate. Also, Lazzarin *et. al* (2005) found out that of solar radiation, about 23% is dissipated by solar reflectivity, 39% by solar absorption, 24% by outside convection, 12% by evapo-transpiration (from green plant on the roof) and 1.3% by thermal accumulation. Therefore, Green roofs benefits environmentally by shielding the buildings against solar energy and temperature fluctuations, thereby bring about reduction in consumption in energy use in building by direct covering, thus, building insulation properties is then improve, causing drastic annual reduction in the energy consumptions, (Morau, Libelle, and Garde, 2012). Capozzoli *et. al* 2013 says with green roof only 8% heat enters the interior rooms, because the green roof has a high solar radiation absorbent. Similarly, Barozzi, Bellazzi, Maffe, and Pollastro, (2017), says green roof causes a reduction of surface temperature and this resulting in indoor temperature reduction.

2.10.3 The roofing sheets performance

The transformation and metamorphosis from traditional roofing system into the modern innovation partly accounted for by the desire to find a durable roof covering resistant enough to the environmental forces, Olomola, (2002). Adesogan, (2018) affirmed that the traditional roof covering such as thatch and grass keeps building cool, though cheap with less skill labour require. This can be installed as a pitched (25°-70°) or low roofs (slope between 10°-24°) respectively. Thatch roofs are example of locally made roofing, is a wouven dried grass. The traditional building roof keep the interior space cool all through the day and ensure all round indoor comfort for the occupant. This type of roofing system keeps buildings cool under tropical climate, they are cheap and do not require great skill for installation. They are not durable, susceptible to termites and rodents attack and require frequent maintenance and can easily catch fire.

2.10.4 The underlay or ceiling performance

Increase ceiling temperature causes interior physiological heat stress, (Kruger, Harimi, Harimi, Kurian and Ideris, 2005). Ceiling is an insulating material made up of different constituents consisting various chemical components with varying thermal conductivities, thermal absorptivities, thermal diffusivities and thermal resistivities, (George, Obianwu, Akpabio, and Obot, 2010). Although, asbestos as typical underlay material contains hydrated mineral silicates which induces fibrosis, lung cancer and mesothelioma, (Onyeaju, Osarolube, Chukwuocha, Ekuma, and Omasheye, 2012). Yet, it has a low density and thermal conductivity but high thermal resistivity, making it a very good insulator material. Asbestos material became a popular insulating material during the industrial revolution, Bozsaky (2015).

Meanwhile, PVC is good thermal insulator because it has high thermal resistivity but low density, low thermal conductivity, (Onyeaju, Osarolube, Chukwuocha, Ekuma, and Omasheye, 2012). Is a polymer material which structurally strong and linear, (Ettah, Egbe, Takim, Akpan, and Oyom, 2016). PVC decreases with temperature increases through mechanically strong bond, which enhance the molecular weight increase, it however decomposes at temperature 140 ℃ while it starts to melt at 160 ℃. It however possesses a

better material for thermal insulation because of its physical appearance, strength, chemical resistance, fire resistance, face-maintenance, non-toxic and odourless nature. However, the one used in most cases for ceiling is heavily plasticized PVC, contains very few additives and additional ingredients that make it less harmful. PVC ceilings are inexpensive, easily install durable and sturdy, little maintenance and last a very long time. Perhaps this explain why is been used mainly in residential houses, not mind its ability to provide indoor thermal comfort.

Pop as an insulating material consist of a quick-setting gypsum plaster comprising of a fine white powder (calcium sulphate hemihydrate), which toughens when moistened and permitted to dry (Ochang *et al* 2018). Plaster of Paris shrinks or crack when dry, making it an excellent medium for casting mould. This has been in use in the past nineteenth century; history has it that John Cranch (1751-1821) used this in painting. It is prepared by heating calcium sulphate hydrate or gypsum to about 120-180ºC, this provides passive fire protection and excellent insulation (Ochang *et al* 2018). Pop was also used in various stucco works, decorative jobs, especially the Chateau du Fontainebleau reliefs' designs and Frieze decoration. Pop board is widely use in most residential buildings with unique designs and styles.

2.11 Thermal comfort and orientation of building

Bekkouch *et.al* (2013) emphasis that orientation of building has opportunities to maximise the passive solar heating when needed, and to avoid solar heat gain during cooling time. The building orientation determines the amount of radiation it receives.

Building orientation affect and influence indoor comfort subject to the interior space(s) favored by the orientation. During the daytime, some indoor space tends to enjoy the configuration of the building, hence, the cost of energy consumption will drastically reduce if correct building orientation is observed and therefore ensure indoor comfort. Submitted that in summer period a high temperature was generated on the roof due solar radiation, which was usually high, either on eastern or western walls but was limited on the south facing wall. Meanwhile, only the diffused solar radiation reaches the northern wall. The dry

season (summer) cooling temperature is set for 25℃, while the wet season (winter) is set for 22℃, Albatayneh *et.al* (2018).

Ahskaya *et.al* 2018, believed that a building oriented to 180 is the perfect orientation for building with minimum solar heat radiation into the indoor space. This will allow solar radiation into the room in the morning and causes heat load on air conditioners to be reduced. But in this part of the world, this may depend on the design arrangement and the orientation of the building. Bekkouch proposed 90℃ for adequate building orientation and ensure reduction in cooling demand before 6:30.

2.12 Modelling

Adesogan (2012) defined model as a set of assumptions, which is logically and mathematically related to increase an understanding of how a system behaves. Many other authors have defined model as the process of describing a particular system. It is expressed as real system represented in a simplified form, while, if simple enough can further allow possibility of use of mathematical methods (such as algebra, calculus, or probability theory) to get precise information on questions of interest and this is termed an analytical solution. Types of models: These include the physical and mathematical models.

2.12.1 Physical models

This is referred to the type of models with physical properties bearing similarity with the real objects. They are either prototypes of the real objects or have characteristics that reflect the function of the real objects.

2.12.2 Mathematical models

They are expressed by an equation that is used to depict a streamlined version of a challenging issue. They serve as a succinct summary of reality. A mathematical model allowed for the manipulation of data in such a way that the output would remain the same regardless of who performed the manipulation. To explain the current problem scenario, it is necessary to express complexity and uncertainty using a mathematical model (Adesogan, 2012).

CHAPTER THREE

MATERIALS AND METHODS

3.1 Preamble

This research methodology involved three phases. These involved the laboratory experiment, the field work (physical model and measurement) and the mathematical simulations (models and formulas).

Phase I: Preliminary investigation

The existing roofing sheets were examined in a preliminary laboratory assessment. These were carried out with the aid of various measuring tools, such as a micrometer screw gauge for measuring material thickness, a measuring scale for weighing specimens, and a measuring steel rule for measuring material length.

Phase II: Experimental tests in the laboratory were conducted to establish the thermophysical characteristics for the materials under study. These consist of thermal diffusivity, thermal absorptivity, thermal diffusivity, thermal conductivity, thermal resistivity, specific heat capacity, and the lagging effects of plywood lined Aluminium roofing (PLAR) sheet.

Phase III: Field experimental tests were conducted for the selected sampled materials, and temperature variations of each sample were measured.

3.2 Survey of the study area

Study location: This study was carried out in Ibadan, Oyo state, south-western part of Nigeria, as presented in Figure 3.1. The study focused on selected residential building roof materials and three (3) sampled roof configurations in the region. Ibadan, being the core city in the western region and the centre of Yoruba speaking states. Oyo state has 33 local government areas and located within the low latitude 7º 3N to 7º 4N and longitude 3º 8 to

3º 9E respectively, (Egbinola *et al.* 2013). Ibadan city has a population of over 3 million, the third most populous city, and situated southwest geographical zone of Nigeria.

The methodology flow chart in Figure 3.2 represents the step by steps procedure through which this research work was conducted, from the literature review to the field work, including various laboratory test conducted and the analysis of the data.

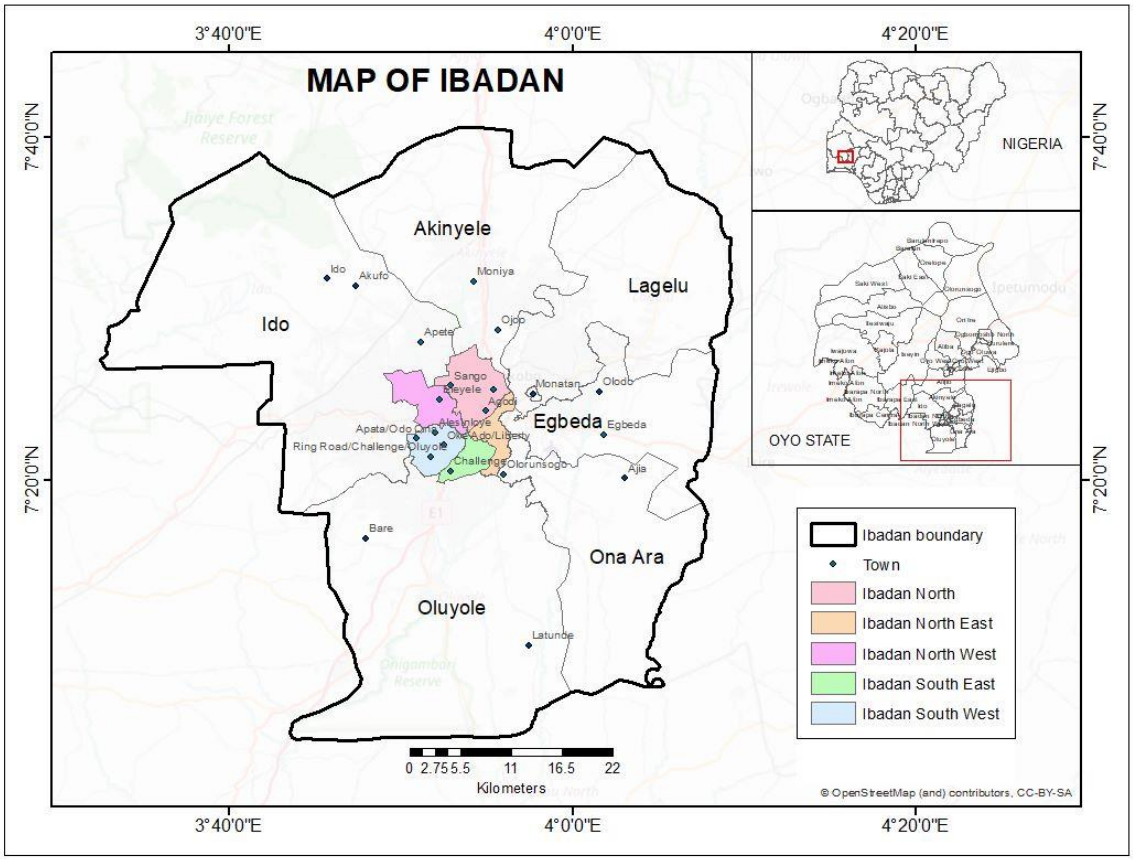

Figure 3.1: Map of the study area

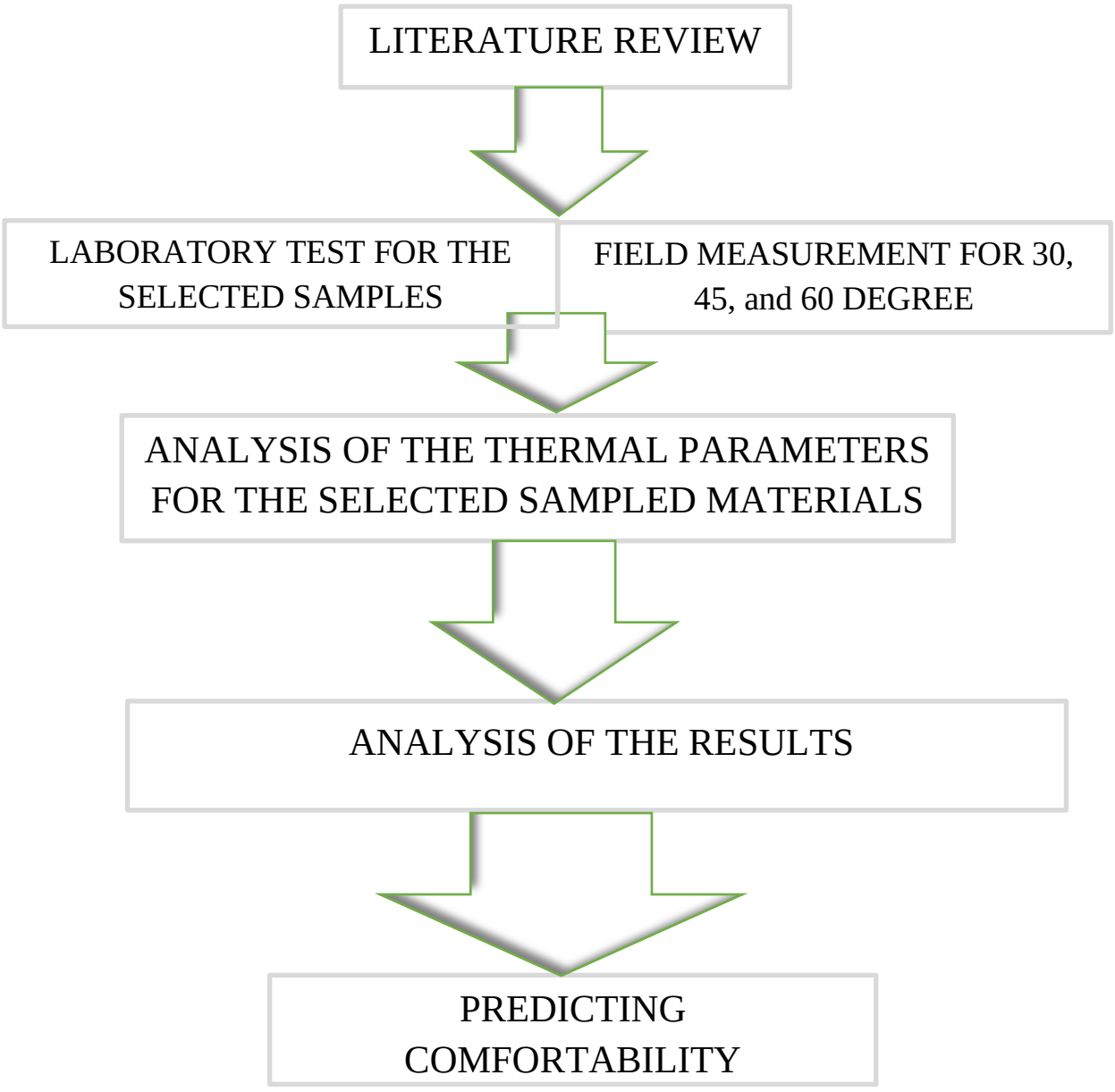

Figure 3.2: Methodology flow chart

3.2.1 Experimental procedure

The thermal performance of selected roofing materials (SRM) and selected ceiling materials (SCM) was tested using the following testing techniques.

Step 1: Thermal conductivity, thermal resistivity, thermal absorptivity, thermal diffusivity, and specific heat capacity tests were conducted on the sample's materials (roofing sheets and ceilings) to determine their main characteristics.

Step 2: The selected samples were cut into sizes and shaped into (180 x 50 mm) and (128 x 128 mm), respectively, based on the configuration of the test apparatus. The test applied the principle of steady-state longitudinal heat and steam flow to the specimen.

Step 3: The selected roofing sheets were tested using the UNE EN standard. The fabricated apparatus was used to test the selected ceiling materials in accordance with the ASTM C518 standard.

The Selected Roofing Sheet SRS were tested using ice and steam apparatus, according to the following procedures (UNE EN standard):

A. I filled the ice mold with water and froze it. I ensured the water did not freeze with the lid on the jar. (Also, a few drops of a non-subsing detergent were added to the water before freezing to help the water flow more freely as it melted, which did not significantly affect the results.)
B. The jar was run under warm water to loosen the ice in the mold.
C. Then the thickness of the sample material was measured and recorded as **h.**
D. The sample material was mounted onto the steam chamber as shown in Figure 3.4. However, the following conditions were strictly adhered to:
E. I ensure I do not attempt to "pry" the ice out of the mold.
F. I ensured the sample material was flushed against the water channel so that water did not leak by tightening the thumbscrews. A bit of grease between the channel and the sample was added to help create a good seal.

G. After which the diameter of the ice block was measured. This was recorded as a value of $\mathbf{d_1}$. The ice was then placed on top of the sample, as shown in Figure 3.4.

H. The ice was allowed to sit for several minutes, so it began to melt and came into full contact with the sample.

I. Subsequently, data for determining the ambient melting rate of the ice was obtained as follows:

   i. By determine the mass of a small container used for collecting the melted ice and record it.
   ii. The melting ice was then collected in the container for a measured time $\mathbf{t_a}$ (approximately 7 minutes).
   iii. Then determine the mass of the container plus water and record it.
   iv. Subtract your first measured mass from your second to determine $\mathbf{m_{wa}}$, the mass of the melted ice.

J. The steam was run into the steam chamber. This took place for several minutes until temperatures stabilized and the heat flow was steady. (A container was placed under the drain spout of the steam chamber, where the water that escapes from the chamber was collected.)

K. The cup used for collecting the melted ice was then emptied. Step 7 was repeated, with the steam running into the steam chamber. The mass of the melted ice and **t**, the time during which the ice melted (5 minutes), were measured and recorded as $\mathbf{m_w}$.

L. The diameter of the ice block was remeasured and recorded as $\mathbf{d_2}$.

M. The test result was calculated to determine the thermal conductivity TC and thermal resistivity TR.

The average of $\mathbf{d_1}$ and $\mathbf{d_2}$ was used to determine $\mathbf{d_{avg}}$, the average diameter of the ice during the experiment. Then, the value of $\mathbf{d_{avg}}$ was used to calculate **A**, the area over which the heat flow between the ice and the steam chamber took place.

I then divide $\mathbf{m_{wa}}$ by $\mathbf{t_a}$ and $\mathbf{m_w}$ by **t** to determine $\mathbf{R_a}$ and **R**, the rates at which the ice melted before and after the steam was turned on. Then, I subtracted $\mathbf{R_a}$ from **R** to determine $\mathbf{R_0}$, the rate at which the ice melted due to the temperature differential alone.

Note: Mc (mass of empty container) = 37.1g; d_1 = Diameter of ice block:
d_2 = Repeat Diameter of ice block; d_{avg} = Average of d_1 and d_2; h = Thickness of sample

$$R_a = \frac{M_{wa}}{t_a} \quad \ldots \quad 3.1$$

$$R = \frac{M_w}{t} \quad \ldots \quad 3.2$$

$$R_0 = R_a - R \quad \ldots \quad 3.3$$

Calculate **k**, the conductivity of the sample: k (cal cm/cm2 sec)
$\Delta\mathbf{T}$ = Boiling point of water (100 ℃ at sea level) - 0℃.
Note: The equation giving the amount of heat conducted through a material is:
$Q = k\ A\ \Delta T\ \Delta t / h$ … 3.4
Therefore, thermal conductivity was calculated by the equation 3.5.

$$\mathrm{k} = (\text{cal cm/cm2 sec}) = \frac{(\text{mass of melted ice})\ (80\ \text{cal/gm})\ (\text{thickness of material})}{(\text{area of ice})\ (\text{time during which ice melted})\ (\text{temp.differential})}$$

$$\mathrm{k} = \frac{(\mathrm{m})(80\mathrm{cal/gm})(\mathrm{h})}{(\mathrm{A})(\mathrm{t})(℃)} \quad \ldots \quad 3.5$$

Meanwhile, the selected ceiling materials test was carried out with the following procedure. The apparatus was set at temperature of 28℃ (usually below 30ºC to avoid damage to the components of the apparatus). Using automatic regulator to stabilised the indicator at 34℃, as configurated. The thermocouple was connected to the data logger to record the inflow temperature at the heat sink and heat source before loading the sample. Then, the heat sink closed to minimise heat loss to the surrounding. As soon as the heater was stabilised to 34°, the samples was then loaded one after the other in the lagged container and tested for 15

minutes. The current rating and voltage were measured using digital AC clamp meter during the heating process. The final temperature at the heat sink was recorded and the temperature gradient evaluated.

The figure shown the physical components of the fabricated apparatus are as follows, 1-Control box, 2-Temperature regulator, 3-Alternating current source cable, 4-Thermocouple cable, 5-Heat source, 6-Sample container, 7-Heat sink.

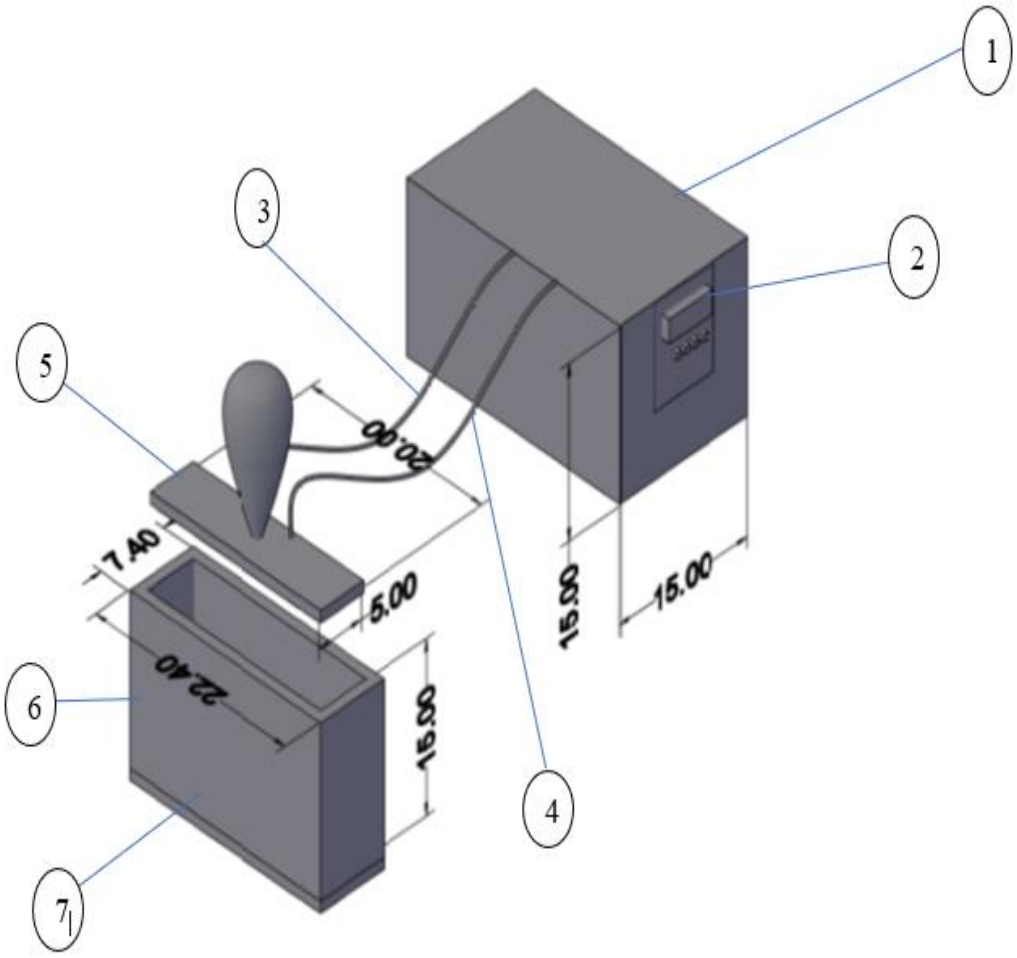

Figure 3.3: Schematic diagram for fabricated experimental conductivity apparatus

Table 3.1 represent the functional components of the apparatus and their function was as follows.

The control box: The control was designed in a cubical form containing temperature regulator. This allowed for control and monitor the steady flow of heat into the heat sink for sample testing.

Temperature regulator, allowed for regulation of temperature from the heat source. Meanwhile, alternating current source cable, conducted electron transfer from the heat source to the sample heat sink.

Thermocouple cable also acted as sensor which indicated the electrical behavior of the sample from the heat sink.

Sample container: this was a rectangular metal fabricated container where material samples were put.

Heat sink: this was lined with glass sheet to prevent heat loss from the sink. The samples were tested there.

Other equipment used were: multi-channels data logger, the kd2 thermal analyser, k type thermometer, mass balance, stop-watch, Bunsen burner, heat source, steel rule, and cutting scissors. Figure 3.4 showing the schematic diagram for the ice and steam apparatus.

Table 3.1: Physical components of the apparatus

S/No	Components
1	Control Box
2	Temperature Regulator
3	Alternating Current Source Cable
4	Thermocouple Cable
5	Heat Source
6	Sample Container
7	Heat Sink

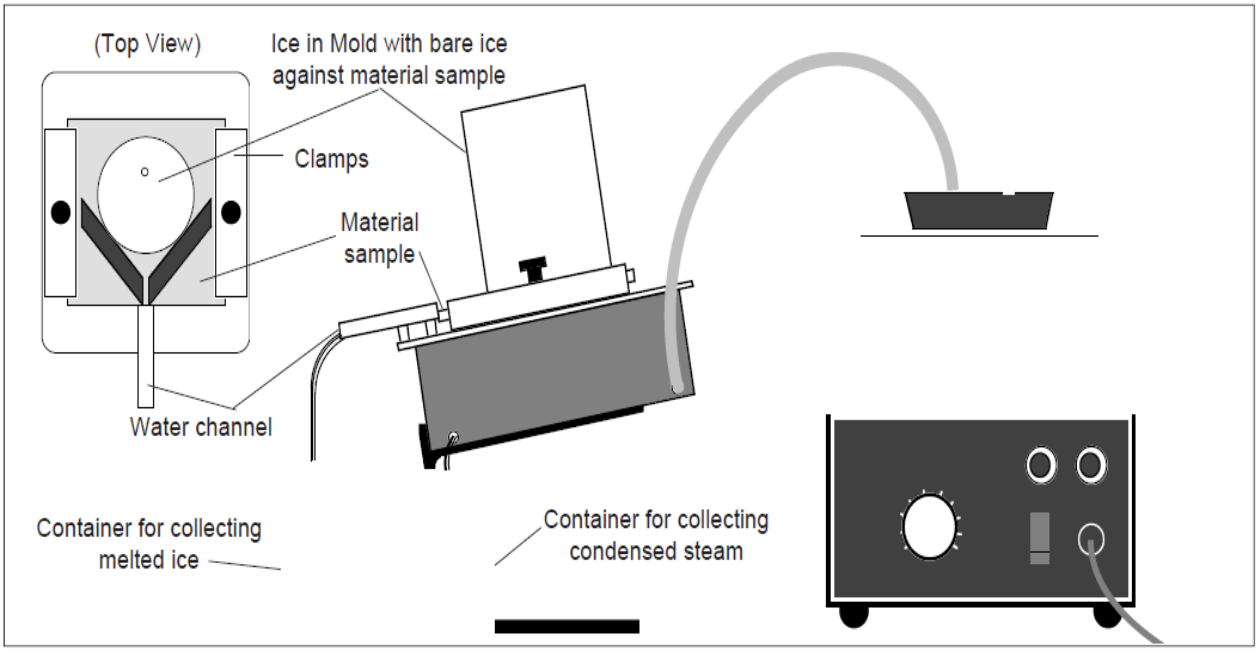

Figure 3.4: Showing schematic experimental setup of ice and steam for thermal conductivity

3.3 Thermal properties test equations

The sample specimens were subjected to both laboratory and the field test. The laboratory experiment was carried out and determined in consonant with UNE EN and ASTM C518 (ISO 6946:2017) standards to evaluate the thermo-physical properties of the material.

3.3.1 Thermal conductivity

The purpose was to know the amount of heat conductivity by the material and transmitted in relation to the time and area of the material surface. According to (Newton, Roy, and Solomon, 2014), this was carried out to examine the effectiveness of materials to conduct heat. This was done in line with Fourier's law of heat conduction. Good insulating materials have low values of thermal conductivities, (Ochang *et al* 2018).

The thermal conductivity was computed with the following formula:

$$K = \frac{Ql}{A(T_o - T_s)} \quad \ldots. \quad 3.6$$

Where K is thermal conductivity in W/mk; Q is rate of heat transferred; l is the thickness of sample; A is surface area of sample in contact with heat source; T_o is temperature at the heat source; T_s is temperature at the heat sink.

3.3.1.1 Thermal resistivity

This is inversely proportional to its conductivity, or the reciprocal of its thermal conductivity. The unit is m k/w. This was done to know the thermal ability of the material to resist heat flow. This depends on the conductivity property of the material.

$$r = {}^{1}/k \quad \ldots. \quad 3.7$$

where, r is the resistivity; k is the conductivity.

Plate 3.1 represent the laboratory procedure for the fabricated conductivity apparatus, while Plate 3.2 showing the laboratory set up for ice and steam apparatus.

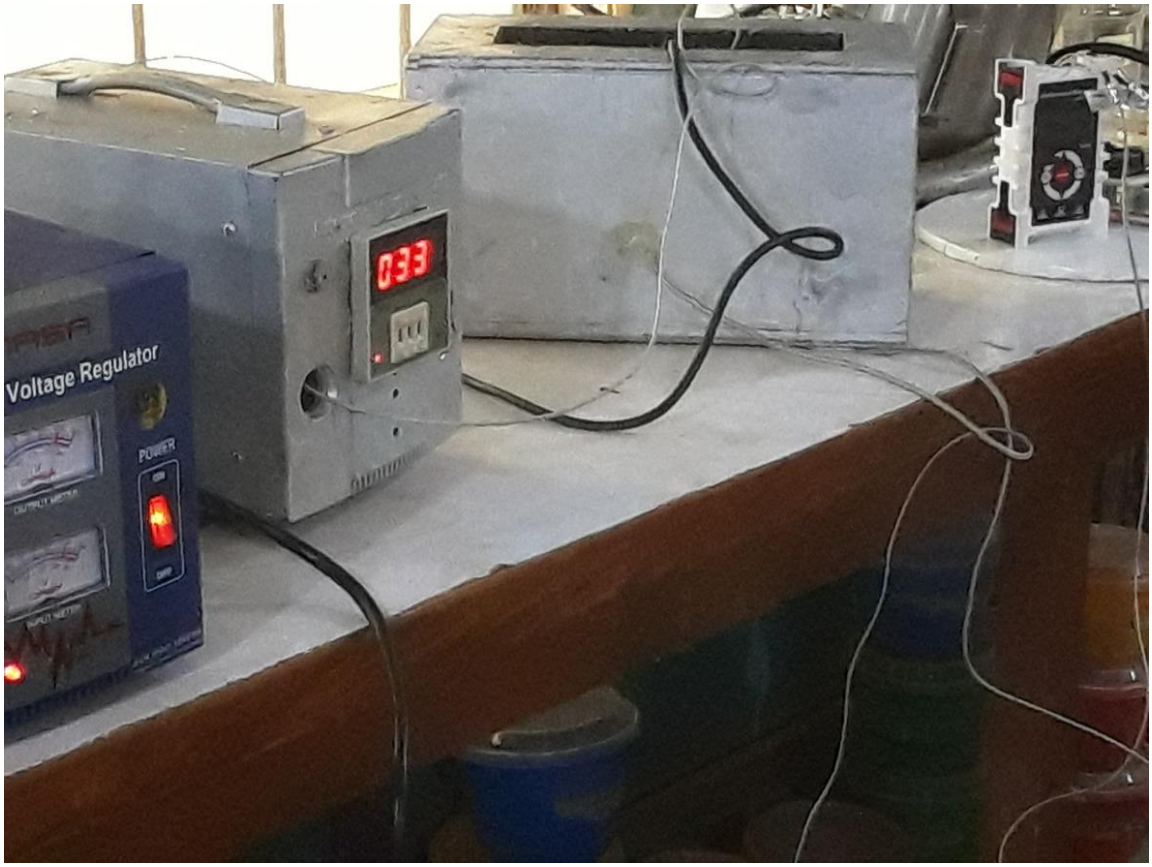

Plate 3.1: Experimental set up for conductivity apparatus

Plate 3.2: Laboratory thermodynamic (ice and steam) apparatus for thermal conductivity

3.3.1.2 Specific heat capacity

This was to determine the thermal storage capacity of the sampled materials. The procedure was as follows: The solid dry was first weighed and recorded as mass M_1. Followed by the weight of the empty calorimeter and stirrer while the water was still boiling and recorded its mass as M_2. The calorimeter was then filled to half its capacity with water. This was recorded as M_3.

We then took the temperature of the water and recorded it as θ_1. The temperature of the boiling water was recorded as θ_2 (i.e., the temperature of a solid). The hot solid was quickly transferred into the calorimeter with water. We then covered up the lid of the calorimeter with the thermometer in place and stirred the water gently with the stirrer.

The thermometer was observed and recorded the highest temperature attained. This was recorded as θ_3.

M_{S1} = Mass of solid M_1 (sample)

M_2 = Mass of empty calorimeter stirrer

M_3 = Mass of calorimeter + stirrer + water

Mass of water = $M_3 - M_2$

θ_1 = Initial temperature of water

θ_2 = Temperature of hot solid

θ_3 = Final temperature of mixture (water + stirrer + calorimeter + solid)

Quantity of heat energy $Q = MC\theta$ … 3.8

Where, M is the mass of the solid

C_s is the specific heat capacity of the solid (sample).

θ is the change in temperature of the solid.

Heat lost by solid is

$M_1 C_s (\theta_2 - \theta_1)$ … 3.9

Heat gained by mixture (water and calorimeter) is

$C_w (M_3\text{-}M_2) (\theta_3 - \theta_1) + M_2 C_c (\theta_3 - \theta_1)$ … 3.10

$C_w [(M_3\text{-}M_2) + M_2 Cc] \times (\theta_3 - \theta_1)$ … 3.11

Note that; C_s = specific heat capacity of the solid =?; C_w = specific heat capacity of water = $4.2x10^3JKg^{-1}K^{-1}$;C_c = specific heat capacity of calorimeter = $0.38x10^3JKg^{-1}K^{-1}$

The unit is measure in joule per kilogram per kelvin (J/kg/K). The equation is given as the quantity of heat to the mass of the material and the temperature different. The Plate 3.3 represent the calorimeter apparatus used for determining the specific heat capacity in the laboratory.

3.3.1.3 Thermal diffusivity

The objective of this was to measure the ability of the sample materials and see how they undergo a temperature changes. Diffusivity is defined as the heat transfer ability of a material relative to its heat storage ability. This is the heat measure from the hot side to the cold side of the materials, (Ochang *et al.* 2018).

Note: material with low thermal diffusivity have a slow rate of heat transfer relative to heat storage. Ochang *et al.* 2018, low value of thermal diffusivity is ascribed as thermal insulators; but high value indicates a good conductor. The unit is m^2/s.

The diffusivity value is calculated through the value of conductivity obtained, divided by the density and specific heat capacity of the material.

$$\alpha = \frac{k}{pc} \qquad \ldots \quad 3.12$$

Plate 3.3: Laboratory calorimeter apparatus for specific heat capacity

3.3.2 Thermal absorptivity

The research also employed this method to determine the capacity of the selected materials to absorb and release heat. Materials with high thermal diffusivity cannot hold heat for long period. This was determined experimentally by estimating the quantity of heat supplied in relation to the conductivity rate, density and specific of the material.

The research also used the polynomial relational equations to factor the amount of heat stored in the samples during the day.

$$\beta = \sqrt{k\rho c} \quad \ldots \quad 3.13$$

where:

κ is the conductivity of the sample material;

ρ is the density in kg/m^3;

C is the specific heat capacity

TA using polynomial relational equation

The polynomial relational equation was adopted in this research to calculate the amount of heat absorbed by the samples. Where the quantity of heat (temperature) absorbed against the time T, was plotted.

The polynomial equation was represented as follow.

$$y = ax^4 - bx^3 + cx^2 - dx + e \quad \ldots \quad 3.14$$

Where, y, represents the quantity of heat material absorbed between the hours of 9am to 9pm for the day period, a, b, c, d represent the measured materials variables in ℃, x is the time in hour at which heat is absorbed, e is the constant.

The equation represented and expressed the relationship between the measured sample variables in temperature, and the time taken x. This was then integrated to determine the quantity of heat absorbed by the shaded area, as represented in Appendix E (Figure E1 – E22).

3.3.2.1 Temperature variations

The study adopted the principle of Maxwell's equation of waves to determine the temperature variation of the penetrating effect of heat on each material. The numbers of wavelength in this case indicate the strength (diffused rate) or how porous the property of such sampled materials. Since heat travels from high temperature to low temperature, it assumed one dimensional transvers wave movement.

Therefore, wavelength is directly proportional to two pie, 2π and inversely proportional to wave number κ.

$$\lambda = \frac{2\pi}{\kappa} \qquad \ldots \qquad 3.16$$

Making k the subject of the formula

We now have

$$\boldsymbol{k = \frac{2\pi}{\lambda}}$$

Where:

K represent the wave number;

λ represent the wave length;

π is the constant pie

Temperature variations for the selected roofing material (SRM) under steady heat supply were examined for about fifteen (15) minutes under regulated standard room temperature. The determine the heat emissivity of the SSM under a regulated steady temperature of 34℃. Table 3.2 presents the different available (eleven (11)) samples for residential roofing materials selected, which include Stone Coated sheet, Plywood lined Aluminium, Aluminium roofing sheets. However, Table 3.3 shows the selected ceiling materials and coded respectively.

Table 3.4 indicates the material source details and manufacturer's address for the sample specimens used to carry out this work. Apparently, most of the roofing sheets and the underlay materials were locally produced. These various sampled roofing sheets were represented in Plates 3.4a, 3.4b, 3.5, 3.6, 3.7 and 3.8. The underlay sampled ceilings also include, asbestos ceiling, polyvinyl chloride ceiling, plaster of Paris ceiling, gypsum ceiling and plywood ceiling board, as shown in Plates 3.9, 3.10, 3.11, 3.11 and 3.12.

Table 3.2: Materials and Code of the selected roofing sheets

S/n	Materials	Sample
1	Stone coated sheet	A
2	Stone coated sheet	B
3	Plywood lined Aluminium	C
4	0.7mm Aluminium sheet	D
5	0.55mm Aluminium sheet	E
6	0.45mm Aluminium sheet	F
7	0.7mm Aluminium sheet	G
8	0.55mm Aluminium sheet	H
9	0.55mm step Aluminium sheet	I
10	0.55mm plain Aluminium sheet	J
11	Galvanized zinc roofing sheet	K

Table 3.3: Materials and code of the selected ceiling materials

s/n	Materials	Sample
1	Polyvinyl chloride	PVC
2	Asbestos	ASB
3	Plaster of Paris POP	POP
4	Gypsum board	GYP
5	Plywood Ceiling board	PCB

Table 3.4: Material specifications for the selected roofing Sheets

Sampled materials	Thickness (mm)	Mass (g)	Area (m^2)
A	1.30	37.40	0.00936
B	1.45	38.10	0.00936
C	9.29	85.60	0.00936
D	0.69	12.10	0.00936
E	0.42	9.70	0.00936
F	0.27	5.70	0.00936
G	0.67	10.10	0.00936
H	0.47	10.00	0.00936
I	0.48	9.90	0.00936
J	0.46	10.6	0.00936
K	0.21	12.8	0.00936

Table 3.5: Material specifications for the sampled ceilings

Sampled materials	Thickness (mm)	Mass (g)	Area (m^2)
PVC	5.43	12.90	0.00936
ASB	3.49	39.00	0.00936
POP	5.20	73.20	0.00936
GYP	6.37	46.70	0.00936
PCB	8.10	44.70	0.00936

Table 3.6: Material source and manufacturers

Material	Manufacturers company address	Company address/location
Stone coated sheet ST-A	New Zealand product	
Stone coated sheet ST-B	Korea product	
Chilatech Aluminium CH-0.7, CH-0.55, CH-0.45	Chilatech Aluminium company limited	Abattoir road, Abule Egba, Lagos state.
Machtech Aluminium MT-0.7, MT-0.55, MT-0.45	Machtech Aluminium company limited	Ile-epo Road, Abule Egba, Lagos state
Balita Aluminium BT-0.55st, BT-0.55	Balita Aluminium company limited	Adjacent Agbala Itura market Lagos/Abeokuta express road.
Sumo Aluminium SU-0.55	Sumo Aluminium company limited	Pleasure bus stop, Iyana Ipaja, Lagos state
Galvanized zinc sheet, GAL		
Polyvinyl chloride PVC	Golden Eva	Ajah, Lagos state
Asbestos ceiling ASB	Nigerite Nigeria plc	Ikeja, Lagos state
Plaster of Paris P.O. P	Site Cast-in-situ	
Gypsum ceiling GYP	China product	China

Source: Field Source

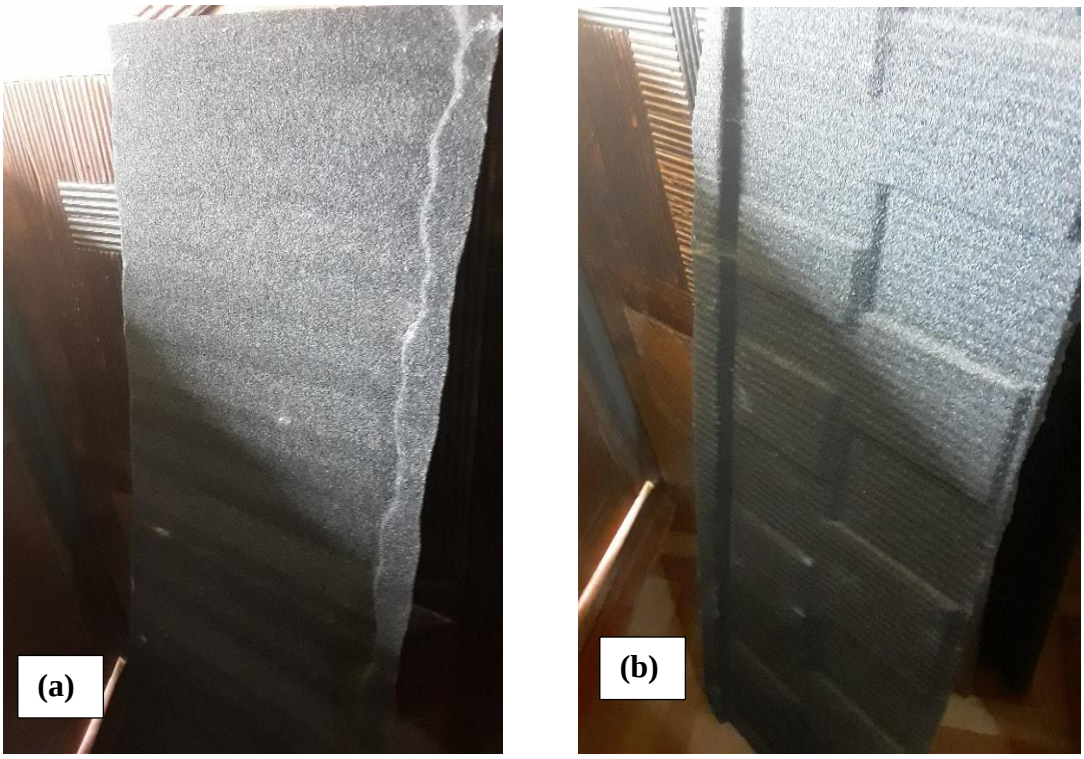

Plate 3.4: Stone coated sheet
(a) New Zealand product (b) Korea product

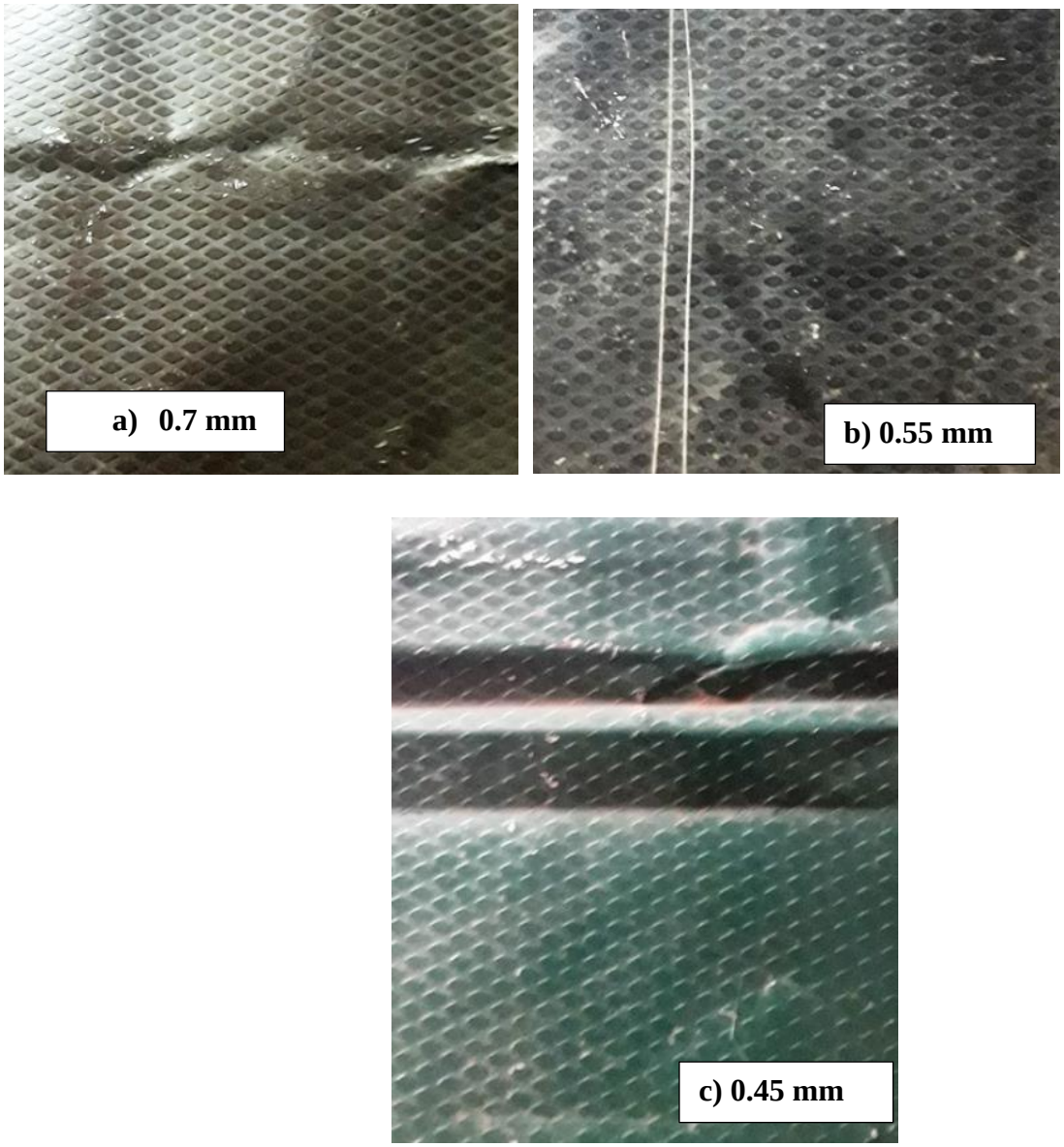

Plate 3.5: Chilatech Aluminium roofing sheets

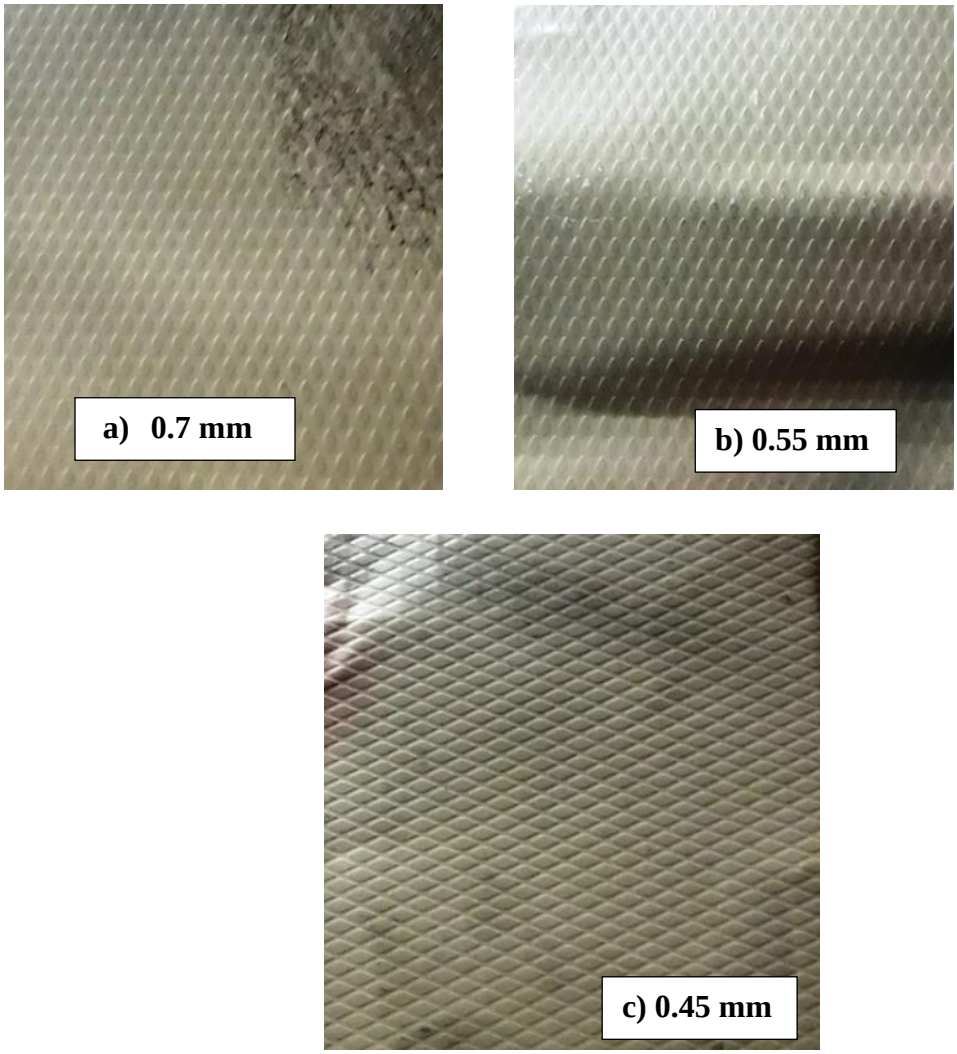

Plate 3.6: Machtech Aluminium roofing sheet

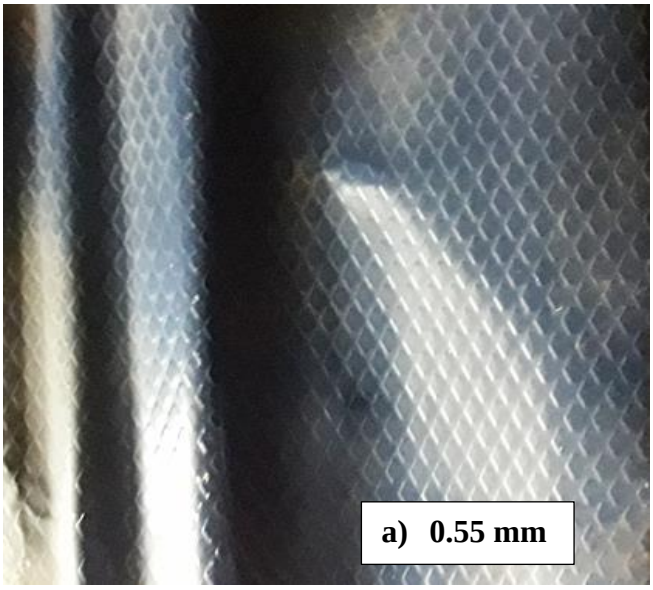

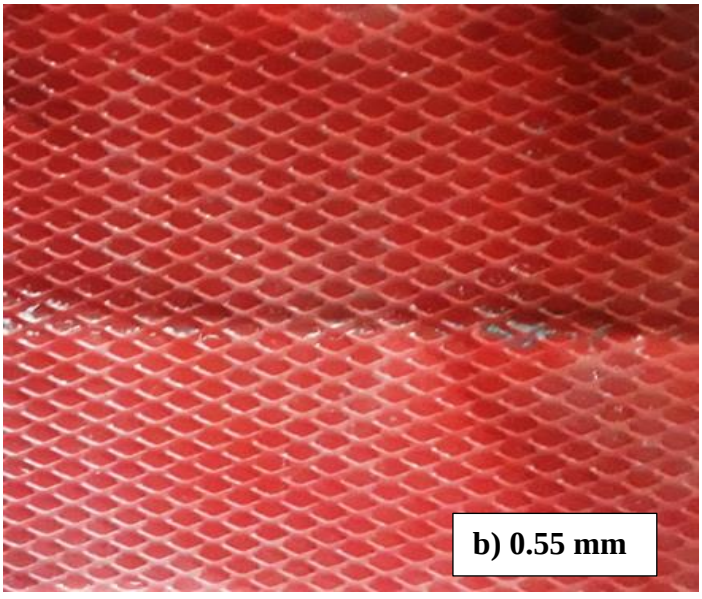

Plate 3.7: Balita step and plain Aluminium roofing sheet

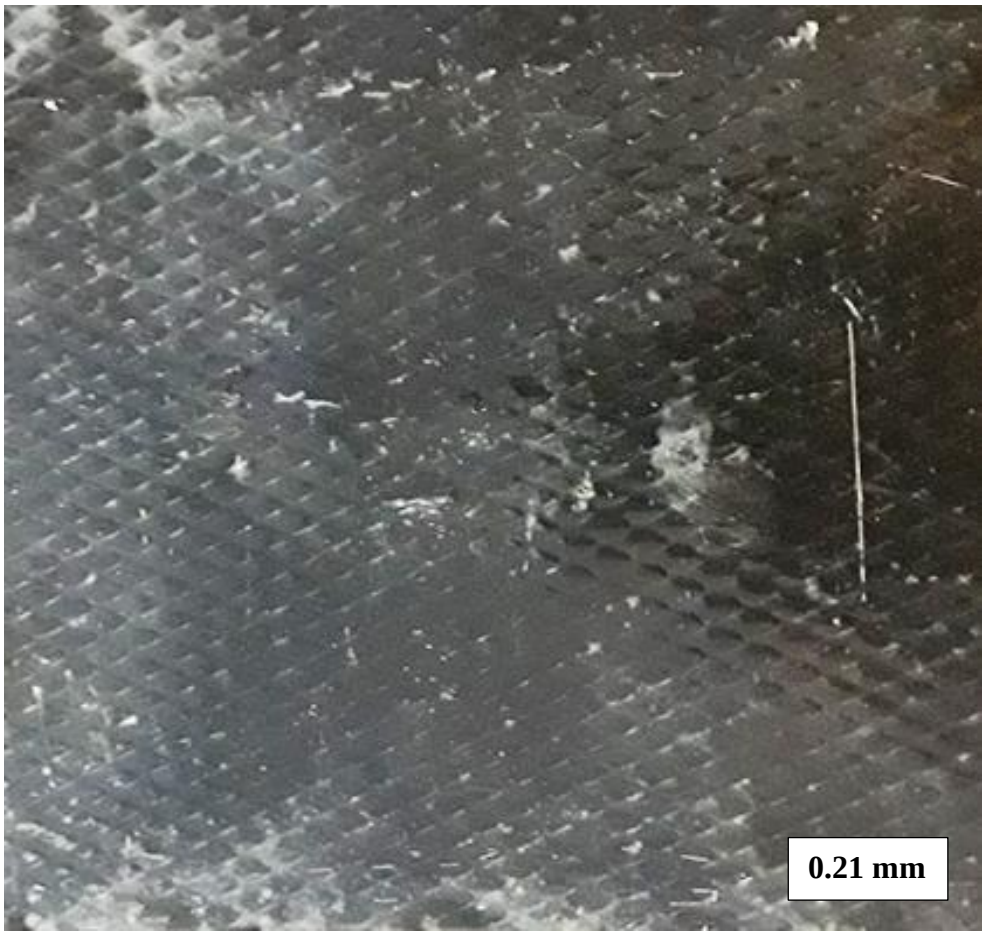

Plate 3.8: Galvanized roofing sheet

Plate 3.9: Sampled polyvinyl chloride ceiling

Plate 3.10: Sampled asbestos ceiling

Plate 3.11: P.O.P sample ceiling materials

Plate 3.12: Sampled gypsum ceiling

3.4 Field test procedure

Forty-five (45) prototype building models were constructed of a factorial combination of three roofing sheet, five (5) ceiling underlays, and three (3) angular configurations of 30, 45 and 60° respectively. The models were positioned north-south orientation. The selected roofing sheets were stone coated roofing sheet (SCS), plywood lined Aluminium roofing sheet and Aluminium roofing sheet. Each selected roofing sheet were configured against all the selected five ceiling samples. The experiment was carried out between January to March 2022, based on this configuration numbers. The daily temperature reading was taken from the ambient temperature, roofing sheet temperature, air space temperature and the ceiling temperature simultaneously. This helped to determined the rate at which heat flow from the outside ambient temperature through the roof air space to the ceiling underneath the roof.

These models were constructed using plywood board material with the building length of 3000 mm (3m), breath and height sizes of 1800 mm (1.8m). The model building has no openings, to minimised heat escape through the windows or doors openings. The Plate 3.13, 3.14, 3.15 represents the model roof configurations set up for plywood lined Aluminium, stone coated roofing sheet, and Aluminium roofs at angles 30, 45, 60 degrees respectively.

Plate 3.13: Experimental set up for plywood-lined Aluminium roofing sheet with selected ceiling materials

Plate 3.14: Experimental set up for stone coated roofing sheet with selected ceiling materials

Plate 3.15: Experimental set up for Aluminium roofing sheet with selected ceiling materials

3.5 Real live field test to validate the roof configurations

The field test was conducted from October to December 2019, March 2020 July 2020, and October 2021 between the hour of 9 am to 10 pm daily. The multi-channel recorder data logger and prime thermometer data logger were used respectively to store the daily temperature.

3.5.1 Field procedure on existing buildings to validate the experiment

The field work was carried on two (2) live simple gable buildings, model 1one was the roof building with stone coated roofing sheet ST-A and P.O.P ceiling (Plate 3.16**).** The model 2 was the roof building with the long span Aluminium roofing sheet and asbestos ceiling as the underlay, as indicated in Plate 3.17. The test was carried out between 8: 45am in the morning till 7pm in the evening. The multi-channel recorder with 4 channels was used to take the temperature reading concurrently. The Appendix 3. and 4. showed the detailed data for the 4-channels. Channel 1 represent the heat temperature at the roofing sheet, channel 2 is the heat temperature within the roof air space, channel 3 gives the heat temperature data on the ceiling and the channel 4 is the ambient air heat temperature.

Similarly, eleven (11) different roofing samples and five (5) different ceiling samples were equally placed outdoor and indoor for a period of six (6) months and the average monthly heat (temperature) absorption were taken and examined, at an interval of 8:30 am, 11:30 am, 2:30 pm, 5:30 pm and 8:30 pm, as indicated in the Plate 3.18 a. and 3.18 b, respectively.

These samples were tested using KD2 thermal Analyzer for both the initial and final temperature, the equipment gave the results for their various thermal conductivity, resistivity, diffusivity, and specific heat capacity of the sample materials respectively.

Plate 3.16: Model 1 (SCS and P.O.P gable roof)

Plate 3.17: Model 2 (ARS and ASB pitched roof)

Plate 3.18a: Experimental outdoor test for selected roofing sheets

Plate 3.18b: Experimental indoor test for selected ceiling materials

3.6 Statistical analysis

The mathematical formula for this work was developed using regression statistical analysis, and it was then verified using the experimental data. ANOVA (Analysis of Variance) was used in the procedure to evaluate and assess the significance of variations between the sample parameters. The threshold for determining statistical significance, 0.05, served as the foundation for the significance test level.

CHAPTER FOUR
RESULTS AND DISCUSSION

4.1 Preamble

This chapter covered the findings of experimental studies on the thermophysical and physical characteristics of selected roofing sheets SRS and selected ceiling materials SCM that were conducted both in the lab and outdoors in accordance with UNE EN and ASTM C518 Standards. Thermal conductivity, thermal resistivity, specific heat capacity, thermal diffusivity, and thermal absorptivity of the sampled specimens were assessed in accordance with the methodology described in chapter three. The four goals of this research were the main topics of debate.

4.2 Preliminary Survey Result

The preliminary finding indicates that there are two categories into which the sampled roofing sheets can be divided: partially insulated roofing sheets and non-insulated roofing sheets. Aluminium sheets with a plywood liner (PLAR) and stone-coated sheets (SCS) are two types of partially insulated roofing sheets. However, all the non-insulated roofing sheets in the sample were made of Aluminium and are known as ARS.

4.3 Thermophysical properties of the partially insulated Selected Sample Materials (SSM)

The results of the mass of the ice after melting are shown in Table 4.1. In comparison to the Stone Coated Sheet SCS tested specimens, which are 16.3 and 16.8 kg, sample C's 9.90 kg (Plywood-Lined Aluminium Roof, PLAR) shows that the mass of the ice that melted was quite small. Which suggested that PLAR has good heat resistance. Evidently, samples A and B (which were stone-coated roofing sheets) exhibit less melted ice in comparison to ARS that are not insulated, because of their capacity to withstand heat infiltration.

The outcome of the melted ice due to the temperature difference R_o was likewise shown in Table 4.2. The findings indicated that on sample C, the ice melted gradually and gently due to PLAR's superior resistance to heat infiltration. This was due to the Aluminium's plywood-lined surface, which improved its resistance to heat influx through surface and displayed semi-insulating capability to the heat flow. According to Joseph, Dirisu, and Odedeji (2021), the choice of insulation and coating will assist reduce excessive heat transfer through the roof, giving composite products a blended and more comfortable thermal behavior than pure materials.

The rate of heat flow was also relatively low in specimens A and B, indicating that stone-coated roofing sheets were an excellent barrier (insulator) to heat inflow. On sample D to J, however, the melting rate accelerated more quickly and steadily. This suggested that aluminum samples, in contrast to plywood-lined aluminum and stone-coated roofing sheets, had low insulating qualities but were good heat conductors. The ice block was apparently able to melt quickly because the aluminum samples transferred heat quickly. The findings of Medina, Kaiser, Lopez, Domizio, and Santian (2021) that materials with poor transmittance due to high thermal conductivity and low specific heat capacity may not be suitable for roofing are supported by the results of this study.

In summary, Table 4.2 showed that sample C had a lagging response to heat inflow because of the insulating effect of plywood coated underneath. As a result, the specimen was better protected against heat transfer from the steam to the ice block. However, the rate of ice melting rose quickly in samples D to J due to their porous character, which causes the specimens to conduct heat more quickly than other sample materials.

Table 4.1: Mass of the ice before and after melted on the SRM

Samples	h(cm)	d_1	d_2	T_a(mins)	M_{wa}	t (mins)	M_w
A	0.178	7.42	7.12	7	16.3	5	31.9
B	0.224	7.92	7.60	7	16.8	5	28.4
C	0.935	7.91	7.73	7	9.90	5	14.0
D	0.052	7.52	7.13	7	22.9	5	74.3
E	0.048	7.33	6.80	7	15.6	5	101.7
F	0.042	7.90	7.63	7	17.5	5	89.4
G	0.053	7.52	7.12	7	16.6	5	88.4
H	0.072	7.84	7.64	7	23.1	5	70.1
I	0.049	7.82	7.52	7	21.1	5	114.1
J	0.029	6.92	6.52	7	12.0	5	97.0

Table 4.2: Rate at which the ice melted due to temperature differential for SRM

Samples	h(cm)	R_a	R	M_{sample}	r	A	R_o
A	0.178	38.81	106.30	2552	3.64	41.52	67.49
B	0.224	40.0	94.67	2272	3.88	47.30	54.67
C	0.935	23.57	46.67	1120	3.91	48.04	23.10
D	0.052	54.53	247.67	5944	3.67	42.20	193.15
E	0.048	37.14	339.00	8136	3.54	39.26	301.86
F	0.042	41.67	298.00	7152	3.89	47.42	256.33
G	0.053	39.52	294.67	7072	3.66	42.09	255.15
H	0.072	55.00	233.67	5608	3.87	47.06	178.67
I	0.049	50.24	380.33	9128	3.84	46.21	330.08
J	0.029	28.5	323.33	7760	3.36	35.47	294.83

4.3.1: Comparison of the thermophysical properties for the Selected Roofing Materials, (SRM)

Table 4.3 displays the findings for the sample materials' Thermal Conductivity (TC), Thermal Resistivity (TR), Specific Heat Capacity (SHC), and Thermal Diffusivity (TD). Although certain roofing sheets share some thermal properties with one another, it was observed that most do not. The outcome showed that when exposed to heat, the SRM's mass (KG) changed by 0.3.

According to Table 4.3, sample C has the maximum thermal conductivity value of k, which indicates that PLAR is a good heat conductor (135.60–150.62 W/mk). As a composite material with strong thermophysical properties, PLAR has a good capacity for storing heat and diffuses less heat into the space as evidenced by its specific capacity of 3.726 x 10-3 j and thermal diffusivity of 1.5070 m2/s. This demonstrates their thermophysical capacity to store heat for a long time and then release the same amount of heat into the surrounding air. The outcome is consistent with the claim made by George, Obianwu, Akpabio, and Obot (2010) that materials with high specific heat capacities have a great potential for storing heat.

The thermophysical characteristics of samples A and B were shown in Table 4.3, with TC values ranging from (83.680 to 97.068 W/mK), SHC values of 3.164 and 8.887 x 10-3, and TD values of 3.095 and 1.390, respectively. The TC values showed that SCS conducted heat slowly due to the texture and property of the material, but the high SHC values implied that they had better heat storage capacity because they are stone coated materials.

Although the SHC of C ranges from 2.839 to 7.309 x 10-3 j and the TD values range from 1.021 to 2.643 m2/s, the non-insulated specimens D to K exhibit comparatively high thermal conductivities (k-values) that range from (76.149 to 123.43 W/mK). The outcome is consistent with the 88 to 251 W/mk ASMI criteria for Aluminium.

The table demonstrates that samples A, B, and C conducted and absorbed more heat away from the surface of the roof to the surroundings. These characteristics aid the materials' ability to stop excessive heat from entering the interior space through the roofing. Additionally, it makes sure that the area(s) beneath such roofs are as comfortable as

possible. Therefore, ST-A, ST-B, and PLAR are superior roofing kinds than Aluminium in tropical regions because to this outstanding quality.

Similar to Table 4.3, it showed that PLAR ST-A and ST-B roofing sheets, which were partially insulated, had TR values that were reasonably low (21.70 mk/w, 19.60 mk/w, and 3.02 mk/w, respectively), suggesting that they had insulating qualities.

Table 4.3: **Comparison of thermal properties of the Selected Roofing Materials (SRM)**

Samples	h(cm)	Density ρ	Conductivity K	Resistivity r	SHC	Diffusivity α
A	0.178	2369	97.068	0.0103	3.164	3.095
B	0.224	1812	83.680	0.0120	8.887	1.390
C	0.936	6412	150.62	0.0066	3.726	1.570
D	0.052	2544	79.496	0.0126	5.847	1.277
E	0.048	2135	123.43	0.0081	5.228	2.643
F	0.042	1887	76.149	0.0131	4.756	2.028
G	0.053	2163.4	107.53	0.0093	7.082	1.680
H	0.072	1542.4	91.630	0.0109	7.309	1.943
I	0.049	1978	117.15	0.0085	6.883	2.057
J	0.029	6657	80.751	0.0124	2.839	1.021

Figure 4.1 demonstrates that among the three partially insulated materials, sample C (PLAR) has the highest density. This demonstrates that PLAR has a greater capacity to absorb and store heat than other sample specimens.

Figure 4.2, on the other hand, revealed that sample C has the maximum thermal conductivity, suggesting that PLAR can conduct heat more quickly. The sample A and B, on the other hand, have low conductivity values when compared to PLAR, indicating that they conducted less heat because of their insulating and surface-texture properties, which let very little heat to pass through their surfaces.

The outcome also demonstrated that PLAR, a composite roofing material made of (CH-A0.7 and PCB), had superb heat resistance properties. To provide a great barrier to heat movement, PLAR combined the insulating and conductivity capabilities of their composite materials. According to (Calderon, 2019), the two roofing materials exhibit the proper qualities for the comfort of the house. This advancement in building design will significantly lessen the amount of heat that enters the inner building space.

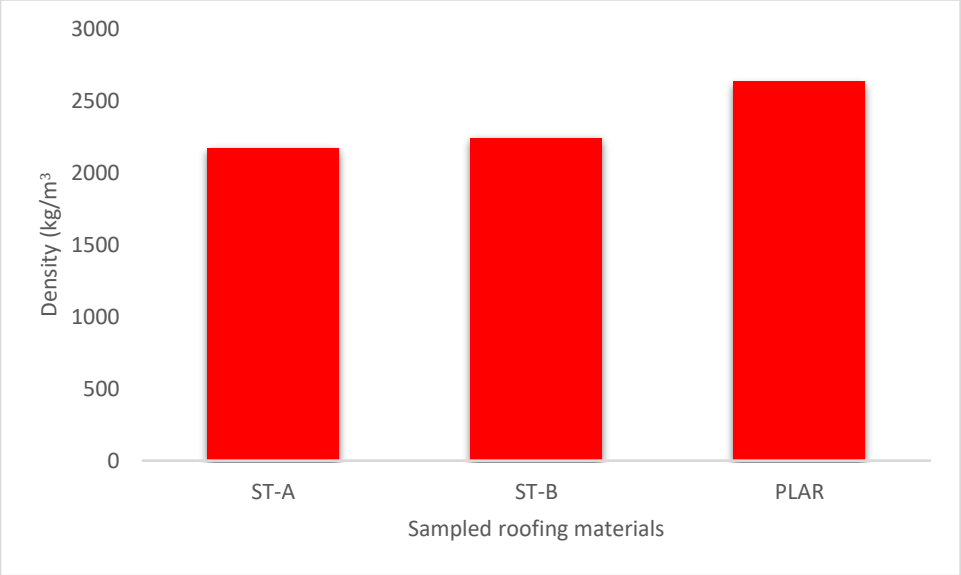

Figure 4.1: Comparison of density for ST-A, ST-B and PLAR

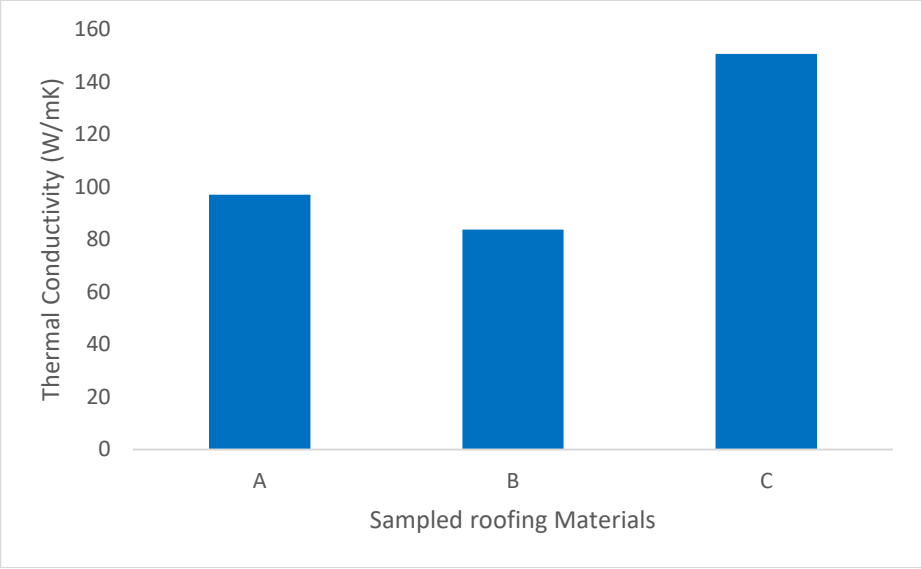

Figure 4.2: Comparison of Thermal Conductivity (TC) for ST-A, ST-B and PLAR

Th The SCS (samples A and B) had a larger TR than sample C, as seen in Figure 4.3. This finding suggests that the material's TR decreases as the TC increases. However, ST-A has the highest TR value of any partially insulated sheet, followed by ST-B. This implies that sample-A (ST-A) tends to resist heat inflow in the form of space temperature, as opposed to ST-B and PLAR. Simply said, the greater the material's TC value, the more heat is reflected and the lower the material's resistivity. As a result, the material's surface radiates heat back into the environment to a greater extent.

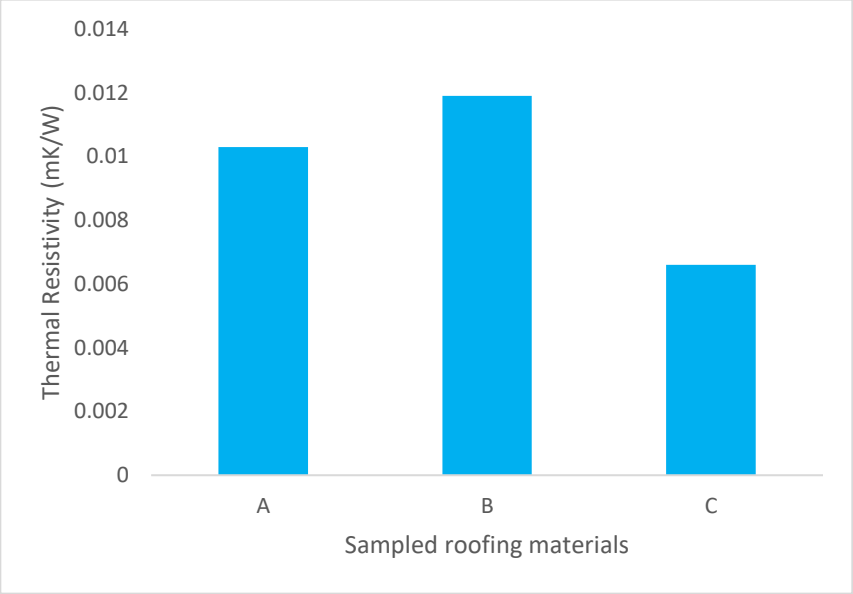

Figure 4.3: Comparison of Thermal Resistivity (TR) for ST-A, ST-B and PLAR

Figure 4.4 illustrates that ST-A, ST-B, and PLAR have the largest specific heat capacities (SHC) and, as a result, have good storage capacities.

The thermal diffusivity for the three partially insulated samples was depicted in Figure 4.5. PLAR diffused heat slowly, whereas ST-A and ST-B did it more quickly. This suggests that the ST-A and ST-B have slightly larger specific heat capacities than the PLAR. The outcome also demonstrates that SCS (ST-A and ST-B) have a greater potential to store heat than PLAR. The outcome is consistent with the findings of Medina, Kaiser, Lopez, Domizio, and Santian (2021), who found that the materials may not be suitable for roofing due to their high thermal conductivity and poor specific heat capacity. This implies that the specific heat capacity of a material decreases with increasing material diffusion rate and vice versa.

The quantity of heat absorbed by the chosen roofing materials (SRM) is depicted similarly in Figure 4.6. The figure showed that SCS had the highest heat absorptivity. In contrast, PLAR also exhibits a potential for good absorptivity.

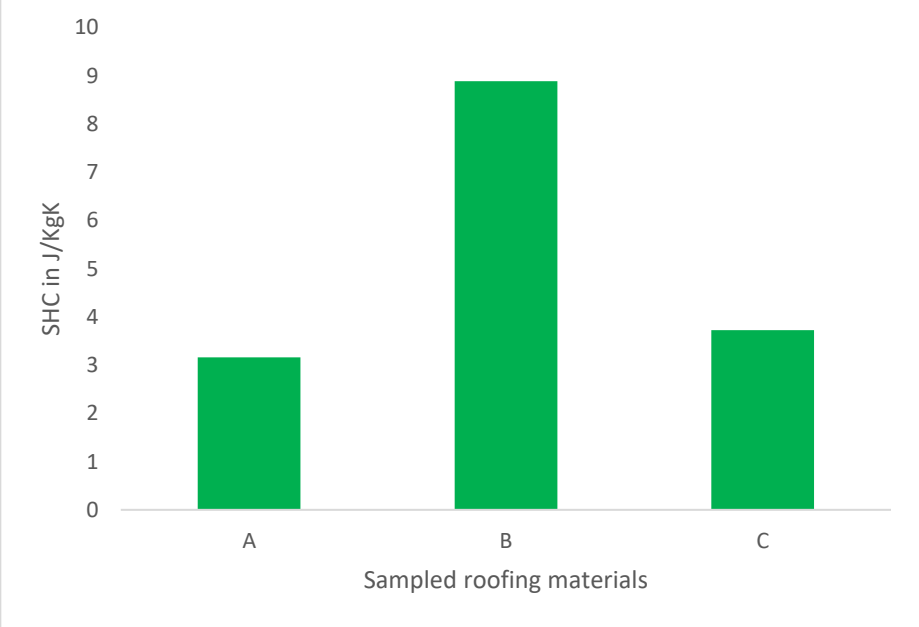

Figure 4.4: Comparison of SHC for ST-A, ST-B and PLAR

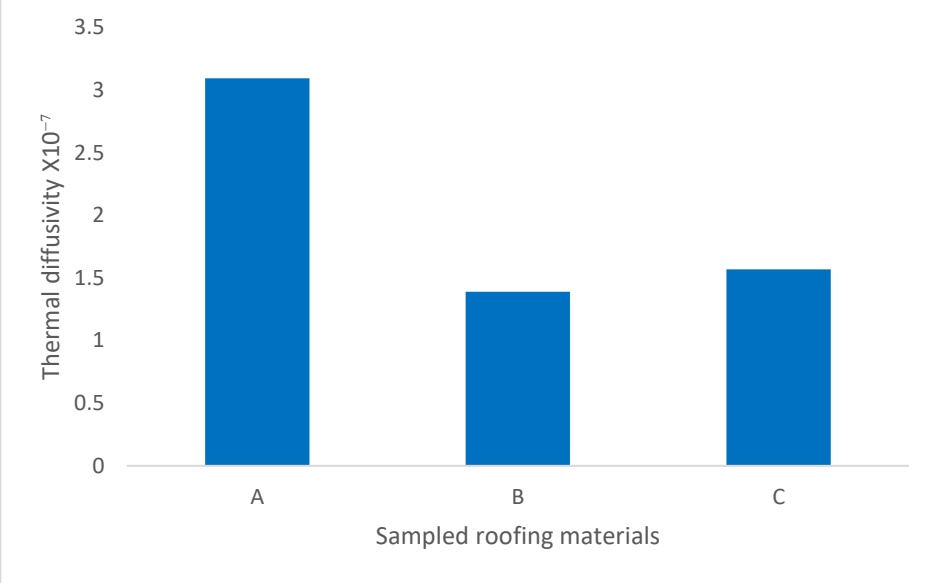

Figure 4.5: Comparison of Thermal Diffusivity (TD) for ST-A, ST-B and PLAR

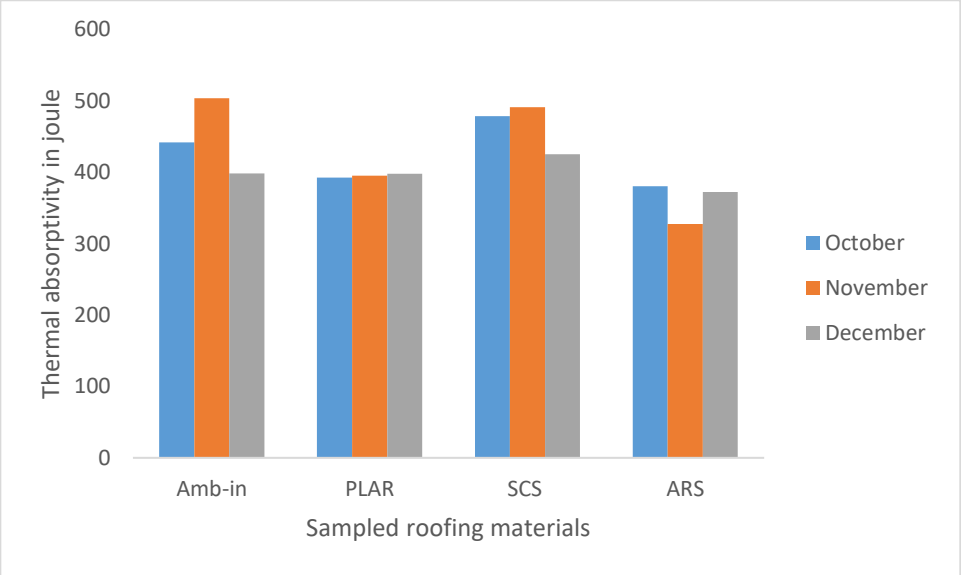

Figure 4.6: Comparison of Thermal Absorptivity (TA) for PLAR, SCS and ARS

Figure 4.7 demonstrates the relatively high density that all the chosen Aluminium roofing sheet (ARS) possessed. This shows that Aluminium may briefly hold heat while simultaneously diffusing and emitting the same amount of heat quickly into the interior region.

The TC for all non-insulated Aluminium materials is shown in Figure 4.8. The results demonstrate the strong heat conductivity of ARS [(CH-A 0.7, 0.55, 0.45), (MT-A 0.7, 0.55, 0.45), (BT-A 0.55st, 0.55), SU-A, and GAL-A]. However, since a material's conductivity and resistivity are inversely related. As a result, the Aluminium with the lowest TC has the highest resistivity rate, which suggests that the more heat an object could resist, the more heat it might conduct. The assumption is that because of their thermo-physical characteristic, which is porous to heat infiltration, ARS were extremely heat-sensitive. The outcome is consistent with the research of Medina, Kaiser, Lopez, Domizio, and Santian (2021), which found that roofing materials with poor transmittance due to high thermal conductivity and low specific heat capacity may not be suitable.

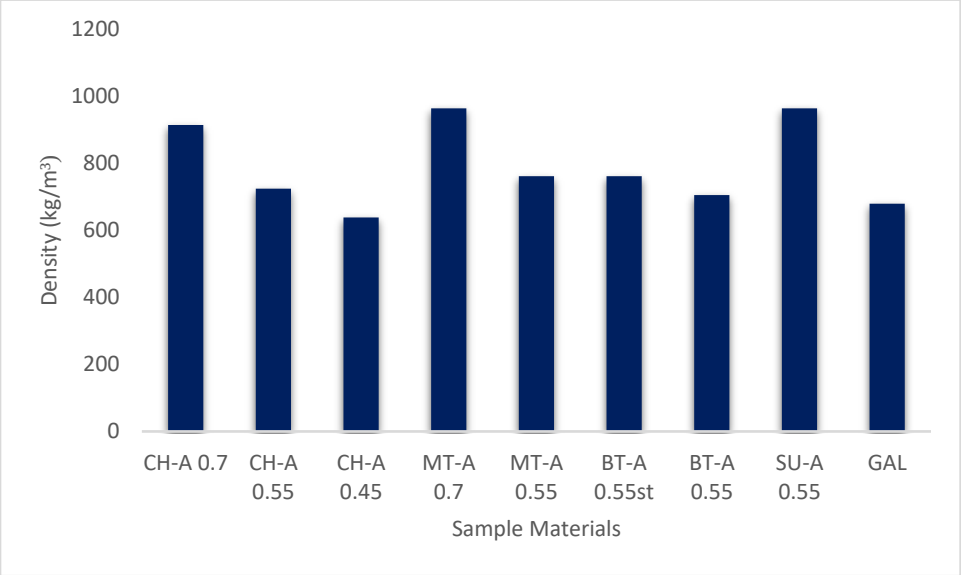

Figure 4.7: Comparison of density for selected Aluminium Roofing Sheets (ARS)

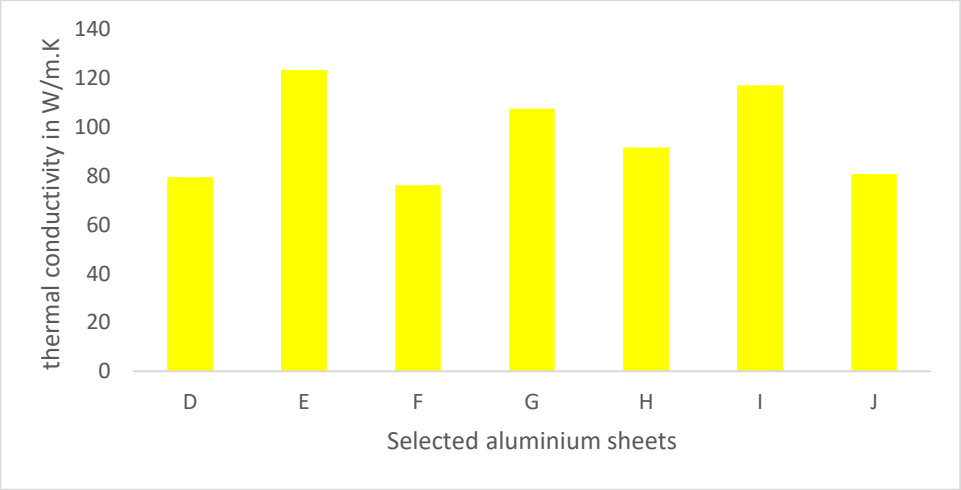

Figure 4.8: Comparison of Thermal Conductivity (TC) for the selected Aluminium roofing sheets

The samples D and G in Figure 4.9 exhibit the highest diffusivity rate among the sampled ARSs. The two specimens imply a decreased storage capacity. Also diffusing heat more quickly than CH-A0.45 and GAL-A were CH-A0.55, MT-A0.55, MT-A0.45, BT-A0.55st, BT-A0.55, and SU-A0.55. The graph demonstrates that all Aluminium roofing sheets typically have extremely limited thermal conductivity (low specific heat capacity), making them incapable of retaining or preserving heat for an extended period. When compared to the amount of heat received, ARS therefore emits and diffuses heat as quickly as it can.

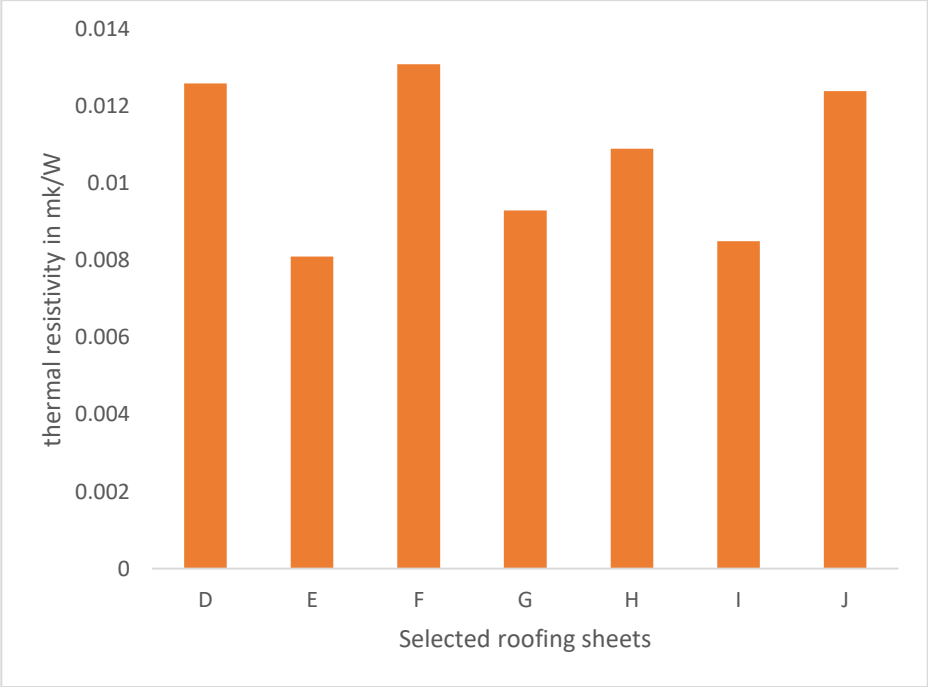

Figure 4.9: Comparison of thermal resistivity for selected Aluminium roofing sheets

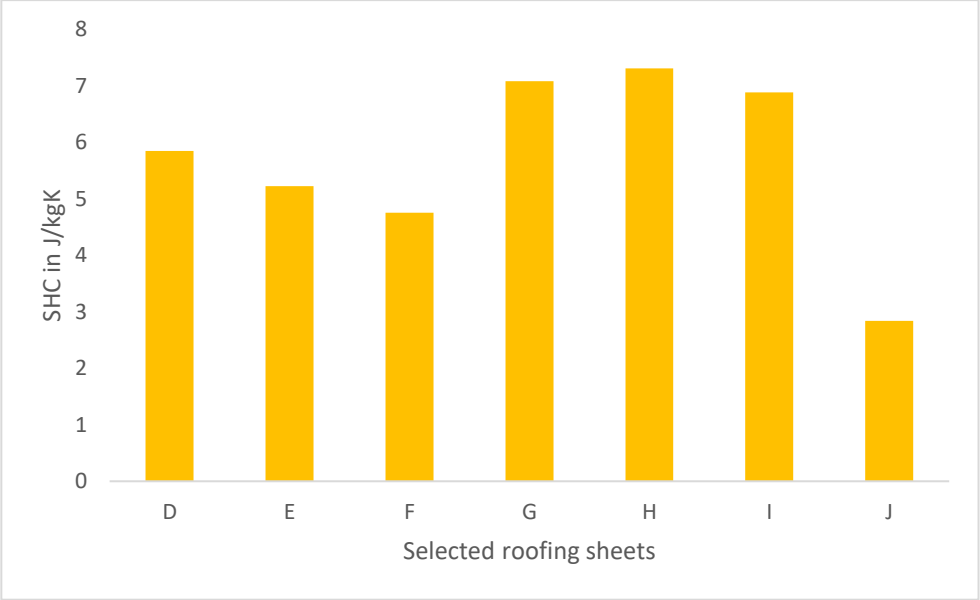

Figure 4.10: Comparison of Specific heat capacity for selected Aluminium roofing sheets

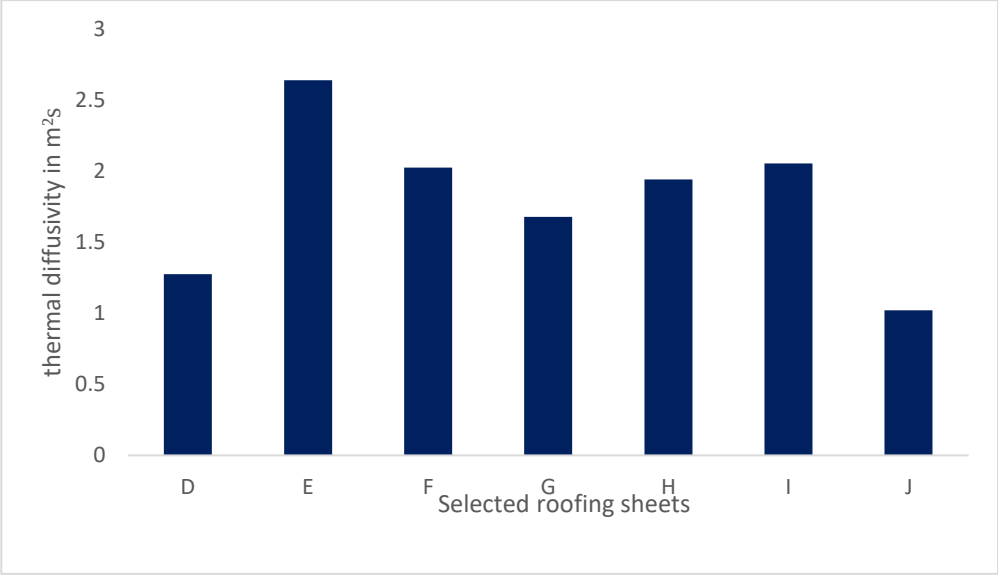

Figure 4.11: Comparison of thermal diffusivity for selected Aluminium roofing sheets

4.3.1.1: Thermophysical properties of the Selected Ceiling Materials (SCM)

Table 4.4's comparative analysis showed that all the sample SCM were effective insulators since their TC values fit within the accepted range of conductivities, which is 0.023 to 2.9 W/mK. This outcome is consistent with research on insulating ceiling materials from Ettah, Egbe, Takim, Akpan, and Oyom (2016) and George, Obianwu, Akpabio, and Oyom (2016).

According to Figures 4.12 and 4.13, PVC has a thermal conductivity of 0.191 W/mK, a thermal resistivity of 5.250 mK/W, and a thermal diffusivity of 3.25 m^2s. P.O.P. has a thermal conductivity value of 0.184 W/mK, thermal resistivity of 5.430 mK/W, and thermal diffusivity of 2.960 m^2/s, while asbestos has a thermal conductivity value of 0.125 W/mK, thermal resistivity of 8.000 mK/W, and thermal diffusivity of 1.345 m^2s. Finally, GYP with the following values for thermal conductivity, resistivity, and diffusivity: 0.228 W/mK, 4.385 mK/W, and 4.539 m^2/s. The outcome demonstrates that ASB offers the best thermal insulation since it has the lowest thermal conductivity and maximum resistivity value, followed by P.O.P, then followed by PVC, and finally GYP, respectively.

Table 4.4: Comparison of thermal properties of Selected Ceiling Materials (SCM)

Sample materials	Density (kg/m^3)	Thermal Conductivity (W/mK)	Thermal Resistivity (mk/w)	Specific heat capacity (J/kgK) x 10^3	Thermal Diffusivity (m/s) x 10^{-7}
PVC	852	0.191	5.240	1.654	1.360
ASB	825	0.125	8.000	2.050	0.399
POP	911	0.184	5.450	1.596	1.266
GYP	784	0.228	4.400	2.070	1.410
PCB	2225	0.283	3.534	2.850	0.456

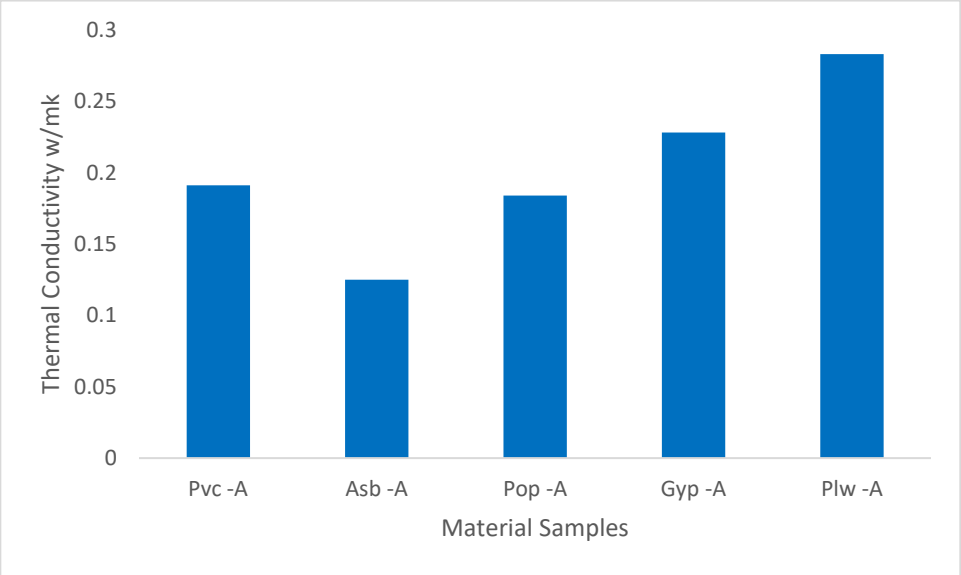

Figure 4.12: Comparison of Thermal Conductivity (TC) for sampled ceiling materials SCM

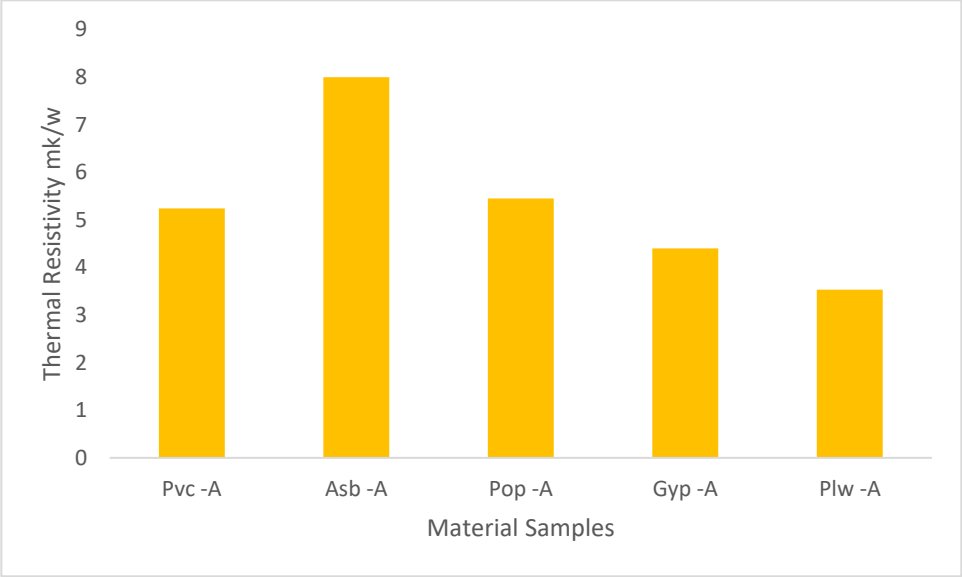

Figure 4.13: Comparison of Thermal Resistivity (TR) for Sampled Ceiling Materials (SCM)

Figure 4.14 demonstrates that PCB has the largest specific heat capacity (2.850 x 10^3 J/kgK) among the specimens studied, indicating that PCB has a higher heat storage capacity than the others. GYP (2.070 x 10^3 J/kgK), ASB (2.050 x 10^3 J/kgK), PVC (1.654 x 10^3 J/kgK), and POP (1.596 x 10^3 J/kgK) were the materials that came next in order. This characteristic demonstrated that PCB is also an excellent insulator material or ceiling material in tropical climates. These results match those of George et al. (2010), who found that PVC (1571.09 ±3.12), Pop (1468.80±6.00), and asbestos (842.90±2.96) all contributed to their findings.

For the chosen ceiling materials, Figure 4.15 displayed the thermophysical diffusivity rate. This finding indicates that PCB (0.456 x 10^{-7} m/s) has a slow rate of heat diffusion through its texture, which implies that PCB holds a very high storage capacity (that is, a very high specific heat capacity) with density ratio. Like ASB (0.399 x 10^{-7}), POP (1.266 x 10^{-7}), PVC (1.360 x 10^{-7}), and GYP (1.410 x10^{-7}) all shown good storage capacity. In line with (George et al 2010, Ettah 2016), this. As a result, the findings also support the notion that a material's particular heat capacity influences its diffusivity rate.

The average monthly thermal absorptivity for the months of October, November, and December was shown in Figure 4.15. The outcome demonstrated that all SCM have high absorptivity values. However, P.O.P. typically has its highest rate of absorption from October to December. However, plywood ceiling boards often have the highest thermal absorptivity, which suggested that PCBs had a considerable amount of storage capacity. The outcome is consistent with the findings of (Calderon, 2019) and (Medina, Kaiser, Lopez, Domizio, and Santian, 2021) that materials with poor transmittance because of their high thermal conductivity and specific heat capacity may not be suitable as ceiling materials when compared to those with thermal absorptivity, such as PCB.

Additionally, the results showed that PCB had the highest specific heat capacity (SHC) among the specimens evaluated, indicating that PCB had superior diffusivity and storage heat capacity to the others. The plywood ceiling board has the highest thermal absorptivity, even though P.O.P.'s absorptivity is constant over a few months. This meant that PCB, having a strong storage capacity, which also put them as an insulating material in the tropics. The outcome is consistent with the findings of Calderon, (2019) and Medina *et al*. (2021), which suggest that materials with poor transmittance because of their high thermal conductivity and specific heat may not be suitable for use as roofing and ceiling materials in comparison to those with thermal absorptivity, such as PCB.

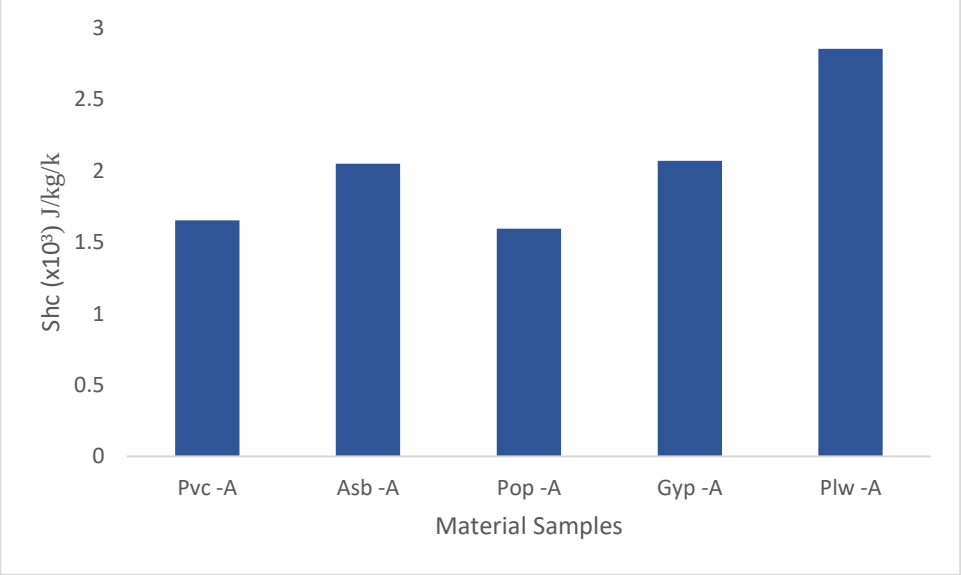

Figure 4.14: Comparison of SHC for Sampled Ceiling Materials (SCM)

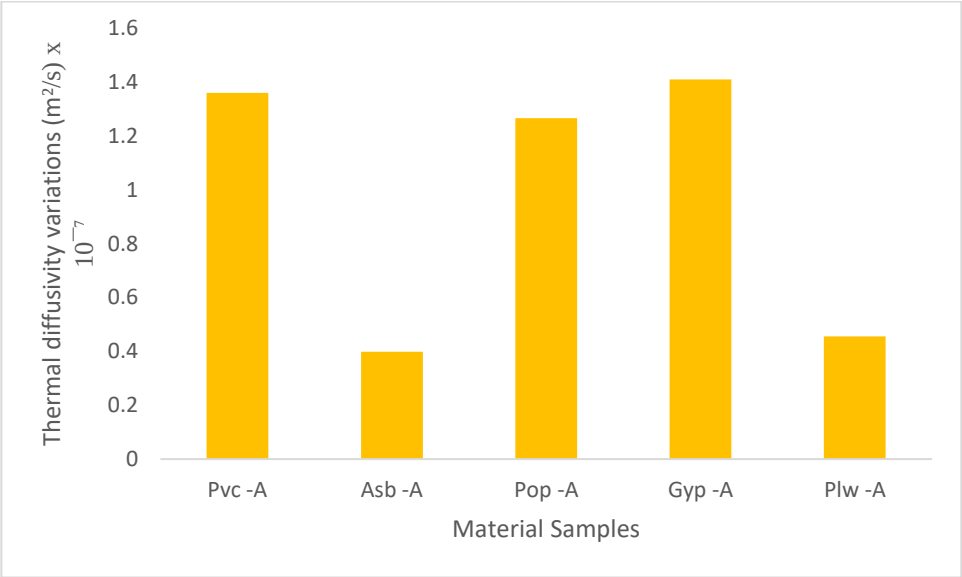

Figure 4.15: Comparison of Thermal Diffusivity (TD) for sampled ceiling SCM

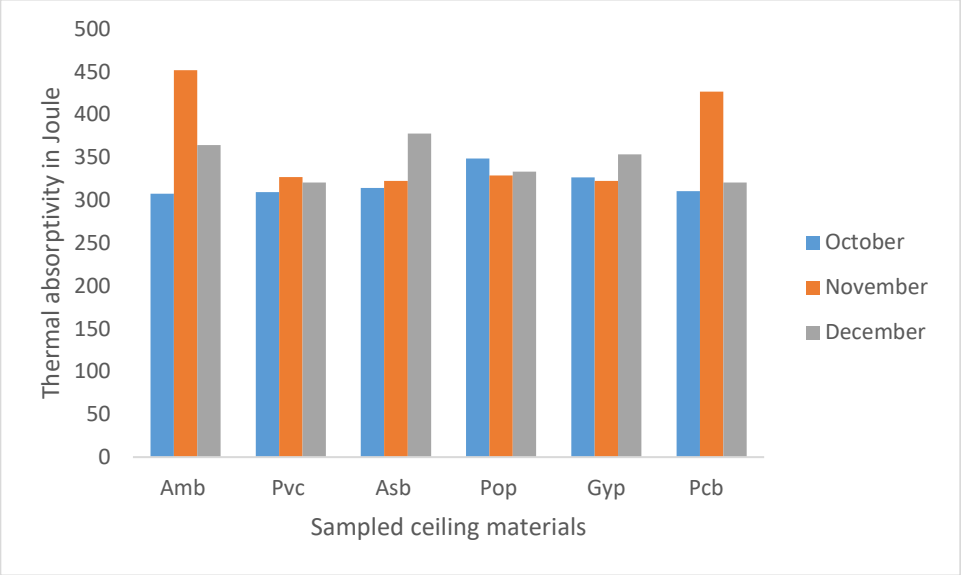

Figure 4.16: Comparison of Thermal Absorptivity (TA) for sampled ceiling SCM

Figure 4.16 shows the Selected Ceiling Materials' (SCM) average temperature absorption from October to December. The outcome demonstrated the great storage capacity of the chosen sample. This demonstrated that the chosen ceiling materials have insulating characteristics.

4.3.2 Comparison of the temperature variations for SRM.

Figures 4.10, 4.11, 4.12, 4.13, 4.14, and 4.15, respectively, depict the sampled roofing sheet's thermophysical behavior under a constant heat source.

According to the ARS, heat is released (emitted) into the space faster and faster the more heat is conducted. The findings also suggested that the thermal emissivity rate (TE) of plywood-lined Aluminium sheet, stone coated Aluminium sheet, and Aluminium roofing materials is high and varies from the brilliant color ARS roof type (E=0.91) to the black color SCS samples (E=0.72). This also supports the idea that materials with high thermal reflectivity typically have low specific heat capacities and low heat storage capacities.

Poor thermal reflectivity materials, such as PLAR and SCS, naturally indicate a possible high heat storage capacity. In conclusion, Figure 4.13 demonstrated the low heat emissivity of PLAR, ST-A, and ST-B. The outcome is consistent with previous studies (Bisam, Marjorie, and Turki, 2017) and the accepted emissivity range of 0.2 to 0.8 (Akbari and Konopacki, 2015).

Figure 4.17 demonstrates that the samples have relatively low rates of emissivity for a partly insulated sheet, it takes between 6 and 9 minutes for the temperature on the SCS to significantly increase. This suggested that SCS was a superior heat insulator and better heat absorber. In contrast to the ARS, which absorbed more heat and expelled it quickly as a good conductor (but poor insulator) to the space, ST-A and ST-B slowly absorbed heat while diffusing it very somewhat.

Comparatively, Figure 4.18 demonstrates that sample-C (PLAR), which emits less heat into the environment than samples-A (ST-A) and sample-B (ST-B), has good heat resistance. It appears that PLAR, which is a composite of both aluminum and plywood, integrated the properties of two materials. PLAR, an excellent heat conductor with outstanding insulating qualities, is the result of the combination of these two features. According to Joseph, Dirisu,

and Odedeji (2021), the choice of insulation and coating will help reduce excessive heat transfer through the roof, which causes thermal discomfort in tropical regions like Nigeria. As a result, the composite products have a blended and more comfortable thermal property than pure material.

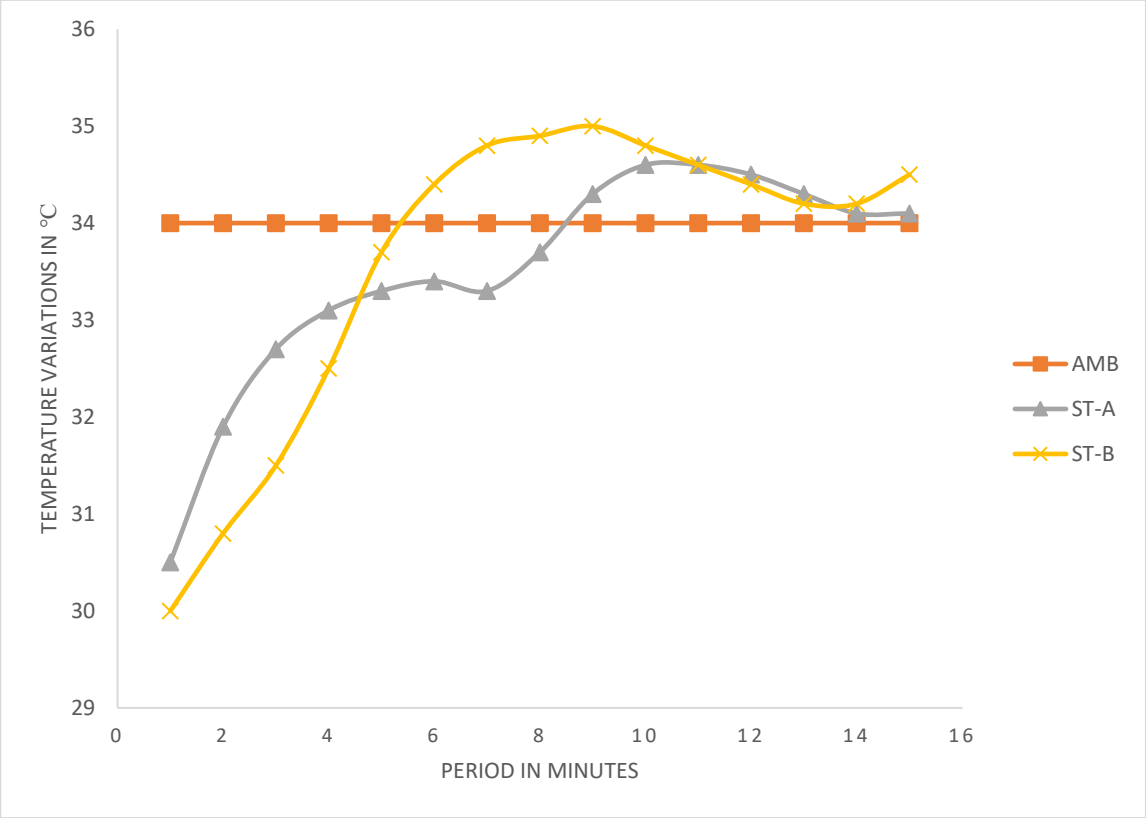

Figure 4.17: Comparison of temperature variations for Thermal Conductivity (TC) between ST-A and ST-B samples

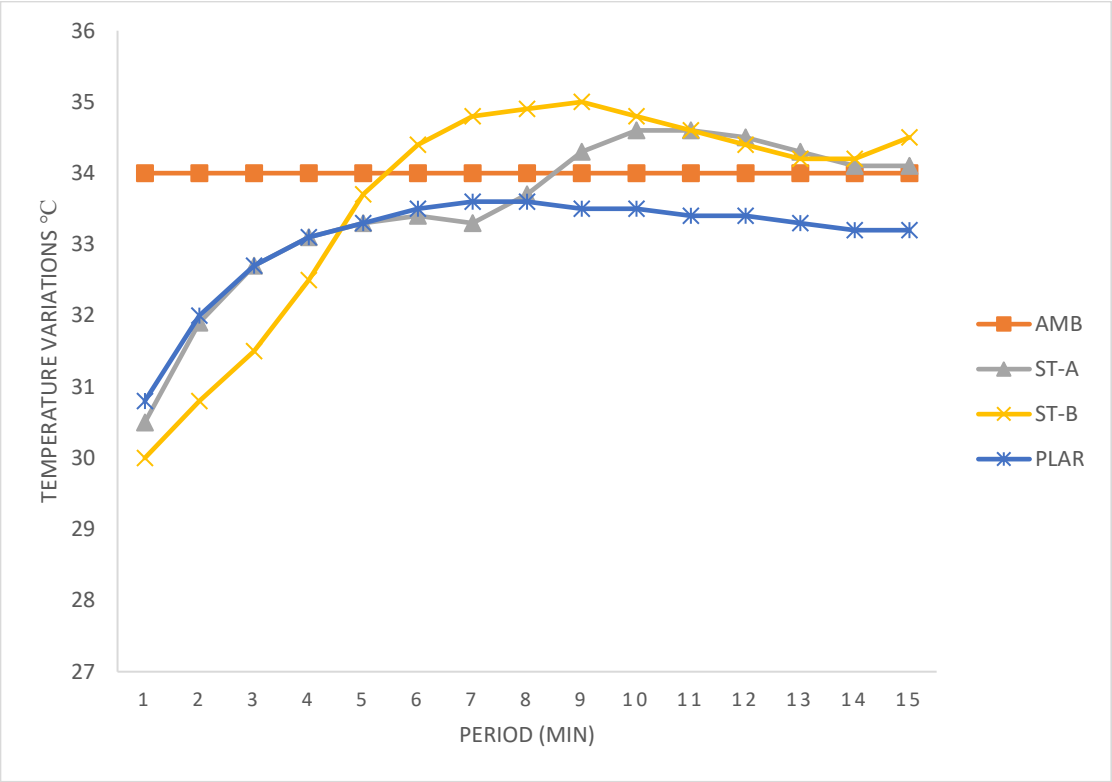

Figure 4.18: Comparison of temperature variations for heat conductivity between PLAR and SCS

Figures 4.19, 4.20, 4.21, and 4.22 show non-insulated ARS samples D to K, which demonstrated a spontaneous and quick increase in temperature with passing time. Since Aluminium samples conducted and dispersed heat more quickly across a wider range of time. The upshot of this was that compared to stone coated roofing sheet (SRS) and PLAR, Aluminium Roofing Sheet (ARS) transmitted and emitted heat more quickly.

Additionally, Aluminium roofing sheets are said to be excellent heat conductors, thus because of their low density to weight ratio and thickness, they diffused heat efficiently and quickly. The truth of this for our constructed environment is that the materials' ability to transfer heat increases with solar radiation intensity.

As a result, materials like Aluminium roofing sheets, ARS sheets, or those with similar qualities tend to heat up quickly, making interior building space less comfortable or unlivable.

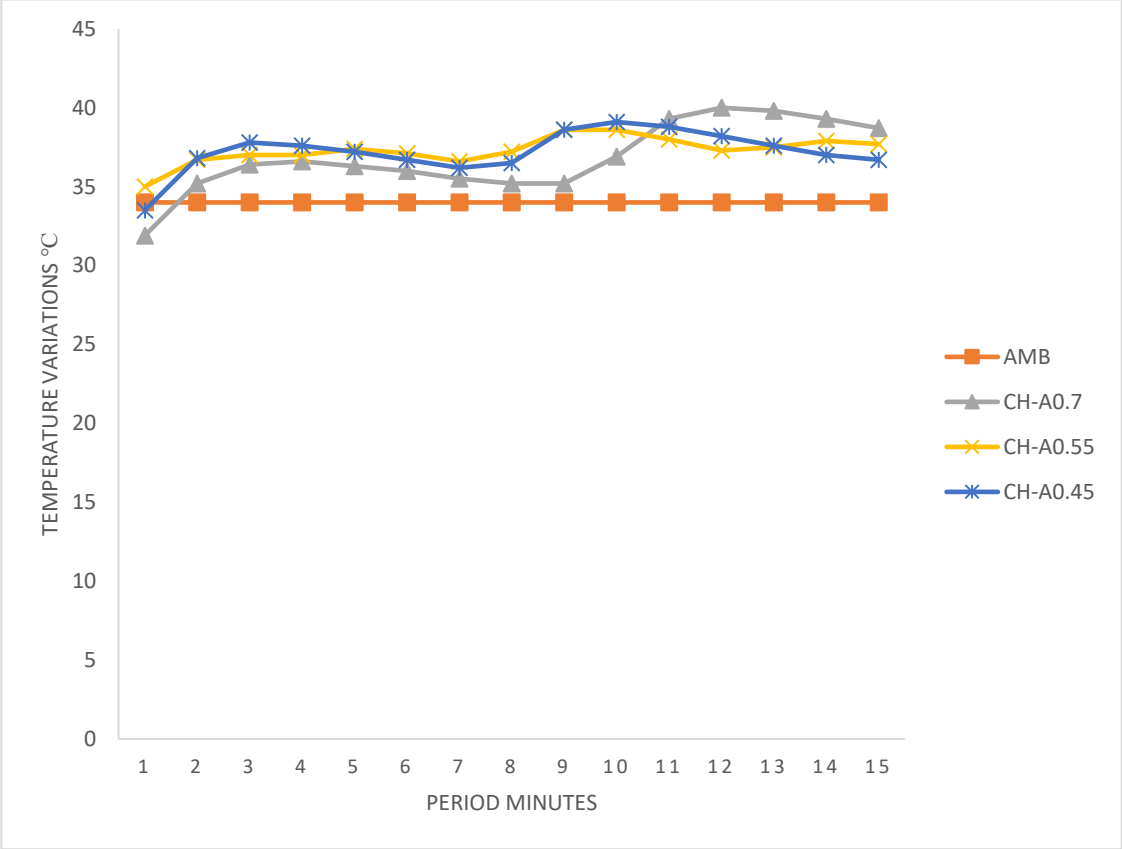

Figure 4.19: Comparison of temperature variations for thermal conductivity between (ARS) chilatech roofing sheets

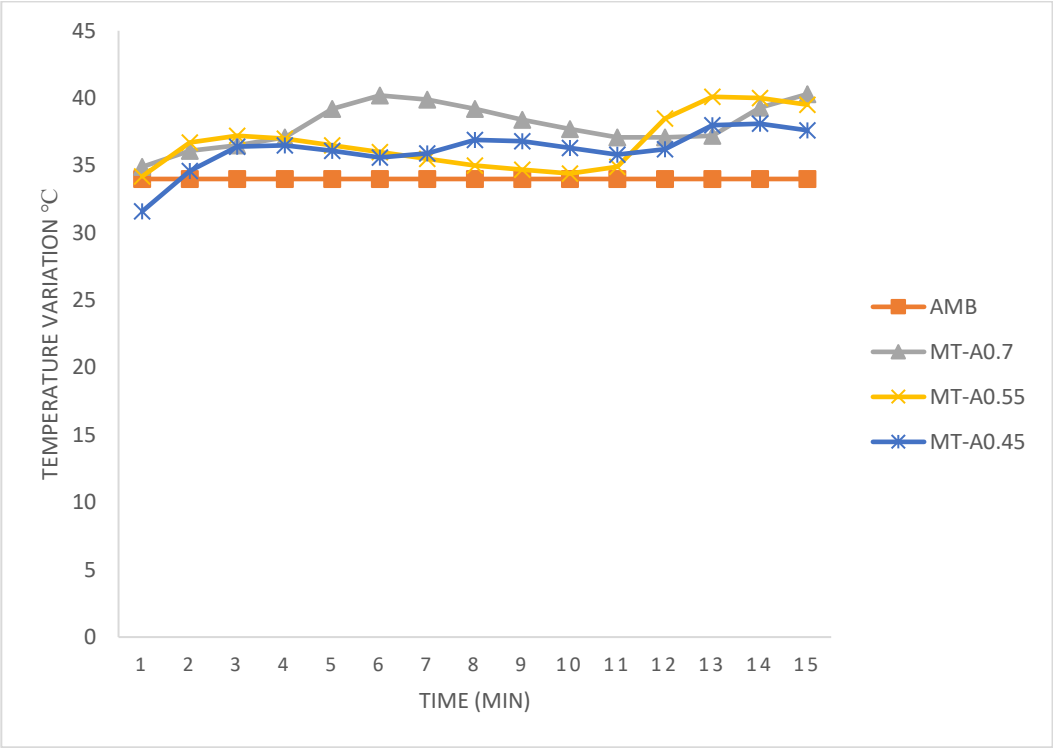

Figure 4.20: Comparison of temperature variations for Thermal Conductivity (TC) between machtech roofing sheets

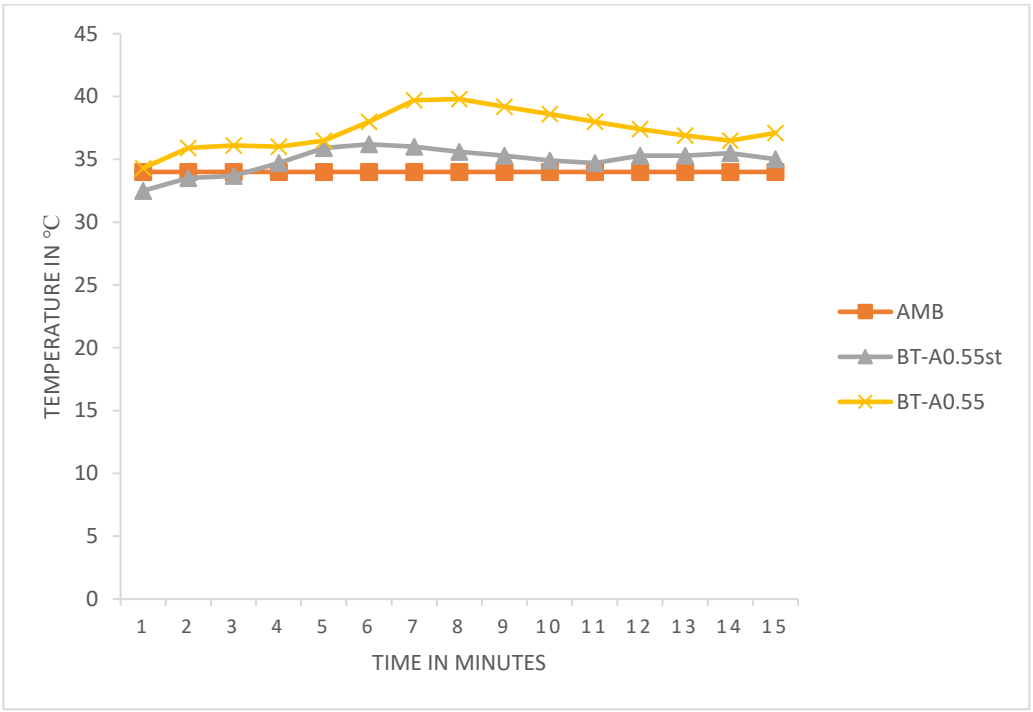

Figure 4.21: Comparison of temperature variations for Thermal Conductivity (TC) between balita roofing sheets

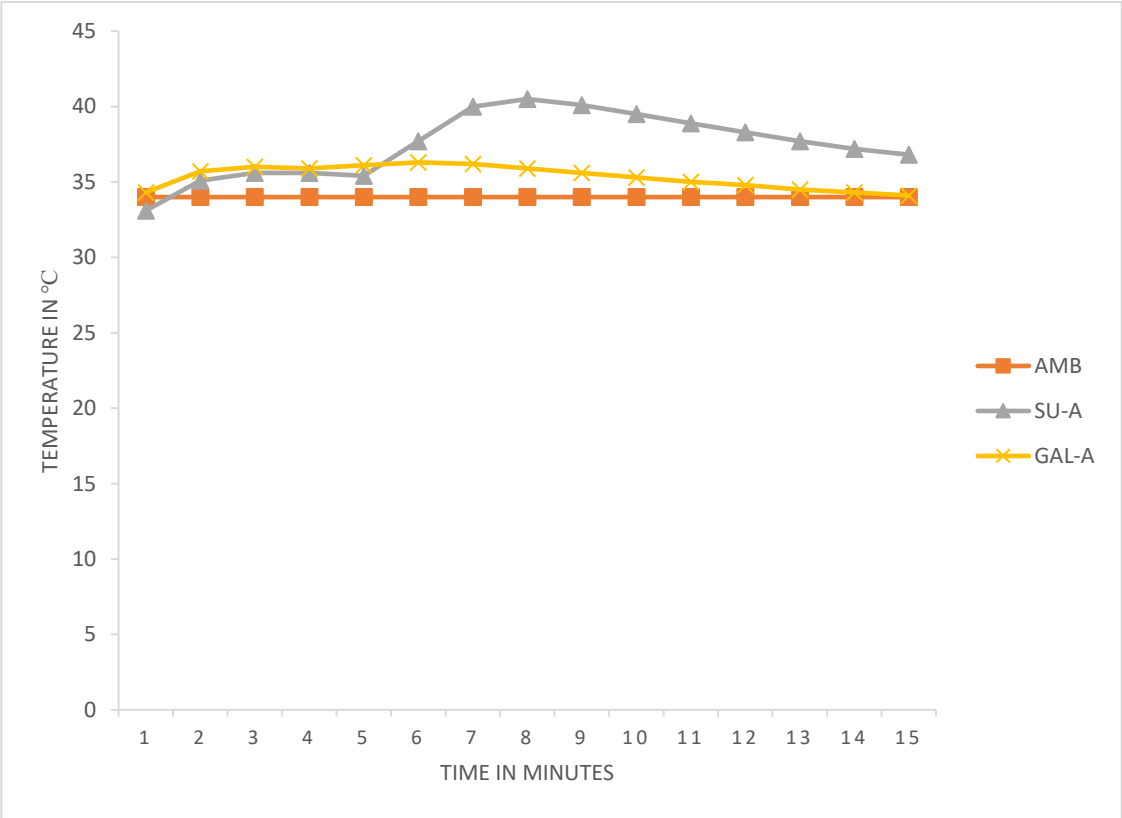

Figure 4.22: Comparison of temperature variations for Thermal Conductivity (TC) between SU-A and GAL-A roofing sheets

4.3.2.1 Comparison of the temperature variations for ceiling

Figure 4.23 showed how the sampled ceiling materials varied in temperature. From 11:30 pm to roughly 3:30 pm, known as the peak hour of the day, there was a temperature imbalance in the building, and the results reveal an increased trend in temperature during that time. But around 5:30 pm, there was a sudden drop in temperature brought on by a reduction in solar radiation, which also caused the temperature of the sample materials to drop.

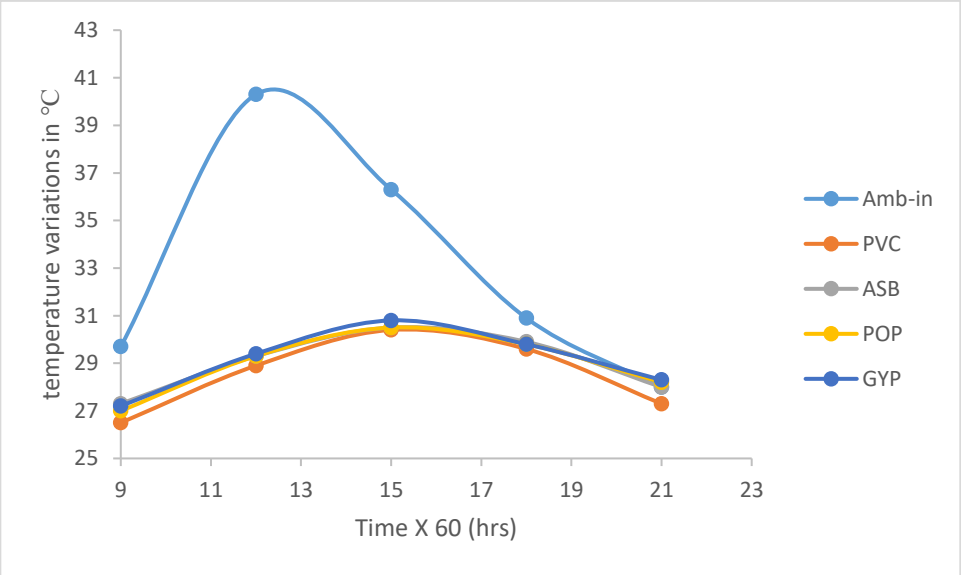

Figure 4.23: Comparison of temperature variations for sampled ceiling SCM

Table 4.5: Temperature variations for the selected ceiling materials

(Regulated temperature = 34°C)

TIME	TEMPERATURE VARIATIONS IN °C			
X 60 SEC	PVC-A	ASB-A	POP-A	GYP-A
1	30.8	33.5	30.2	30.6
2	32.1	33.9	30.4	31.8
3	32.8	34	30.6	32.6
4	32.9	33.9	30.9	33.0
5	33.1	33.8	31.3	33.3
6	33.0	33.9	31.5	33.6
7	37.4	34	31.7	33.9
8	38.3	34	31.9	34.3
9	38.4	34.1	32	34.5
10	38	34.7	32.1	34.8
11	37.5	34.8	32.4	35
12	36.9	34.9	32.6	35.1
13	36.3	34.8	32.8	35.1
14	35.8	34.5	32.9	35.5
15	35.3	34.4	33	36.1

Table 4.5 and Figure 4.24 showed the thermo-physical responses of the sampled ceilings under controlled and constant heat conditions of 34°C. The outcome demonstrates that P.O.P. (Figure 4.24) considerably absorbed and diffused heat with increasing time. When compared to the amount of heat (temperature) received, the amount of heat that was released was comparatively modest. The P.O.P material's particle bond looks to be extremely dense and structurally welded together, which was the cause. This aids the component particles' ability to function as insulating particles. Onyeaju, Osarolube, Chukwuocha, Ekuma, and Omasheye (2012) and Newton, Roy, and Solomon (2014) both support this.

Like P.O.P, gypsum GYP (Figure 4.24) exhibits similar thermophysical characteristics but with a distinct rate of heat absorption. After six minutes of constant heat application, gypsum began to respond to heat gradually. After ten minutes, when the temperature had risen slightly over the set temperature of 34°C, this response became more prominent.

Figure 4.24 shows how the temperature of asbestos ASB changed both gradually and quickly as time went on. The line of 34°C regulation was parallel to the asbestos' heat conductivity and diffusion properties. Because of its dense particle composition, which makes it a good heat insulator (barrier), it was indicated that ASB has a significant ability to store heat.

The figure 4.24 also demonstrated how Polyvinyl Chloride experienced an exponential rise in temperature because of a constant heat source over time. due to its thermoplastic properties, which rapidly conduct heat by expanding when exposed to extreme heat. The double-layered, waffle-like structure of PVC, on the other hand, allows heat to pass through (via conduction and convection) along the vertical and horizontal axes before entering the space, making it an effective insulator.

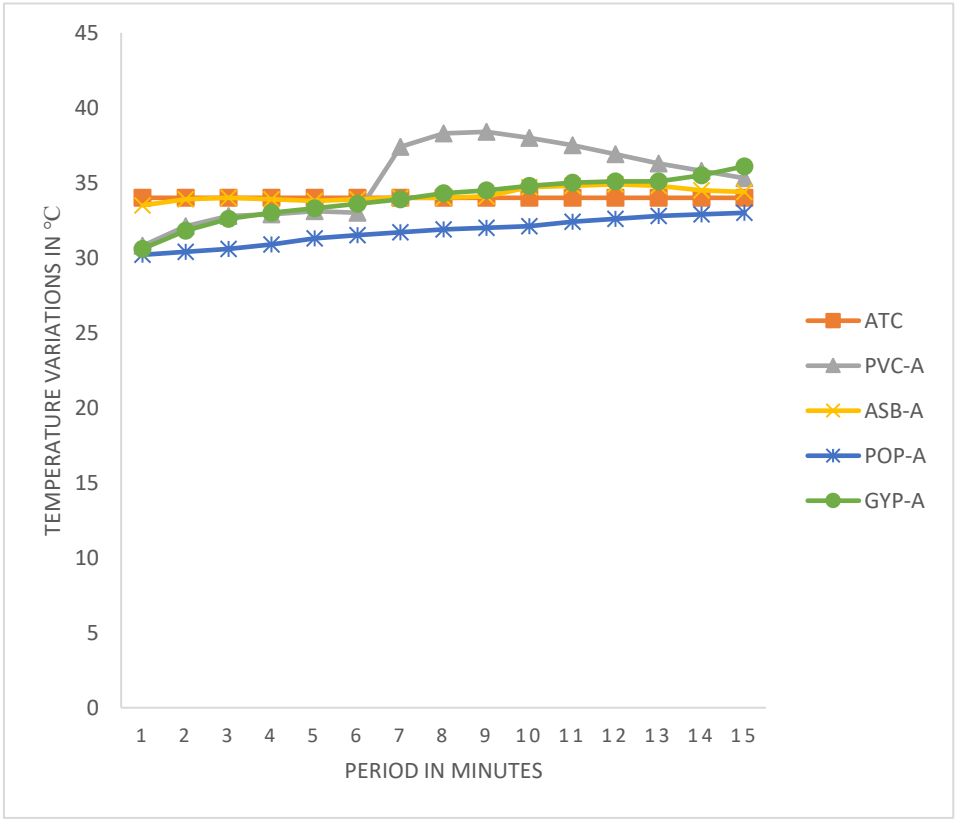

Figure 4.24: comparison of temperature variations of thermal conductivity for Selected Ceiling Materials (SCM)

4.3: Field roof configuration results

This shows the investigation of the angles of inclination of combination of SRM, SCM and ambient at angle 30, 45 and 60°.

4.4: Other predictive model for optimum comfortability roof configurations

Figures 4.25 and 4.26 show, for models 1 and 2, the relative amounts of heat (temperature) input. The findings demonstrated that the temperature at the ceiling was consistently low throughout the day and within a comfortable range of 22–28°C. This suggested that the Gerrard roof's stone-coated roofing sheet SCR (Gerrard roof) served as a good barrier (protector) against the heat influx that occurred as solar radiation from the sun entered the roof's air space hourly. The increase in SCR temperature between 11:30 and 3:00 PM was brought on by this, which absorbed and stored a larger part of the heat that was reaching its surface. proving that the SCR had a larger specific heat capacity, which protected the interior space from an excessive heat inflow.

Due to its high heat conduction, the aluminum roofing sheet, or ARS, as shown in Figure 4.26, creates an excessive influx of heat into the roof's air space. As a result, a lot of heat was allowed to radiate from the ceiling surface, which made the interior's ambient temperature uncomfortable. Due to its insufficient ability to store heat (low specific heat capacity) and high emissivity rate, the ARS also transmitted and expelled more heat into the interior area. As a result, between the early morning at 9:00 am and the late afternoon at 5:30 pm, the temperature at the asbestos ceiling rose quickly.

In contrast to the P.O.P ceiling in model 1, the ASB in model 2 heated up quickly and quickly in the morning, creating a temperature imbalance in the building's interior space that made it less conducive during the daily hour between 10am and 4pm in the tropics, particularly during the height of summer.

In contrast to model 2 in Figure F2, however, model 1 in Figure F1 appears to have a relative heat balance in the air space (space between the roof and ceiling) temperature because of the characteristic of the stone coated roofing sheet SCR. This occurred because of the aluminum roofing sheet's ARS's rate of heat output being equal to the solar heat absorbed.

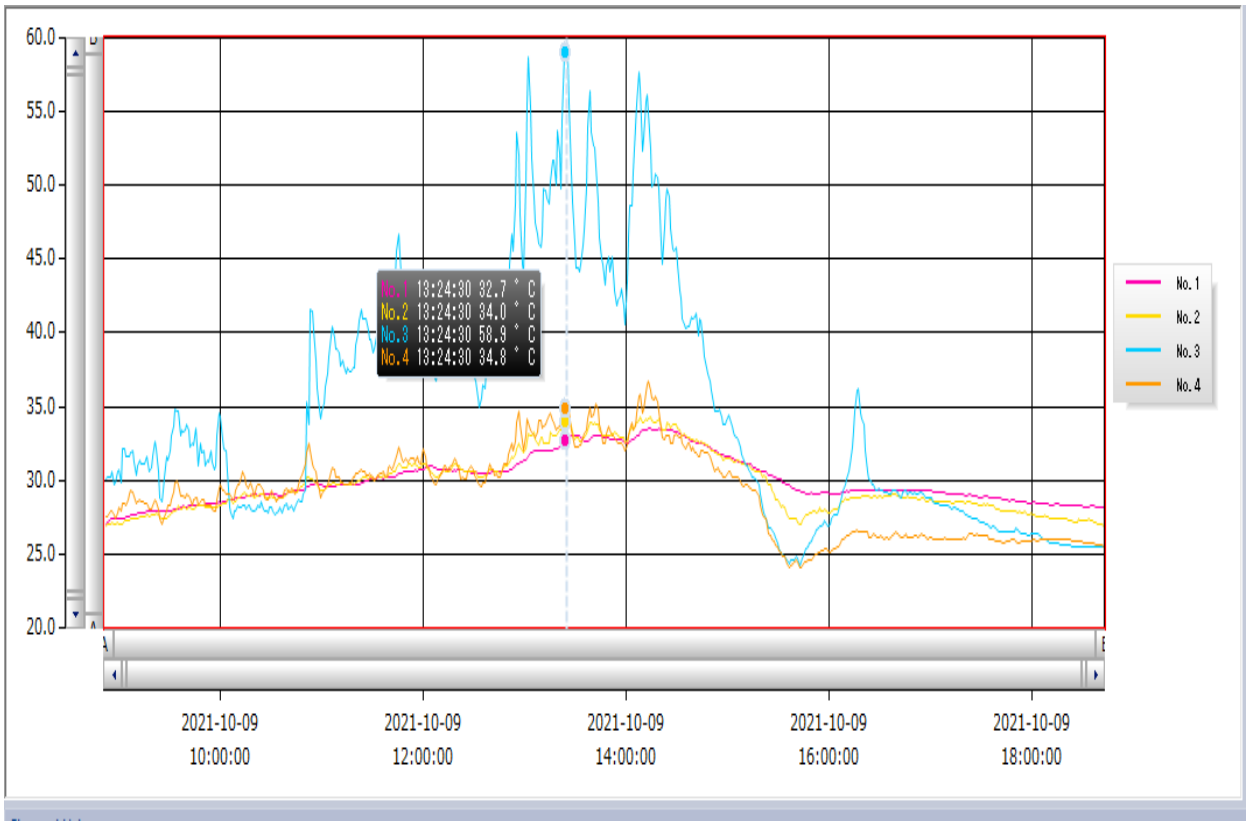

Figure 4.25 Heat influx graph from outside SCS to the inside POP ceiling

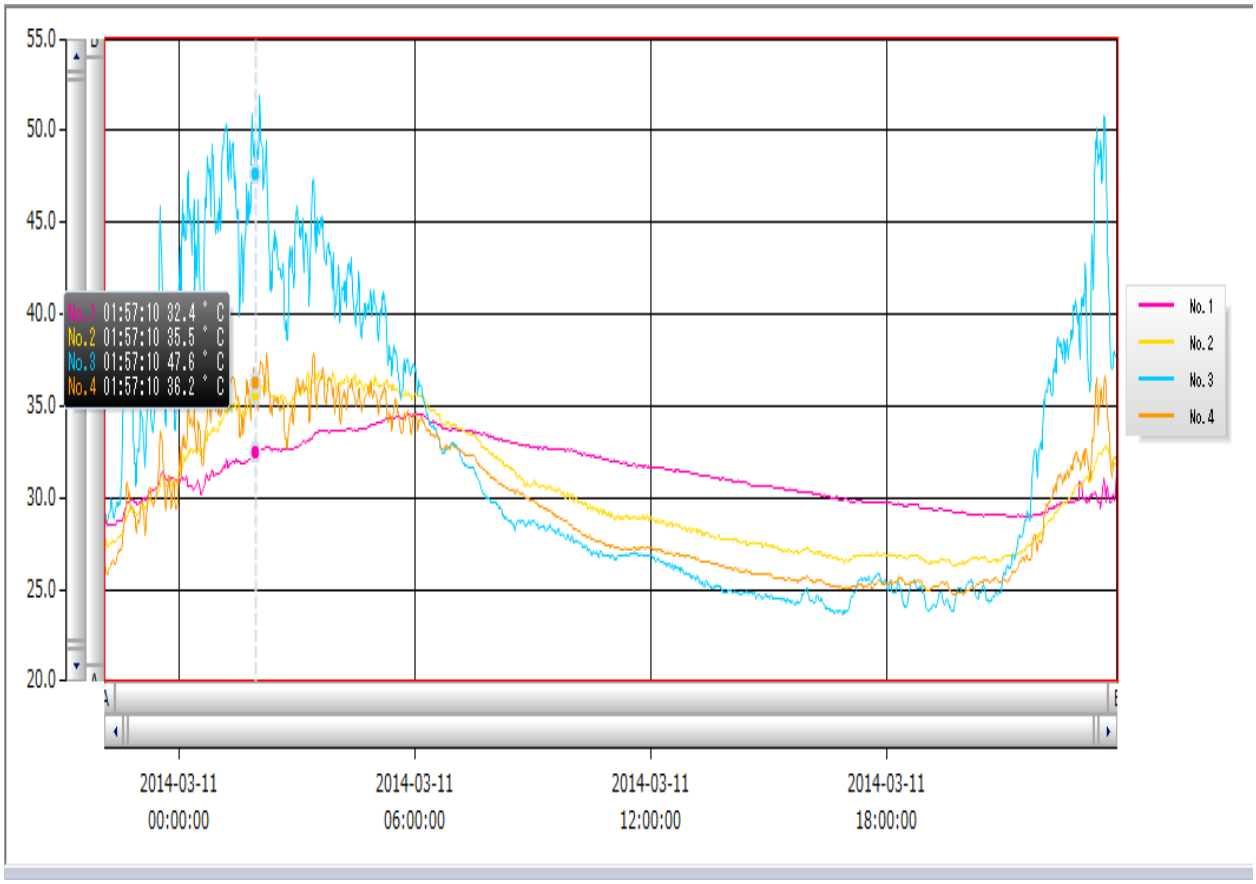

Figure 4.26 Heat influx graph in model 2 from outside ARS to the internal asbestos ceiling

The comparison was made to verify the rate of heat input through Aluminium and stone-coated roofing sheets. According to the findings, stone-coated Aluminium sheet has a lower albedo than Aluminium sheet with a higher albedo (Akbari et al. 2015).

Figure 4.25 displayed a real-time temperature reading for the SCS and P.O.P ceiling roof arrangement of the model building. The findings indicated that the temperature of SCS increased as the ambient temperature rose starting at 11 a.m., as the material absorbed more heat. This reached a crucial point between 12 and 3 PM, when the sun's rays were directed vertically at the surface of the planet. The outcome is consistent with the conclusions made by (Egbinola and Amobichukwu, 2013).

The heat gain during the early morning hours of 9am in this documentation demonstrated that model 2 rapidly gained more heat just as the sun was rising and diffused the same into the interior space, causing the roof air space temperature to rise as the outside ambient air temperature increases and subsequently forcing the trapped heat to radiate the adjacent underlay ceiling leading to an internal temperature imbalance.

The stone coated roofing sheet has a low rate of heat diffusion since the material is a poor conductor of heat, in contrast to model 1, where the roof absorbed the heat and slowly but gently dispersed it into the interior space. This building suggests that it is a superior roofing sheet for this tropical area.

The results of temperature fluctuations in model 1 are likewise depicted in Figure 4.25. Due to the moderate outside temperature recorded by SCS early in the morning, POP's interior space temperature was also reasonable. This occurred because of the very similar air temperatures coming from the roof's external air space (Tamb) and interior air space (Tas).

As a result, the SCS sampled absorbed and established a stable, balanced temperature on the roofing sheet at the place where the heat was intercepted on the roof, which helped to normalise the internal temperature. This was in agreement with the definition, which stated that when the air temperature outside and the air temperature inside are at equilibrium, a person is considered to be at comfort. (Fanger, 2004). The SCS material stabilised the heat by absorbing and diffusing comparatively little air influx into the interior space, which

resulted in a slight increase in temperature on the POP ceiling Tpop, but only between 10:30am and 2:00pm, when the external ambient temperature was steadily higher (solar radiation peak hour) than the air space temperature.

Approximately 25% to 35% of the air temperature absorbed by the chosen stone coated roofing sheet reached the inside space, with a maximum absorption of 65% to 70%. This supports the claim made by Thirumaran and Mathew (2017) that the roofing materials covering the roof are to blame for 60 to 75 percent of internal temperature fluctuations. Between 6:30 and 7:00 pm, when the air temperature had dropped as low as 26°C, which falls within the maximum comfort range of 22 to 28°C, for the tropical region of Ibadan, this mechanism helps SCS roof configuration to enjoy relative all-day thermal comfort.

Figure 4.26 demonstrates that the roof air space AS temperature was high in the morning and that as the air ambient temperature decreased, a high temperature on the Aluminium roofing sheet (ARS) resulted from heat flowing from a medium of high concentration to a medium of low concentration. At 10 a.m., the temperature on the asbestos ceiling reached 47.3°C, while it was 28.9°C on the P.O.P ceiling at the same time. Because Aluminium is typically an excellent conductor of heat but a poor insulator of heat, the heat influx progressively increased as the ambient temperature outside increased (Ariyadara, Muthurathne, and Adikary, 2015).

Heat is discharged into the interior space in direct proportion to how much heat is absorbed. This pattern persisted until 5:00 p.m. and 6:00 p.m., when the sun was almost setting and the ambient air temperature started to drop from 33.1 °F and 30.9 °F to 31 °F and 27.4 °F, respectively.

The area under this roof currently experiences brief thermal comfort until the air temperature is heated up once more. The outcome also showed that the air space temperature and ceiling temperature increased in direct proportion to the outside ambient temperature. Like this, when employed under the same roof conditions, every sampled Aluminium roofing sheet with the same thermal qualities permits heat input. Because the temperature of the ceiling is directly related to the temperature of the interior ambient air space, it is

recommended to always have an insulator laying just above the roof trusses to act as an intermediary or buffer (barrier) to the direct radiation of heat from reaching the ceiling surface.

4.5: Statistical analysis of temperature dynamics between PLAR and SCM

Table 4.6 shows that temperature was generally higher at PLAR compared to the air space AS, SCM and ambient AMB. Also, temperature deviated from the average for PLAR compared to others.

Table 4.6: Summary of temperature for different configurations

	Number of Iterations	Temperature (^{0}C)			
		Minimum	Maximum	Mean	Std. Deviation
SRM	405	22.5	55.2	38.511	8.1377
AS	405	24.2	44.8	34.673	4.8317
SCM	405	24.9	43.4	34.641	4.6392
AMB	405	23.1	42.1	33.830	4.4412
Valid N (listwise)	405				

Table 4.7 summarise the different temperatures on the SRM in comparison to the air space, SCM and ambient, based on different angles of roof configurations. The table shows that the average temperature was highest in Roofing Material, Air space and Ceiling Material for roofing configuration with angle 30^0 in comparison to angles 45^0 and 60^0. Although, it was reported by (Alcivar M, Ramos J, and Velez D, 2022) that the best thermal behaviour inside the house is from the pitched roof orienting towards the west with inclination angles of 20°. However, the present study shows that the best optimum angle of inclination ranges from 30 to 60°.

Table 4.7: Summary of temperature for different angles irrespective of combinations

Angle		Number of Iterations	Temperature (^{0}C) Minimum	Maximum	Mean	Std. Deviation
30 Degrees	SRM	135	27.7	54.1	39.660	8.0752
	AS	135	27.4	44.8	35.866	4.8100
	SCM	135	25.4	43.4	35.468	4.5208
	AMB	135	27.3	41.4	34.416	4.0948
	Valid N (listwise)	135				
45 Degrees	SRM	135	23.6	54.5	36.836	7.8337
	AS	135	24.9	41.8	33.412	4.6178
	SCM	135	24.9	42.0	33.571	4.4721
	AMB	135	25.0	41.2	32.932	4.3531
	Valid N (listwise)	135				
60 Degrees	SRM	135	22.5	55.2	39.039	8.2852
	AS	135	24.2	42.5	34.740	4.7837
	SCM	135	25.8	43.2	34.883	4.7486
	AMB	135	23.1	42.1	34.143	4.7428
	Valid N (listwise)	135				

a. No statistics are computed for one or more split files because there are no valid cases

Table 4.8 summarise the different temperatures on the SRM in comparison to the air space, SCM and ambient, based on different combinations of roofing and ceiling materials irrespective of the angles of roof configurations. The table shows that the average temperature was highest in SRM, air space AS, PCB and ambient when PLAR was combined with PCB, compared with other combinations.

Table 4.8: Summary of temperature for combinations irrespective of the different angles

Combination		Number of Iterations	Temperature (^{0}C) Minimum	Maximum	Mean	Std. Deviation
PLAR vs ASB	SRM	81	27.7	53.8	38.205	7.5536
	AS	81	26.6	44.8	34.686	4.6679
	SCM	81	26.2	43.4	34.730	4.5532
	AMB	81	26.3	41.4	33.590	4.1617
	Valid N (listwise)	81				
PLAR vs GYP	SRM	81	27.4	55.2	38.291	7.7759
	AS	81	26.5	41.5	34.421	4.3862
	SCM	81	26.3	41.5	34.395	4.2899
	AMB	81	26.2	41.8	33.795	4.1733
	Valid N (listwise)	81				
PLAR vs PLW	SRM	81	28.1	54.5	40.110	8.4224
	AS	81	25.5	43.0	35.560	4.7860
	SCM	81	24.9	41.5	35.128	4.5506
	AMB	81	25.7	42.1	34.707	4.4551
	Valid N (listwise)	81				
PLAR vs POP	SRM	81	22.5	52.9	38.249	8.1064
	AS	81	24.2	42.4	34.449	4.7366
	SCM	81	25.8	42.0	34.567	4.5543
	AMB	81	23.1	41.2	33.751	4.5138
	Valid N (listwise)	81				
PLAR vs PVC	SRM	81	23.6	54.1	37.701	8.7629
	AS	81	24.9	44.0	34.246	5.5161
	SCM	81	25.8	43.2	34.384	5.2650
	AMB	81	25.0	42.0	33.307	4.8506
	Valid N (listwise)	81				

Figure 4.27 shows the trend of variation of temperature for different combinations and angles. It is clearly visible from the figure that temperatures for 45 degrees configuration was generally low for the combination of PLAR and PVC.

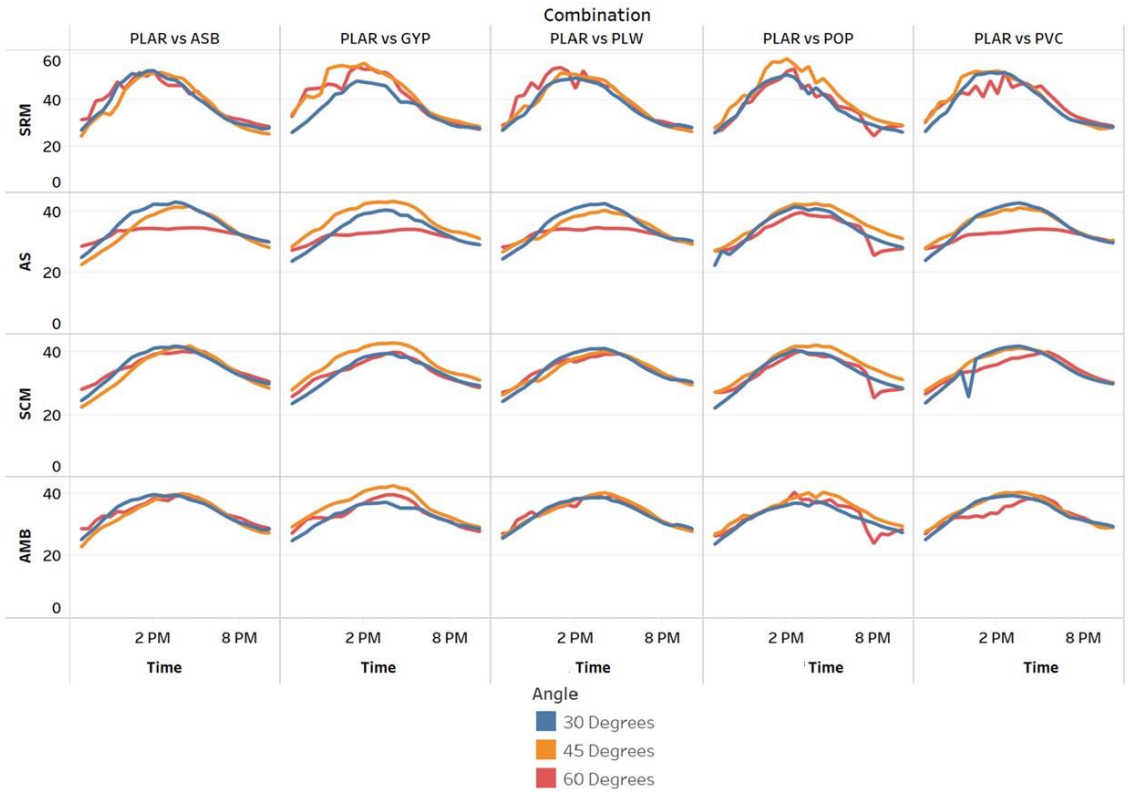

Figure 4.27: Daily temperature variation for different angles with respect to different combinations and materials

4.5.1: Test of hypothesis for Plywood-Lined Aluminium Roof (PLAR)

Null Hypothesis (H_0): There is no significant variations in the temperature of roofing material combinations.

Alternate Hypothesis (H_1): There is significant variations in the temperature of roofing material combinations.

From Table 4.9 above, the null hypothesis is rejected for SRM, SCM, AS and AMB at 30 degrees, and AS at 45 degrees since Sig is less than 0.05. This implies that the angles of configurations cause temperature variations for the five combinations of SRM and SCM, but this variations in temperature were significant for SRM, SCM, AS and AMB and ambient at 30^0 and AS at 45^0. This has practical implications across regions or zones in Nigeria as the difference in angles of inclination could utilization based on the temperature difference across geo-political zones in Nigeria. The findings align with the findings of the study conducted by Jayasingbe *et al*. (2003), melisa Viegas *et al*. (2016); Cobo Fray and Montoya Florez (2021) that in hot climate zones such as Nigeria; materials, insulation, surface colour and the effect of roof orientation; directly influences the maximum interior temperature of housing solutions.

Table 4.9: Analysis of variance of variance in temperature of roofing materials

Angle			Sum of Squares	df	Mean Square	F	Sig.
30 Degrees	SRM	Between Groups	1451.061	4	362.765	6.255	.000
		Within Groups	7539.067	130	57.993		
		Total	8990.129	134			
	AS	Between Groups	717.192	4	179.298	9.350	.000
		Within Groups	2492.872	130	19.176		
		Total	3210.064	134			
	SCM	Between Groups	574.521	4	143.630	8.170	.000
		Within Groups	2285.327	130	17.579		
		Total	2859.848	134			
	AMB	Between Groups	545.527	4	136.382	7.737	.000
		Within Groups	2291.659	130	17.628		
		Total	2837.186	134			
45 Degrees	SRM	Between Groups	395.769	4	98.942	1.656	.164
		Within Groups	7769.208	130	59.763		
		Total	8164.977	134			
	AS	Between Groups	236.295	4	59.074	2.810	.028
		Within Groups	2733.115	130	21.024		
		Total	2969.409	134			
	SCM	Between Groups	157.546	4	39.387	2.087	.086
		Within Groups	2453.306	130	18.872		
		Total	2610.852	134			
	AMB	Between Groups	101.139	4	25.285	1.495	.207
		Within Groups	2198.256	130	16.910		
		Total	2299.395	134			
60 Degrees	SRM	Between Groups	181.851	4	45.463	.644	.632
		Within Groups	9183.002	130	70.638		
		Total	9364.853	134			
	AS	Between Groups	47.674	4	11.919	.496	.738
		Within Groups	3121.634	130	24.013		
		Total	3169.308	134			
	SCM	Between Groups	63.296	4	15.824	.666	.617
		Within Groups	3088.535	130	23.758		
		Total	3151.831	134			
	AMB	Between Groups	49.213	4	12.303	.591	.670
		Within Groups	2704.779	130	20.806		
		Total	2753.992	134			

Decision: Reject H_0 when Sig. is less than 0.05

4.5.2 Statistical analysis of temperature dynamics between SCS and POP

Table 4.10 shows that temperature was generally higher at stone coated sheet (SCS) compared to the air space (AS), plaster of paris (POP) and ambient temperature (AMB). Also, temperature deviated from the average for SCS compared to others. SCS possess high specific heat capacity which enable it to absorb and acted as good heat storage. This excellent thermophysical property placed SCS roofing material above other available roofing sheet in this tropical zone.

Table 4.10: Summary of temperature for different configurations

	Number of Iterations	Temperature (^{0}C)			
		Minimum	Maximum	Mean	Std. Deviation
SRM	405	22.4	61.2	39.143	10.4015
AS	405	24.6	61.9	37.069	8.1673
SCM	405	20.9	58.6	35.553	6.7489
AMB	405	22.0	62.1	34.816	7.3650
Valid N (listwise)	405				

Table 4.11 summarise the different temperatures on the selected roofing materials (SRM) in comparison to the air space AS, POP, and ambient AMB, based on different angles of roof configurations. The table shows that the average temperature was highest in Air space for roofing configuration with angle 30^0; due to the gentleness in the pitch between the roofing sheet and the underlay ceiling, causing high concentration of heat within the air space while it was lowest for SRM based on angles 45^0 and 60^0 respectively. Because the air space within angle 45^0 and 60^0 was sufficiently high causing adequate heat conduction effect to take place without any interference. This also allowed free flow of air circulations from the underlay ceiling to the exterior roofing sheet.

Table 4.11: Summary of temperature for different angles irrespective of combinations

Angle		Number of Iterations	Temperature (^{0}C) Minimum	Maximum	Mean	Std. Deviation
30 Degrees	SRM	135	22.6	61.2	37.973	9.7382
	AS	135	21.6	61.9	39.189	10.1632
	SCM	135	21.9	58.6	36.894	8.0658
	AMB	135	22.0	62.1	38.909	9.9072
	Valid N (listwise)	135				
45 Degrees	SRM	135	22.4	60.3	40.025	11.4859
	AS	135	23.7	49.6	35.926	6.9692
	SCM	135	23.0	44.3	34.790	5.9895
	AMB	135	23.2	39.4	32.439	4.4839
	Valid N (listwise)	135				
60 Degrees	SRM	135	23.7	56.3	39.429	9.8579
	AS	135	23.5	46.2	36.092	6.5148
	SCM	135	20.9	43.7	34.975	5.8014
	AMB	135	23.1	40.3	33.100	4.4435
	Valid N (listwise)	135				

Table 4.12 summarise the different temperatures on the SRM in comparison to the air space, POP and ambient, based on different combinations of roofing and ceiling materials irrespective of the angles of roof configurations. The table shows that the average temperature was highest in SRM, air space AS, PCB and ambient when SCS was combined with POP, compared with other combinations.

Table 4.12: Summary of temperature for combinations of SRM and SCM irrespective of the different angles

Combination		Number of Iterations	Temperature (^{0}C) Minimum	Maximum	Mean	Std. Deviation
SCS vs ASB	SRM	82	23.6	54.4	38.6939	8.6226
	AS	82	23.7	52.5	37.2634	7.1251
	SCM	82	23.6	43.5	35.0768	5.0579
	AMB	82	22.6	39.5	32.9902	3.8357
	Valid N (listwise)	82				
SCS vs GYP	SRM	81	23.2	61.2	38.8864	11.2069
	AS	81	22.2	53.3	36.7482	8.2320
	SCM	81	20.9	58.6	35.8667	7.7551
	AMB	81	22.3	53.9	34.6148	7.5996
	Valid N (listwise)	81				
SCS vs PCB	SRM	80	22.6	57.0	40.7787	10.3990
	AS	80	23.5	61.5	38.4300	8.5369
	SCM	80	21.9	54.1	36.5663	6.9510
	AMB	80	22.0	55.3	36.1488	8.3888
	Valid N (listwise)	80				
SCS vs POP	SRM	81	22.4	56.4	39.0173	10.6739
	AS	81	24.1	49.7	35.5568	7.1019
	SCM	81	22.9	47.5	35.1309	7.1199
	AMB	81	23.2	54.3	34.9827	8.2469
	Valid N (listwise)	81				
SCS vs PVC	SRM	81	23.0	60.3	38.3617	11.0084
	AS	81	21.6	61.3	37.3605	9.5335
	SCM	81	22.0	53.5	35.1432	6.6222
	AMB	81	23.1	62.1	35.3815	7.6282
	Valid N (listwise)	81				

Figure 4.28 shows the trend of temperature variations for different combinations and angles. It was deduced from the figure that ambient temperature was lowest (below 40^0) for the combination of SCS and ASB. While temperature of ASB did not change much for the different angles in the combination of SCS and ASB. In addition, Angle 30 has the lowest temperature when SCS is combined with PVC.

Figure 4.29 implied that the average Ambient temperature was highest for the different combination with SCS during the day for 30 degrees, while it dropped at night.
Figure 4.30 indicated that the average AS temperature was highest for the different combinations with SCS during the day for the 30 degrees, while it dropped at night.
Similarly, Figure 4.31 revealed that the average SCM temperature was highest at 30 degrees for the different combinations with SCS during the day between 10am and 2pm, while it dropped at Night between 7pm and 10pm. This is in tandem with the (Harimi, Harimi, Kurian, and Nurmin, 2005) finding that the tropical temperature dropped as the sunset.

Apparently, Figure 4.32 showed that the average SRM temperature was highest at 45 degrees for the different combinations with SCS during the day between 10 am to 2 pm, while it dropped at Night between 4 pm and 10 pm.
But for Figure 4.32 the average temperature of SCS Vs POP was highest in the day and reduce at Night, while temperature of SCS Vs ASB was lower during the day and highest at Night.

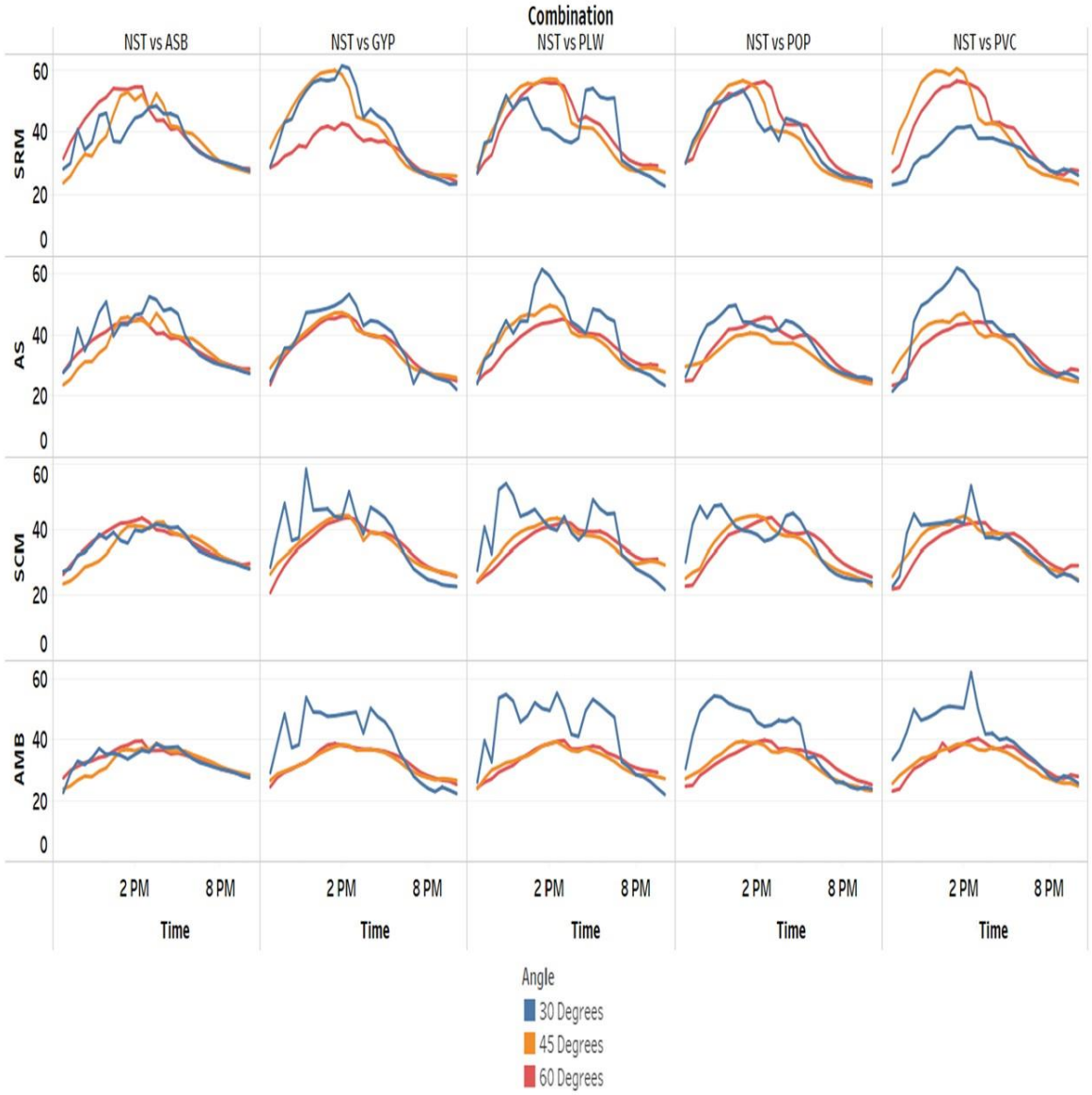

Figure 4.28: Daily temperature variation for different angles with respect to different combinations and materials

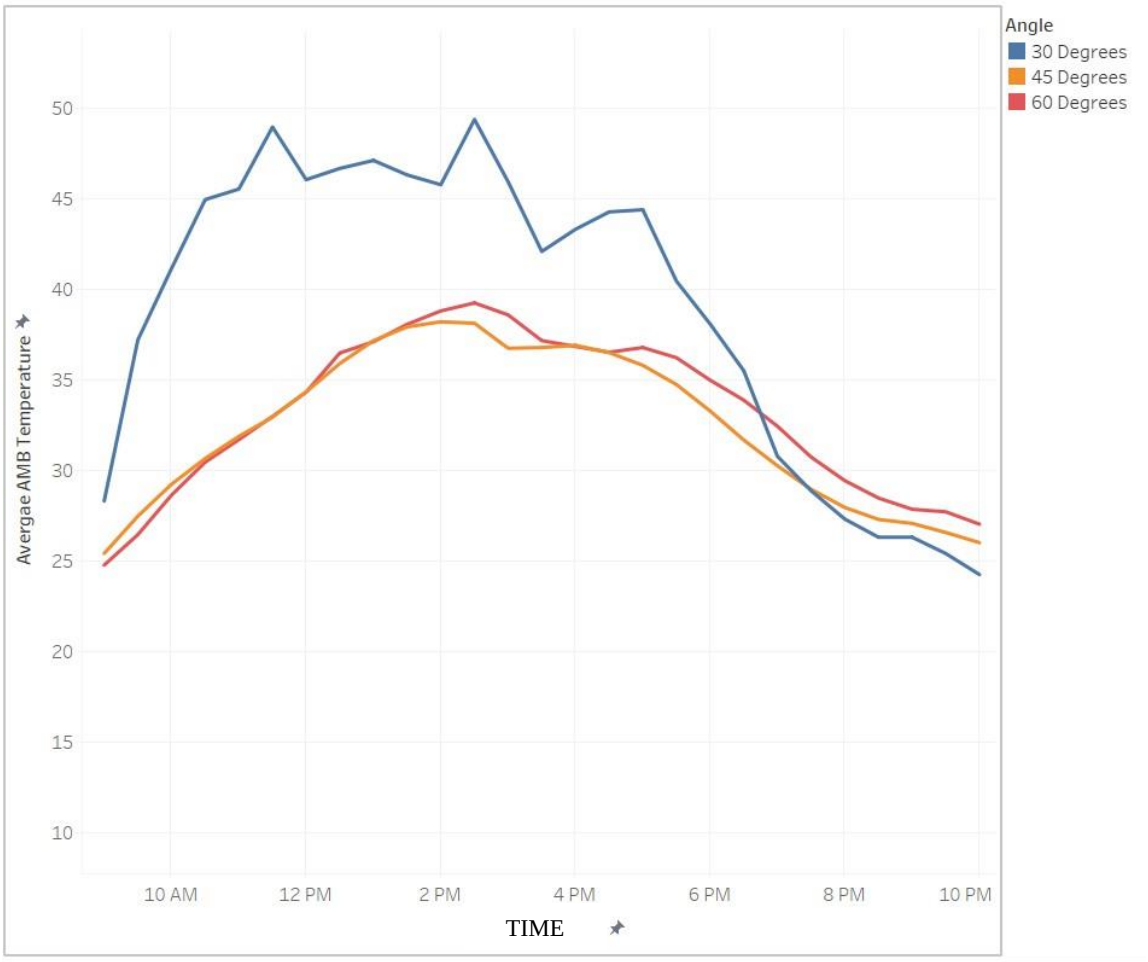

Figure 4.29: Average ambient temperature for the different angles of SCM vs SRM irrespective of combinations

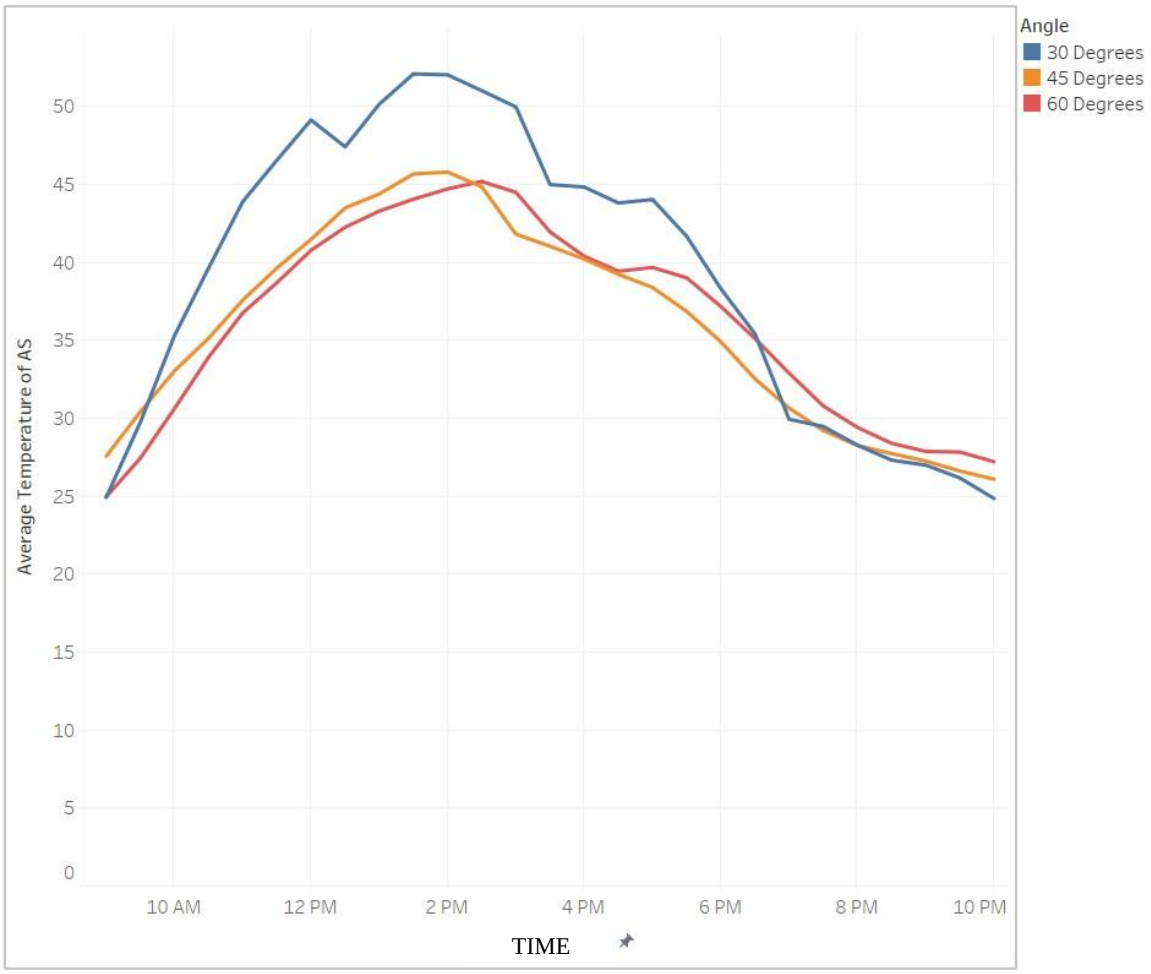

Figure 4.30: Average air space temperature for the different angles of SCM vs SRM irrespective of combinations

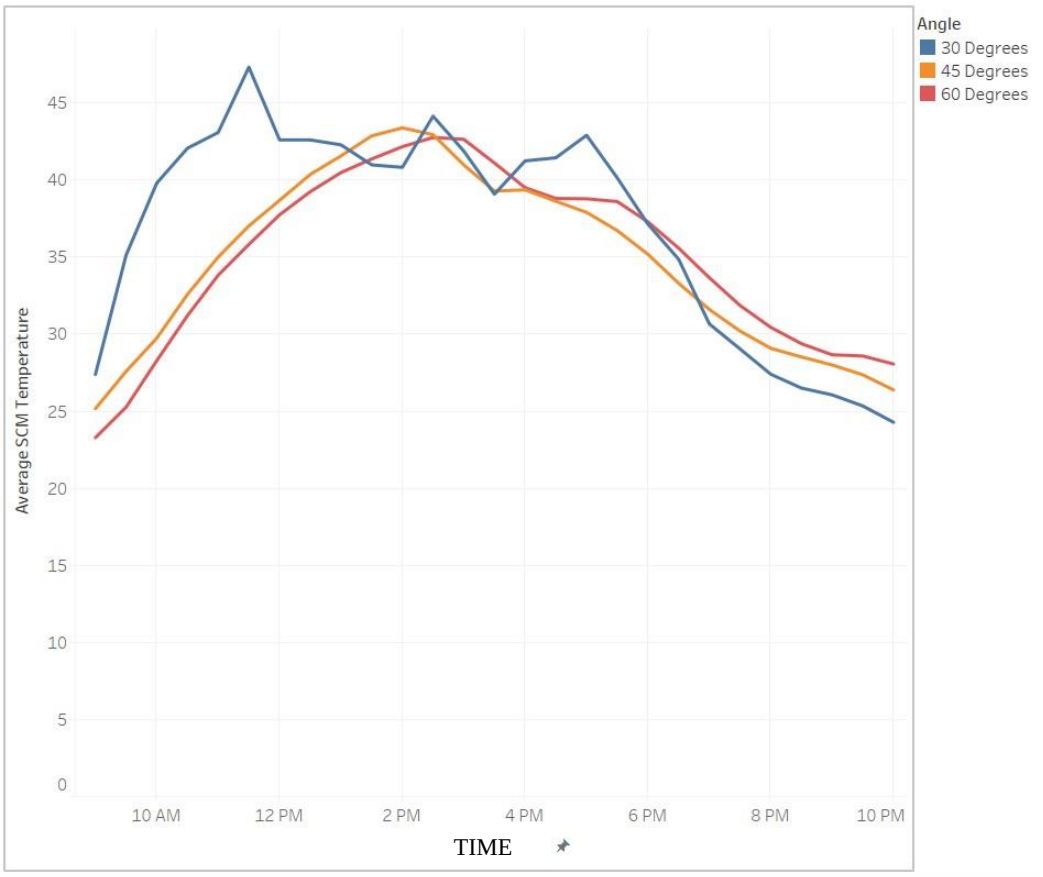

Figure 4.31: Average ceiling material temperature for the different angles of SCS vs SCM irrespective of combinations

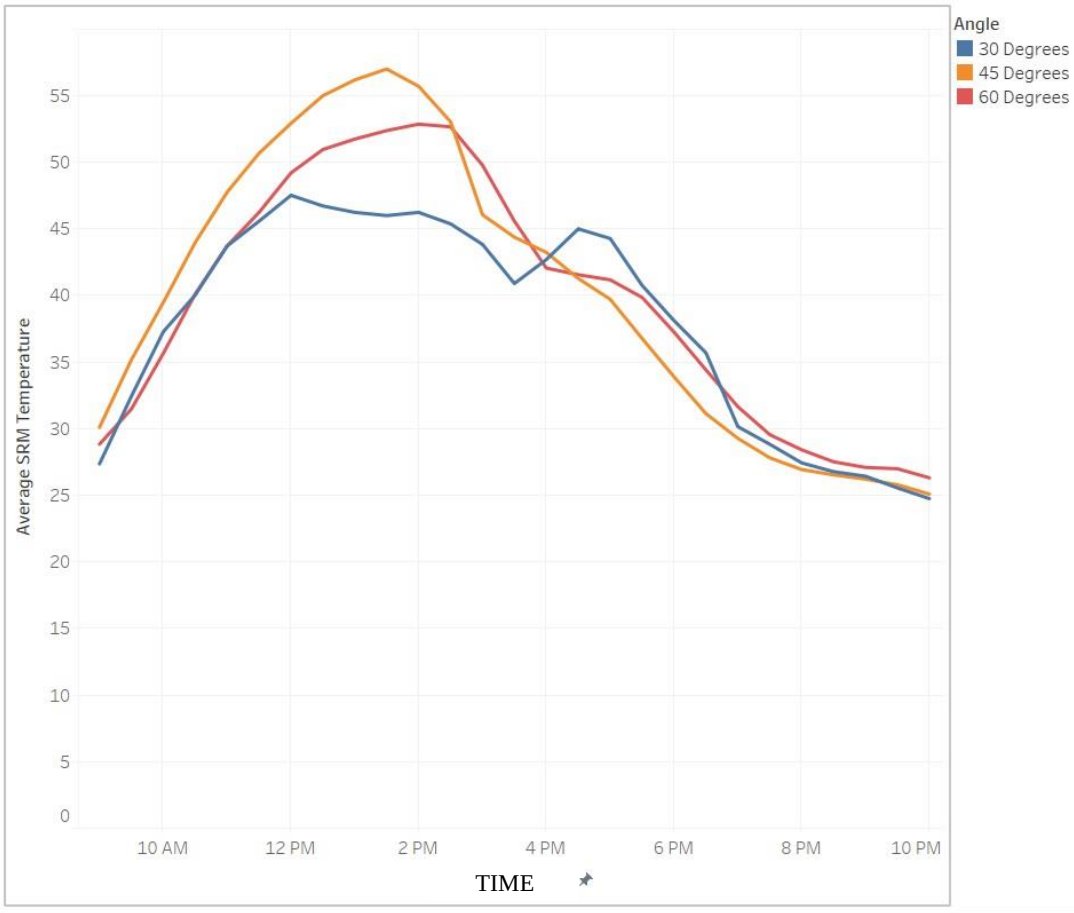

Figure 4.32: Average roofing material temperature for the different angles of SCS vs SRM irrespective of combinations

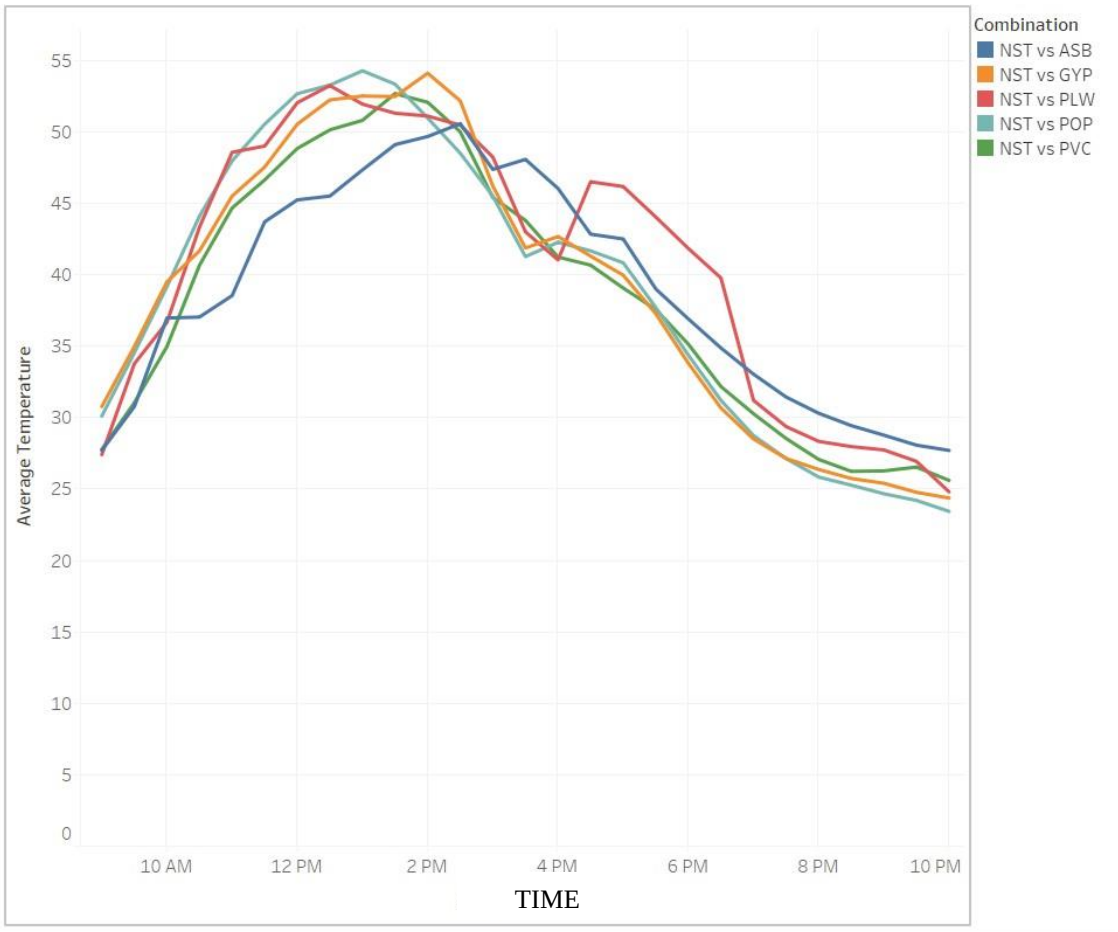

Figure 4.33: Average temperature for the different combination of SCM vs SRM irrespective of the angles

4.5.3: Test of hypothesis for stone coated roof configurations

Null Hypothesis (H_0): There is no significant variations in the temperature of roofing material combinations.

Alternate Hypothesis (H_1): There is significant variations in the temperature of roofing material combinations.

From Table 4.13 above, the null hypothesis is rejected for SCS and AMB at 30 degrees, and SCS at 60 degrees since Sig is less than 0.05. This implies that the angles of configurations cause temperature variations for the five combinations of SRM and SCM, but this variations in temperature were significant for SCS and ambient at 30^0 and SCS at 60^0. This has practical implications across regions or zones in Nigeria as the difference in angles of inclination could utilization based on the temperature difference across geo-political zones in Nigeria. The finding aligns with the findings of the study conducted by (Jayasingbe M, Attalage, and Jayawardena, 2003), (Melisa, Walsh, and Barros, 2016) and (Cobo and Montoya, 2021) that in hot climate zones such as Nigeria; materials, insulation, surface colour and the effect of roof orientation; directly influences the maximum interior temperature of housing solutions.

Table 4.13: Analysis of variance of variance in temperature of roofing materials

Angle			Sum of Squares	df	Mean Square	F	Sig.
30 Degrees	SRM	Between Groups	1142.291	4	285.573	3.210	.015
		Within Groups	11565.398	130	88.965		
		Total	12707.689	134			
	AS	Between Groups	202.419	4	50.605	.482	.749
		Within Groups	13638.534	130	104.912		
		Total	13840.953	134			
	SCM	Between Groups	253.913	4	63.478	.975	.424
		Within Groups	8463.682	130	65.105		
		Total	8717.595	134			
	AMB	Between Groups	1267.469	4	316.867	3.466	.010
		Within Groups	11884.901	130	91.422		
		Total	13152.369	134			
45 Degrees	SRM	Between Groups	286.800	4	71.700	.536	.710
		Within Groups	17391.554	130	133.781		
		Total	17678.354	134			
	AS	Between Groups	302.635	4	75.659	1.585	.182
		Within Groups	6205.664	130	47.736		
		Total	6508.299	134			
	SCM	Between Groups	27.032	4	6.758	.184	.946
		Within Groups	4780.125	130	36.770		
		Total	4807.157	134			
	AMB	Between Groups	5.616	4	1.404	.068	.991
		Within Groups	2688.524	130	20.681		
		Total	2694.140	134			
60 Degrees	SRM	Between Groups	1064.824	4	266.206	2.894	.025
		Within Groups	11957.037	130	91.977		
		Total	13021.861	134			
	AS	Between Groups	23.991	4	5.997	.138	.968
		Within Groups	5663.311	130	43.564		
		Total	5687.301	134			
	SCM	Between Groups	33.975	4	8.494	.247	.911
		Within Groups	4475.920	130	34.430		
		Total	4509.894	134			
	AMB	Between Groups	16.531	4	4.133	.204	.936
		Within Groups	2629.249	130	20.225		
		Total	2645.780	134			

Decision: Reject H_0 when Sig. is less than 0.05

4.5.4: Statistical analysis of temperature dynamics between ARS and SCM

Table 4.14 shows that temperature was generally higher at ARS compared to the air space AS, SCM and ambient AMB. Also, temperature deviated from the average for ARS compared to others.

Table 4.14: Summary of temperature for different configurations

		Temperature (^{0}C)			
	N	**Minimum**	**Maximum**	**Mean**	**Std. Deviation**
SRM	405	22.4	57.9	39.589	8.7637
AS	405	22.4	43.3	34.374	4.6638
SCM	405	22.1	43.0	34.752	4.7795
AMB	405	22.9	42.6	33.879	4.1422
Valid N (listwise)	405				

Table 4.15 summarise the different temperatures on the SRM in comparison to the air space, SCM and ambient, based on different angles of roof configurations. The table shows that the average temperature was highest in roofing material at 45^0, in Air space at 30^0 and in Ceiling Material at 60^0 in compared to others.

Table 4.15: Summary of temperature for different angles irrespective of combinations

Angle		Number of Iterations	Temperature (^{0}C) Minimum	Maximum	Mean	Std. Deviation
30 Degrees	SRM	135	22.6	57.9	39.364	9.0995
	AS	135	22.4	43.3	34.992	5.1589
	SCM	135	22.1	43.0	34.752	5.0916
	AMB	135	23.8	42.6	33.716	4.3223
	Valid N (listwise)	135				
45 Degrees	SRM	135	26.4	54.5	39.792	8.4255
	AS	135	24.0	42.8	34.070	4.4466
	SCM	135	23.7	42.0	34.676	4.6005
	AMB	135	25.2	40.4	33.924	3.9003
	Valid N (listwise)	135				
60 Degrees	SRM	135	24.4	54.1	39.613	8.8131
	AS	135	22.7	43.1	34.060	4.3145
	SCM	135	22.4	42.1	34.827	4.6660
	AMB	135	22.9	40.3	33.997	4.2181
	Valid N (listwise)	135				

Table 4.16 summarise the different temperatures on the SRM in comparison to the air space, SCM and ambient, based on different combinations of roofing and ceiling materials irrespective of the angles of roof configurations. The table shows that the average temperature was highest in SRM, when ARS was combined with GYP, compared to other combinations.

Table 4.16: Summary of temperature for combinations irrespective of the different angles

Combination		Number of Iterations	Temperature (^{0}C)			
			Minimum	Maximum	Mean	Std. Deviation
ARS vs POP	SRM	81	25.8	54.5	39.329	8.8861
	AS	81	22.4	41.5	33.549	4.2957
	SCM	81	22.1	40.7	33.975	4.5929
	AMB	81	23.8	40.3	33.344	4.0379
	Valid N (listwise)	81				
ARS vs GYP	SRM	81	26.4	57.9	40.673	9.2643
	AS	81	24.0	42.8	34.837	4.6688
	SCM	81	23.7	42.3	35.179	4.8019
	AMB	81	25.2	40.5	34.264	3.9729
	Valid N (listwise)	81				
ARS vs PVC	SRM	81	24.6	53.5	39.179	8.9683
	AS	81	25.0	43.1	34.938	4.9432
	SCM	81	24.5	42.0	34.811	4.9006
	AMB	81	24.1	40.5	33.954	4.4866
	Valid N (listwise)	81				
ARS vs PCB	SRM	81	24.4	52.2	38.383	8.0350
	AS	81	22.7	41.8	33.386	4.5722
	SCM	81	22.4	42.1	34.074	4.8543
	AMB	81	22.9	40.0	33.104	3.9710
	Valid N (listwise)	81				
ARS vs ASB	SRM	81	26.9	56.0	40.383	8.6329
	AS	81	24.5	43.3	35.159	4.6272
	SCM	81	24.2	43.0	35.718	4.6279
	AMB	81	25.7	42.6	34.728	4.1078
	Valid N (listwise)	81				

Figure 4.33 shows the trend of temperature variations for different combinations and angles. It was noted from the figure that ambient temperature and SCM had similar patterns for the three angles of configuration.

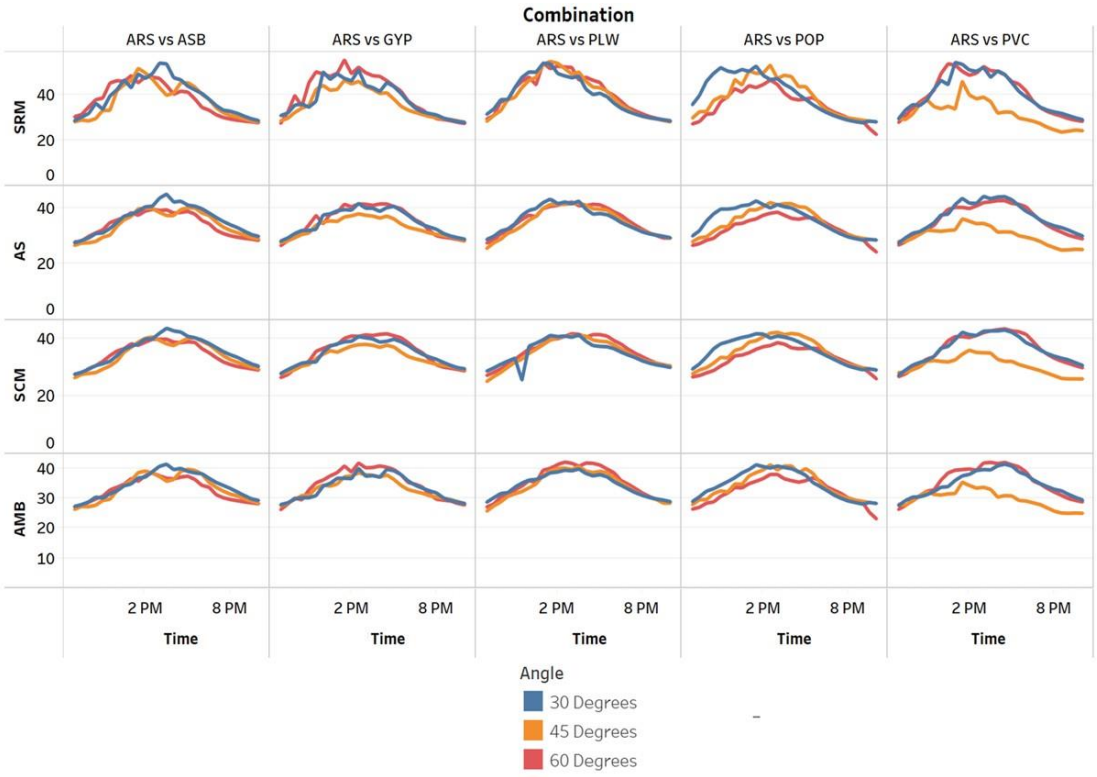

Figure 4.34: Daily temperature variation for different angles with respect to different combinations and materials

4.5.5: Test of hypothesis for Aluminium Roofing Sheet (ARS)

Null Hypothesis (H_0): There is no significant variations in the temperature of roofing material combinations.

Alternate Hypothesis (H_1): There is significant variations in the temperature of roofing material combinations.

From Table 4.17 above, the null hypothesis is rejected for SRM, SCM, AS and AMB at 30 degrees, and AS at 45 degrees since Sig is less than 0.05. This implies that the angles of configurations cause temperature variations for the five combinations of SRM and SCM, but this variations in temperature were significant for SRM, SCM, AS and AMB and ambient at 30^0 and AS at 45^0 and 60^0.

Table 4.17: Analysis of variance in temperature of roofing materials

Angle			Sum of Squares	df	Mean Square	F	Sig.
30 Degrees	SRM	Between Groups	814.800	4	203.700	2.576	.041
		Within Groups	10280.552	130	79.081		
		Total	11095.352	134			
	AS	Between Groups	336.460	4	84.115	3.386	.011
		Within Groups	3229.821	130	24.845		
		Total	3566.281	134			
	SCM	Between Groups	305.401	4	76.350	3.133	.017
		Within Groups	3168.436	130	24.373		
		Total	3473.837	134			
	AMB	Between Groups	272.487	4	68.122	3.970	.005
		Within Groups	2230.910	130	17.161		
		Total	2503.397	134			
45 Degrees	SRM	Between Groups	144.618	4	36.155	.502	.735
		Within Groups	9367.863	130	72.060		
		Total	9512.481	134			
	AS	Between Groups	396.487	4	99.122	5.719	.000
		Within Groups	2253.015	130	17.331		
		Total	2649.501	134			
	SCM	Between Groups	44.832	4	11.208	.522	.720
		Within Groups	2791.338	130	21.472		
		Total	2836.169	134			
	AMB	Between Groups	32.493	4	8.123	.526	.716
		Within Groups	2005.916	130	15.430		
		Total	2038.409	134			
60 Degrees	SRM	Between Groups	85.028	4	21.257	.268	.898
		Within Groups	10322.768	130	79.406		
		Total	10407.796	134			
	AS	Between Groups	249.601	4	62.400	3.614	.008
		Within Groups	2244.823	130	17.268		
		Total	2494.424	134			
	SCM	Between Groups	58.952	4	14.738	.670	.614
		Within Groups	2858.457	130	21.988		
		Total	2917.409	134			
	AMB	Between Groups	28.793	4	7.198	.397	.810
		Within Groups	2355.346	130	18.118		
		Total	2384.139	134			

Decision: Reject H_0 when Sig. is less than 0.05

4.5.6: Mathematical model

The results of the daily temperature variations for the PLAR, SRS and ARS were analyzed using ANOVA and modelled with regression equation due to the nature of data generated and in consonant with objectives four of this research. For every situation, two hypotheses were tested, and the results are presented.

4.5.6.1: Regression model equations

The predictive mathematical models for Optimum Comfortability Roof (OCR) for PLAR, SRS and ARS were developed with external ambient temperature AMB, selected roofing temperature SRM, air space AS temperature and selected ceiling temperature SCM, considered as parameters. The output below suggested that the regression model for PLAR, SCS, and ARS has 95.0%, 70.0% and 90.0% of model fit (predictive abilities) respectively, showing that the relationship among the independent variables is strong. This is in accordance with (Lawal and Ojo, 2011) submission on coefficient of correlation.

4.5.6.2: Derivation of mathematical model for PLAR configurations

Combination: PLAR Vs {POP, GYP, PVC, ASB, PLW}

4.5.6.2.1: MODEL 1: To predict temperature of roofing material based on ambient temperature and time (GMT) for the different combinations.

To predict temperature based on thermo-physical properties, a mathematical model was created. The equation 4.0 represents the developed model to predict temperature of the roofing material at a given time with respect to angle of inclinations.

$$Y_i = \beta_0 + \beta_1 X_{i1} + \beta_2 X_{i2} + \beta_3 X_{i3} \quad \ldots \quad 4.0$$

where Y_i is Temperature of Roofing Material, X_1 is Time, X_2 is Ambient Temperature, X_3 is Angle of configuration; β_0 is the intercept of the fit, while $\beta_1 - \beta_3$ are the coefficient of the independent variables.

After fitting the factors and the temperature in a regression model and deriving their respective coefficient. The equation 4.1 summarised their relationship and its presented below:

$$SRM = -7.9340 - 0.8995X_1 + 1.7551X_2 - 0.014X_3 \quad \ldots \quad 4.1$$

The model's variables coefficients values are used for assessing the impact of factors on temperature of the roofing materials irrespective of the selected combinations are presented in Table 4.18.

Table 4.18: Summary of linear regression model parameters

Dep. Variable:	SRM	R-squared:	0.857
Model:	OLS	Adj. R-squared:	0.856
Method:	Least squares	F-statistic:	800.6
Date:	Fri, 24 Feb. 2023	Prob (F-statistic):	7.17e-169
Time:	13:52:48	Log-Likelihood:	-1059.5
No. Observations:	405	AIC:	2127.
Df. Residuals:	401	BIC:	2143.
Df. Model:	3		
Covariance Type:	Nonrobust		

	Coef	std err	T	P> |t|	[0.025	0.975]
Intercept	-7.9340	1.624	-4.884	0.000	-11.127	-4.741
Time	-0.8995	0.042	-21.196	0.000	-0.983	-0.816
AMB	1.7551	0.040	43.912	0.000	1.677	1.834
Angle	0.0426	0.014	3.159	0.002	0.016	0.069

Omnibus:	16.915	Durbin-Watson:	0.440
Prob (Omnibus):	0.000	Jarque-Bera (JB):	18.333
Skew:	0.520	Prob (JB):	0.000104
Kurtosis:	2.947	Cond. No.	582

From Table 4.18, the coefficient of the intercept is -7.9340, which implies that there is a decrease in the unit temperature of the roofing material for every increase in other variables that are not included in the model, while the other independent variables are held constant. It also shows that the coefficient of the Time is -0.8995, that implies that the unit temperature of the roofing material decreases as time increases from 9:00 to 24:00, while the other variables are held constant.

It also shows that the ambient temperature (AMB) coefficient is 1.7551, which signifies there is an increase in the unit temperature of the roofing material for every ambient temperature increment. The result is in line with (Lawal and Ojo, 2011) findings that say increase in ambient temperature lead to an increase in roof temperature, while other variables are held constant. While on further observation in the table, the configuration angle coefficient is 0.0426, which means a decrease in the unit temperature of the roofing material for every increase in the angle of configuration in the order of 30^0, 45^0 and 60^0, while the other variables are held constant. The coefficient of p values shows that the coefficients are statistically significantly different from zero since all the values is less than 0.05, expect for angle of configuration. This implies that the angle of configuration does not significantly affect the temperature of Air Space based on the combined SRM and SCM.

Coefficient of Determination (R^2) depicted in the table has a value of 0.857 that shows the measure of the overall strength of the model. It can be observed that since the R^2 is approximately 0.9, which is not far from 1, it can be concluded that the model is adequate in determining the temperature of roofing material based on the experimentally observed independent variables, (Lawal and Ojo, 2011) (Lawal, Akinpade, and Makinde, 2017). There are indications also that these variables are not the only factors responsible for the thermal conditions of the roofing material.

The table further shows that null hypothesis F test affirm that all the model coefficients are equal to Zero. Since the p value for the f test is <0.00 which is less than 0.05, it can be resolved that all the coefficients are none zero, which infer there is a relationship between the selected independent variables and the temperature of the roofing material.

4.5.6.2.2: MODEL 2: To predict temperature of ceiling material based on ambient temperature and time (GMT) for the different combinations.

To predict temperature based on thermo-physical properties, a mathematical model was formulated. The equation 4.3 represents the developed model to predict temperature of the ceiling materials at a given time with respect to angle of inclinations.

$$Y_i = \beta_0 + \beta_1 X_{i1} + \beta_2 X_{i2} + \beta_3 X_{i3} \quad \ldots \quad 4.3$$

where Y_i is Temperature of Ceiling Material, X_1 is Time, X_2 is Ambient Temperature, X_3 is Angle of configuration; β_0 is the intercept of the fit, while $\beta_1 - \beta_3$ are the coefficient of the independent variables.

After fitting the factors and the temperature in a regression model and deriving their respective coefficient. The equation 4.4 summarised their relationship and its presented below:

$$SCM = -5.7487 + 0.2108X_1 + 1.1078X_2 - 0.0062X_3 \quad \ldots \quad 4.4$$

The model's variables coefficient values are used for assessing the impact of factors on temperature of the ceiling materials irrespective of the selected combinations are presented in Table 4.19.

Table 4.19: Summary of linear regression model parameters

Dep. Variable:	SCM	R-Squared:	0.949
Model:	OLS	Adj. R-Squared:	0.949
Method:	Least Squares	F-Statistic:	2511.
Date:	Fri, 24 Feb. 2023	Prob (F-Statistic):	1.84e-259
Time:	13:28:03	Log-Likelihood:	-603.25
No. Observations:	405	AIC:	1215.
Df. Residuals:	401	BIC:	1231.
Df. Model:	3		
Covariance Type:	Nonrobust		

	coef	std err	T	p>|t|	[0.025	0.975]
Intercept	-5.7487	0.527	-10.918	0.000	-6.784	-4.714
Time	0.2108	0.014	15.326	0.000	0.184	0.238
AMB	1.1078	0.013	85.509	0.000	1.082	1.133
ANGLE	-0.0062	0.004	-1.414	0.158	-0.015	0.002

Omnibus:	254.806	Durbin-Watson:	0.991
Prob (Omnibus):	0.000	Jarque-Bera (JB):	8525.618
Skew:	-2.098	Prob (JB):	0.00
Kurtosis:	25.082	Cond. No.	582.

From Table 4.19, the coefficient of the intercept is -5.7487, which implies that there is a decrease in the unit temperature of the ceiling material as other variables increases that are not included in the model, while the other independent variables are held constant. It also shows that the coefficient of the Time is 0.2108, there is an increase in the unit temperature of the ceiling material as time increases from 9:00 to 24:00, while the other variables are held constant.

It also shows that the ambient temperature (AMB) coefficient is 1.1078, which signifies there is an increase in the unit temperature of the ceiling material as the ambient temperature increases, while other variables are held constant. While further observation from the table shows that the configuration angle of coefficient is -0.0062, which signifies there is decrease in the unit temperature of the ceiling material for every increase in the angle of configuration in the order of 30^0, 45^0 and 60^0, while other variables are held constant. The coefficient of p values shows that the coefficients are statistically significantly different from zero since all the values is less than 0.05, expect for angle of configuration. This implies that the angle of configuration does not significantly affect the temperature of Air Space based on the combined SRM and SCM.

Coefficient of Determination (R^2) depicted in the table has a value of 0.965 that shows the measure of the overall strength of the model. It can be observed that since the R^2 is approximately 1, it can be concluded that the model is adequate in determining the temperature of ceiling material based on the experimentally observed independent variables. There are indications also that these factors are not the only factors responsible for the thermal conditions of the ceiling material.

The table further shows that null hypothesis F test proved that all the model coefficients are equal to Zero. Since the p value for the f test is <0.00 which is less than 0.05, it inferred that all coefficients are none zero, which implies there is a relationship among the selected independent variables and the temperature of the ceiling material.

4.5.6.2.3: MODEL 3: To predict temperature of Air Space (AS) based on ambient temperature and time (GMT) for the different combinations.

To predict temperature based on thermo-physical properties, a mathematical model was formulated. The equation 4.5 represents the developed model to predict the temperature within the air space AS, at a given time with respect to the angle of inclinations.

$$Y_i = \beta_0 + \beta_1 X_{i1} + \beta_2 X_{i2} + \beta_3 X_{i3} \quad \ldots \quad 4.5$$

where Y_i is Temperature of Air Space, X_1 is Time, X_2 is Ambient Temperature, X_3 is Angle of configuration; β_0 is the intercept of the fit, while $\beta_1 - \beta_3$ are the coefficient of the independent variables.

After fitting the factors and the temperature in a regression model and deriving their respective coefficient. The equation 4.6 summarise their relationship and presented below:

$$AS = 1.4224 - 0.1441X_1 + 1.0229X_2 - 0.0872X_3 \quad \ldots \quad 4.6$$

The model's variables coefficients values are used for assessing the impact of factors on temperature of the Air Spaces irrespective of the selected combinations are presented in table 4.20.

Table 4.20: Summary of linear regression model parameters

Dep. Variable:		AS		R-Squared:		0.884
Model:		OLS		Adj. R-Squared:		0.884
Method:		Least Squares		F-Statistic:		1023.
Date:		Fri, 24 Feb. 2023		Prob (F-Statistic):		1.84e-187
Time:		13:28:00		Log-Likelihood:		-760.80
No. Observations:		405		AIC:		1530.
Df. Residuals:		401		BIC:		1546.
Df. Model:		3				
Covariance Type:		Nonrobust				
	coef	std err	t	P>|t|	[0.025	0.975]
Intercept	1.4224	0.777	1.831	0.068	-0.105	2.950
Time	0.1441	0.020	7.097	0.000	0.104	0.184
AMB	1.0229	0.019	53.513	0.000	0.985	1.061
ANGLE	-0.0872	0.006	-13.503	0.000	-0.100	-0.074
Omnibus:		40.712		Durbin-Watson:		0.306
Prob (Omnibus):		0.000		Jarque-Bera (JB):		50.801
Skew:		-0.790		Prob (JB):		9.30e-12
Kurtosis:		3.715		Cond. No.		582.

From Table 4.20, above coefficient of the intercept is 1.4224, which implies that there is a unit increase in the temperature of the Air Space for every increase in other variables that are not included in the model, while the other independent variables were held constant. From the table, further deduction show that the coefficient of the Time is 0.144, there is a unit increase in the temperature of the Air Space as time increase from 9:00 to 24:00, while other variables are held constant.

It also shows that the ambient temperature (AMB) coefficient is 1.023, which signifies that there is an increase in the unit temperature of the Air Space as the ambient temperature increases, (Lawal and Ojo 2011), while other variables are held constant. While on further observation from the table configuration angle coefficient is -0.087, which implies there is a unit temperature decrease of the Air Space for every increase in the angle of configuration in the order of 30^0, 45^0 and 60^0, while other variables are held constant. The coefficient of p values shows that the coefficients are statistically significantly different from zero since all the values is less than 0.05, expect for the intercept. This implies that the other factors contributing to temperature dynamics of building material do not significantly affect the temperature of Air Space based on the combined SRM and SCM.

Coefficient of Determination (R^2) depicted in the table has a value of 0.884 that shows the measure of the overall strength of the model. It can be observed that since the R^2 is approximately 0.9, which is not far from 1, it can be concluded that the model is adequate in determining the temperature of Air Space based on the experimentally observed independent variables. There are indications also that these factors are not the only factors responsible for the thermal conditions of the Air Space.

The table further shows that null hypothesis F test affirms that all the model coefficients are equal to Zero. Since the p value for the f test is <0.00 which is less than 0.05, it can be summarised that all the coefficients are none zero, which implies there is a correlation between the selected independent variables and the temperature of the Air Space.

4.5.6.3: Derivation of mathematical model for stone coated configuration Combination: SCS Vs {POP, GYP, PVC, ASB, PLW}

4.5.6.3.1: MODEL 1: To predict temperature of roofing material based on ambient temperature and time (GMT) for the different combinations.

To predict temperature based on thermo-physical properties, a mathematical model was developed. The equation 4.7 represented the developed model as obtainable below:

$$Y_i = \beta_0 + \beta_1 X_{i1} + \beta_2 X_{i2} + \beta_3 X_{i3} \quad \ldots \quad 4.7$$

where Y_i is Temperature of Roofing Material, X_1 is Time, X_2 is Ambient Temperature, X_3 is Angle of configuration; β_0 is the intercept of the fit, while $\beta_1 - \beta_3$ are the coefficient of the independent variables.

After fitting the factors and the temperature in a regression model and deriving their respective coefficient. Thus, equation 4.8 summarized their relationship as presented below:

$$SRM = 12.56 - 0.8547X_1 + 0.8630X_2 + 0.2157X_3 \quad \ldots \quad 4.8$$

The model's variables coefficient values are used for assessing the impact of factors on temperature of the roofing materials irrespective of the selected combinations are presented in table 4.21.

Table 4.21: Summary of linear regression model parameters

Dep. Variable:		SRM		R-Squared:		0.562
Model:		OLS		Adj. R-squared:		0.599
Method:		Least Squares		F-statistic:		171.6
Date:		Sat, 18 Feb. 2023		Prob (F-Statistic):		1.48e-71
Time:		17:37:13		Log-Likelihood:		-1355.4
No. Observations:		405		AIC:		2719.
Df. Residuals:		401		BIC:		2735.
Df. Model:		3				
Covariance Type:		Nonrobust				
	coef	std err	t	P>|t|	[0.025	0.975]
Intercept	12.5578	3.327	3.774	0.000	6.017	19.099
Time	-0.8547	0.093	-9.164	0.000	-1.038	-0.671
AMB	0.8630	0.052	16.538	0.000	0.760	0.966
ANGLE	0.2157	0.030	7.238	0.000	0.157	0.274
Omnibus:		3.119		Durbin-Watson:		0.219
Prob (omnibus):		0.210		Jarque-Bera (JB):		3.516
Skew:		-0.020		Prob (JB):		0.172
Kurtosis:		3.455		Cond. No.		578.

From Table 4.21, above coefficient of the intercept is 12.56, which implies that there is a unit increase in the temperature of the roofing material for every increase in other variables that are not included in the model, while the other independent variables were held constant. It can be deduced that the coefficient of the Time is -0.86, there is a decrease in the unit temperature of the roofing material as time increase from 9:00 to 24:00, while the other variables were held constant.

It also shows that the ambient temperature (AMB) coefficient is 0.863, which means there is an increase in the unit temperature of the roofing material as the ambient temperature increases, while other variables are held constant. While on further observation from in the table, the configuration angle coefficient is 0.216, which means there is an increase in the unit temperature of the roofing material for every increase in the angle of configuration in the order of 30^0, 45^0 and 60^0, while other variables are held constant. The coefficient of p values shows that the coefficients are statistically significantly different from zero since all the values is less than 0.05.

Coefficient of Determination (R^2) depicted in the table has a value of 0.56 that shows the measure of the overall strength of the model. It can be observed that since the R^2 is approximately 0.6, which is not far from 1, it can be concluded that the model is adequate in determining the temperature of roofing material based on the experimentally observed independent variables. There are indications also that these factors are not the only factors responsible for the thermal conditions of the roofing material.

The table further shows that the null hypothesis F test affirms that all the model coefficients are equal to Zero. Since the p value for the f test is <0.00 which is less than 0.05, it showed that all the coefficients are none zero, which implies there is a correlation between the selected independent variables and the temperature of the roofing material.

4.5.6.3.2: MODEL 2: To predict temperature of ceiling material based on ambient temperature and time (GMT) for the different combinations

To predict temperature based on thermo-physical properties, a mathematical equation was formulated. Thus, equation 4.9 present a developed modelling for determine the temperature reaching the roof ceiling at certain period with respect to the angle of inclinations.

$$Y_i = \beta_0 + \beta_1 X_{i1} + \beta_2 X_{i2} + \beta_3 X_{i3} \quad \ldots \quad 4.9$$

where Y_i is Temperature of Ceiling Material, X_1 is Time, X_2 is Ambient Temperature, X_3 is Angle of configuration; β_0 is the intercept of the fit, while $\beta_1 - \beta_3$ are the coefficient of the independent variables.

After fitting the factors and the temperature in a regression model and deriving their respective coefficient. The equation 4.10 summarized their relationship as presented below:

$$SRM = 4.2517 - 0.2162X_1 + 0.9371X_2 + 0.0782X_3 \quad \ldots \quad 4.10$$

Therefore, the model's variables coefficient values are usually use for assessing the impact of factors on temperature of the ceiling materials irrespective of the selected combinations are presented in Table 4.22.

Table 4.22: Summary of linear regression model parameters

Dep. Variable:		AS		R-Squared:		0.729
Model:		OLS		Adj. R-Squared:		0.727
Method:		Least Squares		F-Statistic:		359.1
Date:		Sat, 18 Feb. 2023		Prob (F-Statistic):		3.35e-113
Time:		17:37:18		Log-Likelihood:		-1160.5
No. Observations:		405		AIC:		2329.
Df. Residuals:		401		BIC:		2345.
Df. Model:		3				
Covariance Type:		Nonrobust				
	coef	std err	t	P>|t|	[0.025	0.975]
Intercept	4.2517	2.056	2.068	0.039	0.209	8.294
Time	-0.2162	0.058	-3.750	0.000	-0.329	-0.103
AMB	0.9371	0.032	29.060	0.000	0.874	1.001
ANGLE	0.0782	0.018	4.248	0.000	0.042	0.114
Omnibus:		32.933		Durbin-Watson:		0.395
Prob (Omnibus):		0.000		Jarque-Bera (JB):		120.894
Skew:		-0.215		Prob (JB):		5.60e-27
Kurtosis:		5.624		Cond. No.		578.

From Table 4.22, above coefficient of the intercept is 4.252, which implies that there is a unit increase in the temperature of the ceiling material for every increase in other variables that are not included in the model, while the other independent variables were held constant. It was revealed that the coefficient of the Time is -0.22, there is a decrease in the unit temperature of the ceiling material as time increase from 9:00 to 24:00, while the other variables were held constant.

It also shows that the ambient temperature (AMB) coefficient is 0.937, which means there is an increase in the unit temperature of the ceiling material as the ambient temperature increases, while other variables are held constant. While further observation from in the table show that the configuration angle coefficient is 0.078, which means there is an increase in the unit temperature of the ceiling material for every increase in the angle of configuration in the order of 30^0, 45^0 and 60^0, while the other variables are held constant. The coefficient of p values shows that the coefficients are statistically significantly different from zero since all the values is less than 0.05.

Coefficient of Determination (R^2) depicted in the table has a value of 0.729 that shows the measure of the overall strength of the model. It can be observed that since the R^2 is approximately 0.7, which is not far from 1, it can be concluded that the model is adequate in determining the temperature of ceiling material based on the experimentally observed independent variables. There are indications also that these factors are not the only factors responsible for the thermal conditions of the ceiling material.

The table further shows that null hypothesis F test affirmed that all the model coefficients are equal to Zero. Since the p value for the f test is <0.00 which is less than 0.05, it can be inferred that all the coefficients are none zero, which implies there is a relationship among the selected independent variables and the temperature of the ceiling material.

4.5.6.3.3: MODEL 3: To predict temperature of Air Space (AS) based on ambient temperature and time (GMT) for the different combinations.

To predict temperature based on thermo-physical properties, a mathematical modelling was adopted. The formulated model is denoted by equation 4.11 as showed below:

$$Y_i = \beta_0 + \beta_1 X_{i1} + \beta_2 X_{i2} + \beta_3 X_{i3} \quad \ldots \quad 4.11$$

where Y_i is Temperature of Air Space, X_1 is Time, X_2 is Ambient Temperature, X_3 is Angle of configuration; β_0 is the intercept of the fit, while $\beta_1 - \beta_3$ are the coefficient of the independent variables.

After fitting the factors and the temperature in a regression model and deriving their respective coefficient. The correlation is summarised in equation 4.12 as described below:

$$SRM = 12.5578 - 0.8547X_1 + 0.8630X_2 + 0.2157X_3 \quad \ldots \quad 4.12$$

The model's variables coefficients represent the values for assessing the impact of factors on temperature of the Air Spaces irrespective of the selected combinations are presented in Table 4.23.

Table 4.23: Summary of linear regression model parameters

Dep. Variable:	SRM	R-Squared:	0.562
Model:	OLS	Adj. R-Squared:	0.599
Method:	Least Squares	F-Statistic:	171.6
Date:	Sat, 18 Feb. 2023	Prob (F-Statistic):	1.48e-71
Time:	17:37:23	Log-Likelihood:	-1355.4
No. Observations:	405	AIC:	2719.
Df. Residuals:	401	BIC:	2735.
Df. Model:	3		
Covariance Type:	Nonrobust		

	coef	std err	t	P>|t|	[0.025	0.975]
Intercept	12.5578	3.327	3.774	0.000	6.017	19.099
Time	-0.8547	0.093	-9.164	0.000	-1.038	-0.671
AMB	0.8630	0.052	16.538	0.000	0.760	0.966
ANGLE	0.2157	0.030	7.238	0.000	0.157	0.274

Omnibus:	3.119	Durbin-Watson:	0.219
Prob (Omnibus):	0.210	Jarque-Bera (JB):	3.519
Skew:	-0.020	Prob (JB):	0.172
Kurtosis:	3.455	Cond. No.	578.

From Table 4.23, above coefficient of the intercept is 12.56, which implies that there is a unit increase in the temperature of the Air Space for every increase in other variables that are not included in the model, while the other independent variables are held constant. It was revealed that the coefficient of the Time is -0.86, this imply a unit temperature decrease of the Air Space as time increases from 9:00 to 24:00, while other variables are held constant.

It also shows that the ambient temperature (AMB) coefficient is 0.86, which means there is an increase in the unit temperature of the Air Space as the ambient temperature increases, while other variables are held constant. While further observation show that the configuration angle coefficient is 0.216, which implies there is an increase in the unit temperature of the Air Space for every increase in the angle of configuration in the order of 30^0, 45^0 and 60^0, while holding the other variables constant. The coefficient of p values shows that the coefficients are statistically significantly different from zero since all the values is less than 0.05.

Coefficient of Determination (R^2) depicted in the table has a value of 0.56 that shows the measure of the overall strength of the model. It can be observed that since the R^2 is approximately 0.6, which is not far from 1, it can be concluded that the model is adequate in determining the temperature of Air Space based on the experimentally observed independent variables. There are indications also that these factors are not the only factors responsible for the thermal conditions of the Air Space.

The table further shows that null hypothesis F test proved that all the model coefficients are equal to Zero. Since the p value for the f test is <0.00 which is less than 0.05, it is therefore, concluded that all the coefficients are none zero, which indicate there is a relationship amongst the selected independent variables and the temperature of the Air Space.

4.5.6.4: Derivation of mathematical model for Aluminium roof Configurations Combination: ARS Vs {POP, GYP, PVC, ASB, PLW}

4.5.6.4.1: MODEL 1: To predict temperature of Selected Roofing Material (SRM) based on ambient temperature and time (GMT) for the different combinations.

To predict temperature based on thermo-physical properties, a mathematical model was established. The is denoted by equation 4.13:

$$Y_i = \beta_0 + \beta_1 X_{i1} + \beta_2 X_{i2} + \beta_3 X_{i3} \quad \ldots \quad 4.13$$

where Y_i is Temperature of Roofing Material, X_1 is Time, X_2 is Ambient Temperature, X_3 is Angle of configuration; β_0 is the intercept of the fit, while $\beta_1 - \beta_3$ are the coefficient of the independent variables.

After fitting the factors and the temperature in a regression model and deriving their corresponding coefficient. The equation 4.14 summarized their relationship as presented below:

$$SRM = -3.0039 - 0.7229X_1 + 1.5649X_2 - 0.065X_3 \quad \ldots \quad 4.14$$

The model's variables coefficients are the values used for assessing the impact of factors on temperature of the roofing materials irrespective of the selected combinations are presented in table 4.24.

Table 4.24: Summary of linear regression model parameters

Dep. Variable:	SRM	R-Squared:	0.878
Model:	OLS	Adj. R-Squared:	0.877
Method:	Least Squares	F-Statistic:	959.3
Date:	Fri, 24 Feb. 2023	Prob (F-Statistic):	1.60e-182
Time:	01:22:02	Log-Likelihood:	-997.75
No. Observations:	405	AIC:	2003.
Df. Residuals:	401	BIC:	2020.
Df. Model:	3		
Covariance Type:	Nonrobust		

	coef	std err	t	P>|t|	[0.025	0.975]
Intercept	-3.0039	1.367	-2.197	0.029	-5.692	-0.316
Time	-0.7229	0.036	-19.818	0.000	-0.795	-0.651
AMB	1.5649	0.032	48.836	0.000	1.502	1.628
ANGLE	-0.0065	0.012	-0.560	0.576	-0.029	0.016

Omnibus:	21.044	Durbin-Watson:	0.508
Prob (Omnibus):	0.000	Jarque-Bera (JB):	23.202
Skew:	0.585	Prob (JB):	9.16e-06
Kurtosis:	3.068	Cond. No.	570.0

From Table 4.24, above coefficient of the intercept is -3.0039, which implies that there is a decrease in the unit temperature of the roofing material for every increase in other variables that are not included in the model, while the other independent variables are held constant. Further observation revealed that the coefficient of the Time is -0.7229, showing a decrease in the unit temperature of the roofing material as time increase from 9:00 to 24:00, while other variables are held fixed.

It also shows that the ambient temperature (AMB) coefficient is 1.5649, which means there is an increase in the unit temperature of the roofing material as the ambient temperature increases, this is in tandem with (Harimi, Harimi, Kurian, and Nurmin, 2005) findings, while other variables are held constant. While further observation from the table shows that the configuration angle coefficient is -0.0065, which implies there is a decrease in the unit temperature of the roofing material for every increase in the angle of configuration in the order of 30^0, 45^0 and 60^0, while the other variables were held constant. The coefficient of p values shows that the coefficients are statistically significantly different from zero since all the values is less than 0.05, expect for angle of configuration. This implies that the angle of configuration does not significantly affect the temperature of Air Space based on the combined SRM and SCM.

Coefficient of Determination (R^2) depicted in the table has a value of 0.878 that shows the measure of the overall strength of the model. It can be observed that since the R^2 is approximately 0.9, which is not far from 1, it can be concluded that the model is adequate in determining the temperature of roofing material based on the experimentally observed independent variables. There are indications also that these factors are not the only factors responsible for the thermal conditions of the roofing material.

The table further shows that null hypothesis F test proved that all the model coefficients are equal to Zero. Since the p value for the f test is <0.00 which is less than 0.05, the conclusion is that not all coefficients are equal to zero, this denote there is a relationship among the selected independent variables and the temperature of the roofing material.

4.5.6.4.2: MODEL 2: To predict temperature of Selected Ceiling Material (SCM) based on ambient temperature and time (GMT) for the different combinations

To predict temperature based on thermo-physical properties, a mathematical model was developed. The equation 4.15 represented the formulated model for the prediction of ceiling temperature at a given period with a specific inclination angle.

$$Y_i = \beta_0 + \beta_1 X_{i1} + \beta_2 X_{i2} + \beta_3 X_{i3} \quad \ldots \quad 4.15$$

where Y_i is Temperature of Ceiling Material, X_1 is Time, X_2 is Ambient Temperature, X_3 is Angle of configuration; β_0 is the intercept of the fit, while $\beta_1 - \beta_3$ are the coefficient of the independent variables.

After fitting the factors and the temperature in a regression model and deriving their respective coefficient. The relationship is summed up in the equation 4.16 as presented below:

$$SCM = -0.644833 + 0.081303X_1 + 1.019626X_2 - 0.010241X_3 \quad \ldots \quad 4.16$$

The model's variables coefficients values used for assessing the impact of factors on temperature of the ceiling materials irrespective of the selected combinations are presented in table 4.25.

Table 4.25: Summary of linear regression model parameters

Dep. Variable:	SRM	R-Squared:			0.953
Model:	OLS	Adj. R-Squared:			0.953
Method:	Least Squares	F-Statistic:			2728.
Date:	Sat, 18 Feb. 2023	Prob (F-Statistic):			2.62e-266
Time:	17:37:23	Log-Likelihood:			-575.26
No. Observations:	405	AIC:			1159.
Df. Residuals:	401	BIC:			1175.
Df. Model:	3				
Covariance Type:	Nonrobust				

	coef	std err	t	P>|t|	[0.025	0.975]
Intercept	-0.6448	0.482	-1.339	0.181	-1.592	0.302
Time	0.0813	0.013	6.326	0.000	0.056	0.107
AMB	1.0196	0.011	90.310	0.000	0.997	1.042
ANGLE	-0.0102	0.004	-2.507	0.013	-0.018	-0.002

Omnibus:	3.119	Durbin-Watson:	1.072
Prob (Omnibus):	0.210	Jarque-Bera (JB):	1.3237.315
Skew:	-0.020	Prob (JB):	0.00
Kurtosis:	3.455	Cond. No.	570.

From Table 4.25, the intercept coefficient is -0.644833, which implies a unit temperature decrease of the ceiling material for every increase in other variables that are not included in the model, while the other independent variables are held constant. Further observation shows that the coefficient of the Time is 0.081303, showing a unit temperature decrease of the ceiling material as time increases from 9:00 to 24:00, while other variables are held constant.

It also shows that the ambient temperature (AMB) coefficient is 1.019626, which implies there is an increase in the unit temperature of the ceiling material as the ambient temperature increases, (Lawal, Akinpade, and Makinde, 2017), while other variables are held constant. While further observation from the table show that the configuration angle coefficient is -0.010241, which signifies that there is a decrease in the unit temperature of the ceiling material for every increase in the angle of configuration in the order of 30^0, 45^0 and 60^0, while other variables remain constant. The coefficient of p values shows that the coefficients are statistically significantly different from zero since all the values is less than 0.05, expect for intercept. This implies that the other factors that were not considered for the model do not significantly affect the temperature of Air Space based on the combined SRM and SCM.

Coefficient of Determination (R^2) depicted in the table has a value of 0.953 that shows the measure of the overall strength of the model. It can be observed that since the R^2 is approximately 1, it can be concluded that the model is adequate in determining the temperature of ceiling material based on the experimentally observed independent variables. There are indications also that these factors are not the only factors responsible for the thermal conditions of the ceiling material.

The table further shows that null hypothesis F test affirmed that all the model coefficients are equal to Zero. Since the p value for the f test is <0.00 which is less than 0.05, the conclusion is that not all the coefficients are equal to zero, this means there is a relationship among the selected independent variables and the temperature of the ceiling material.

4.5.6.4.3: MODEL 3: To predict temperature of Air Space (AS) based on ambient temperature and time (GMT) for the different combinations.

To predict temperature based on thermo-physical properties, a mathematical modelling was formulated. The equation 4.17 is the model for predicting temperature at the air space, as depicted in the equation below.

$$Y_i = \beta_0 + \beta_1 X_{i1} + \beta_2 X_{i2} + \beta_3 X_{i3} \quad \ldots \quad 4.17$$

where Y_i is Temperature of Air Space, X_1 is Time, X_2 is Ambient Temperature, X_3 is Angle of configuration; β_0 is the intercept of the fit, while $\beta_1 - \beta_3$ are the coefficient of the independent variables.

After fitting the factors and the temperature in a regression model and deriving their respective coefficient. Hence, equation 4.18 summarized their relationship as presented below:

$$AS = 0.6819 - 0.044X_1 + 1.0617X_2 - 0.028X_3 \quad \ldots \quad 4.18$$

The model's variables coefficient values are used for assessing the impact of factors on temperature of the Air Spaces irrespective of the selected combinations are presented in Table 4.26.

Table 4.26: Summary of linear regression model parameters

Dep. Variable:	SRM	R-Squared:	0.965
Model:	OLS	Adj. R-Squared:	0.965
Method:	Least Squares	F-Statistic:	3718
Date:	Fri, 24 Feb. 2023	Prob (F-Statistic):	3.49e-292
Time:	01:54:12	Log-Likelihood:	-531.54
No. Observations:	405	AIC:	1071.
Df. Residuals:	401	BIC:	1087.
Df. Model:	3		
Covariance Type:	Nonrobust		

	coef	std err	t	P>|t|	[0.025	0.975]
Intercept	0.6819	0.432	1.577	0.116	-0.168	1.532
Time	-0.0436	0.012	-3.780	0.000	-0.066	-0.021
AMB	1.0617	0.010	104.754	0.000	1.042	1.082
ANGLE	-0.0426	0.004	-7.605	0.000	-0.035	-0.021

Omnibus:	73.589	Durbin-Watson:	0.525
Prob (Omnibus):	0.000	Jarque-Bera (JB):	178.117
Skew:	0.906	Prob (JB):	2.10e-39
Kurtosis:	5.696	Cond. No.	570.

From Table 4.26, coefficient of the intercept is 0.6819, which implies that there is an increase in the unit temperature of the ceiling material for every increase in other variables that are not included in the model, while the other independent variables were held constant. Further observation revealed that the coefficient of the Time is -0.044, this implies a decrease in the unit temperature of the ceiling material as time increase from 9:00 to 24:00, while other variables are held constant.

It shows also that the ambient temperature (AMB) coefficient is 1.062, which means there is a unit increase in the temperature of the ceiling material for every rise in the ambient temperature, which in accordance with (Lawal, Akinpade, & Makinde, 2017) findings, while other variables are constant. While further observation from the table revealed that the configuration angle coefficient is -0.028, which implies there is a decrease in the unit temperature of the ceiling material for every increase in the angle of configuration in the order of 30^0, 45^0 and 60^0, while other variables remain constant. The coefficient of p values shows that the coefficients are statistically significantly different from zero since all the values is less than 0.05, expect for intercept. This implies that the other factors that were not considered for the model do not significantly affect the temperature of Air Space based on the combined SRM and SCM.

Coefficient of Determination (R^2) depicted in the table has a value of 0.965 that shows the measure of the overall strength of the model. It can be observed that since the R^2 is approximately 1, it can be concluded that the model is adequate in determining the temperature of ceiling material based on the experimentally observed independent variables. There are indications also that these factors are not the only factors responsible for the thermal conditions of the ceiling material.

The table further shows that null hypothesis F test showed that all the model coefficients are equal to Zero. Since the p value for the f test is <0.00 which is less than 0.05, the conclusion show that all the coefficients are none zero, which shows there is a correction between the selected independent variables and the temperature of the ceiling material.

4.5.7.1 Regression model for SCS and POP roof configuration

Table 4.27 presents the regression model for the combination of SCS and P.O.P, the result revealed R, of 0.89 which is a correlation value between SCS and POP. The R value that SCS and POP are highly correlated. The R^2 of 0.89 shows that the SCS and POP accounted for 89.0% of the total variance that occurred in the Model leaving remaining 11.0% to error of other variables that were not in the model. The F value equally shows that the combination of POP and SCS allowed reliable prediction of Ambient internal temperature $F_{(4,493)} = 519.897$, $p < 0.001$)

Table 4.27: Combination of POP and stone coated roofing sheet

Model		Sum of squares	df	Mean Square	F	Sig.
1	Regression	3327.914	4	831.979	519.897	.000[b]
	Residual	788.935	493	1.600		
	Total	4116.850	497			

Model Summary: Model 1; R .899[a]; R Square .808; Adjusted R Square .807; Std. Error of the Estimate1 .26502

Table 4.28: Summary for combination of POP and SCS

Model		Unstandardised Coefficients		Standardised Coefficients	T	Sig.
		B	Std. Error	Beta		
	(Constant)	8.726	1.584		-5.508	.000
	POP	-.444	.206	-.250	-2.152	.032
	AIRSPACE	2.886	.233	1.998	12.375	.000
	SRS	.047	.018	.134	2.594	.010
	AMBOUT	-2.077	.066	-2.054	-31.698	.000

a. Dependent Variable: HEIGHT

Table 4.28: shows the model Summary for the prediction of optimal ambient internal temperature for the combination of POP and SCS. The result shows that the internal ambient temperature to achieve maximum comfortability for materials with the same parameters as SCS and POP is 8.726.

Using a regression model $Y= c+X_1+X_2+X_3……+e$

where C is a constant representing the air space height within the roof and the ceiling. Then y is internal Temperature T_{in}, X_1 is Temperature on the P.O.P T_{POP}, X_2 is Temperature at air space, X_3 is Temperature on the stone coated sheet, while X_4 is Temperature outside T_{AMB}.

$$Y = 8.73-444X_1+2.886X_2+0.047X_3-2.077X_4 \quad \ldots \quad 4.20$$

The mathematical expression implied that for optimum internal ambient for POP and SCS combinations, the air space must be put at 8.726m. This also applicable to the materials with similar thermal properties.

Trigonometrically, the inclination angle gave 60°. This is in line with optimal pitch angle for self-support roof trusses which is said to be 55^0. (Mijinyawa, Adesogan , & Ogunkoya , 2007).

Table 4.29: Combination of roofing material (long span) and ceiling (asbestos)

Model		Sum of squares	df	Mean Square	F	Sig.
1	Regression	3190.322	4	797.580	257.815	.000[b]
	Residual	1605.588	519	3.094		
	Total	4795.910	523			
Model Summary						
Model		1				
R		.816[a]				
R Square		.665				
Adjusted R Square		.663				
Std. Error of the Estimate		1.7588				

4.5.7.2 Regression model for ARS and ASB roof configuration

Table 4.29 presents the regression model for the combination of ARS and ASB, the result revealed R, of 0.82 which is a correlation value between ARS and ASB. The R value that ARS and ASB are highly correlated. The R^2 of 0.67 shows that the ARS and ASB accounted for 67.0% of the total variance that occurred in the Model leaving remaining 23.0% to error of other variables that were not in the model. The F value equally shows that the combination of ARS and ASB allowed reliable prediction of Ambient internal temperature $F(4,519) = 257.815$, $p < 0.001$)

Table 4.30: Model summary for combination of ARS and ASB

Model		Unstandardised Coefficients		Standardised Coefficients	T	Sig.
		B	Std. Error	Beta		
1	(Constant)	39.486	3.015		13.096	.000
	ASB	-.026	.005	-.153	-5.674	.000
	AIRSPACE	-4.848	.230	-2.095	-21.082	.000
	ARS	3.656	.140	2.553	26.028	.000
	AMBOUT	.000	.001	-.017	-.653	.514

a. Dependent Variable: HEIGHT

Table 4.30: shows the model summary for the prediction of ambient internal temperature for the combination of ASB and ARS. The result shows that for the ambient temperature to achieve maximum comfortability for these materials or any with the same parameters as ARS and ASB, the constant C, must be 39.48m.

Using a regression model $Y= c+X_1+X_2+X_3……+e$ where C is a constant representing the air space height within the roof and the ceiling. Therefore, to achieve internal ambient for combination ARS and ASB the air space must be put at 39.48m, applicable to other materials with similar thermal parameters.

$$Y = 39.486-0.26X_1-4.848X_2+3.656X_3+1.000X_4 \quad \ldots \quad 4.21$$

The implication of this result is that thermal comfortability through this configuration and similar roofing and ceiling parameters will only achieve desired comfortability unless the air space height is 39.48m, which is extremely impossible.

4.5.8 Model validation

The field data was used to validate the model obtained from the laboratory. Data validated was in term with the existing literature after comparison.

4.5.8.1 Roof height

The modelled optimal roof height is given as 8.72m for stone coated roofing and P.O.P ceiling with similar parameters, this compared favorably with prevailing roof height in this same region.

4.5.8.2 Roof angle

The modelled comfort roof angle was given to be 74.6°, which validate that the optimum comfortability angle should not be less than 45° to 60°. This result is in tandem with 55° pitch angle recommended by Adesogan (2012).

The model and the result of the prediction show that SRM and SCM are responsive to the temperature and angle of inclination. This implies that there are two major factors that determine the conduciveness of the combination of roofing and ceiling material chosen for a house covering in Nigeria. Also, the result also gives allowance for other external factors

which could be dependent on the regional differences in Nigeria. This result aligns with the findings of Ogah and Josiphiah (2015) who reported that roofing and ceiling material and style should be dependent upon the regional availability of materials and climatic conditions.

CHAPTER FIVE

SUMMARY, CONCLUSION AND RECOMMENDATIONS

5.1 Summary

According to empirical findings thus far, the following conclusions and recommendations have been made as optimal combinations between the selected roofing materials (SRM) and the selected ceiling materials (SCM) for moderate internal building comfort in Ibadan, Nigeria. The chosen roofing sheets SRS underwent testing based on UNE EN Standard. This was done to assess the thermo-physical qualities of the Stone Coated Sheet (SCS), the Aluminum Roofing Sheet (ARS), and the Plywood-line Aluminium roofing (PLAR), while the Selected Ceiling Materials (SCM) were utilizing ASTM standards. To create the Optimum Comfortability Roof (OCR), fieldwork was conducted on an enclosed model using three different roofing materials and five different ceiling underlays at angles of 30°, 45°, and 60°, respectively.

The thermal conductivity (TC) of PLAR, SCS, and ARS affects how much heat passes through these sample materials, which in turn affects how much heat is absorbed or released into the interior space. The TR, TA, SHC, and TD all significantly affect how quickly heat enters the sample materials.

While SCS and PLAR values were reasonably high between the hours of 11:30am and 3:30pm in all the months under consideration when this experiment was done, TA was noticeably low in all the sampled Aluminium roofing sheets ARS. TE in PLAR was (=0.73) around 20%, whereas SCS (ST-A (=0.78) and ST-B (=0.72)) account for over 25% and less than 30% of heat ingress, respectively. In contrast, ARS (CH-A, MT-A, BT-A, SU-A, and GAL-A) account for 65% to 70% of heat penetration into the interior area. All aluminum roofing sheets, particularly the CH-A0.45 and GAL-A, have low TR, rendering them unsuitable for usage in residential structures. Like how ASB has a higher TR than other

sampled ceilings, it traps more heat in the room. Although the TC in P.O.P and PVC, positioned them to be better insulators of heat.

5.2 Conclusion

1. Thermo-physical properties (TC, TR TD, SHC and TA) of PLAR and SCM offered a suitable heat performance as roofing and ceiling material, as stipulated by ASME and ISO 7730, standard.
2. PLAR exhibited good lagging property in regulating heat influx to the indoor space.
3. The Optimum Comfortability Roof (OCR) was obtained through roof configured between PLAR, SCS with POP or PVC at angle between 45 and 60°, as stipulated by ISO 7730 Standard.
4. Predictive model developed for PLAR, SCS and ARS also provided OCR, adequate for residential buildings in Ibadan.

5.3 Recommendations

The following recommendations were drawn:

i. PLAR should be used in tropical zones for optimal internal ambient temperature.
ii. Adequate lining of all types of ARS before installation for comfortability of every individual, should be ensure for optimal ambient internal temperature.
iii. All roofing sheets should not be use in isolation but be lined with plywood to act as an insulator and barrier to heat influx through the roof.
iv. Established roof configuration angle should be between 45° and 60°, for maximum internal ambient comfort temperature between 22 - 29° based on ISO standard.

5.4 Contributions to knowledge

This research will contribute immensely to the building construction industry and act as template by government for roof design specifications for both state and federal housing authorities. The following are the contributions to knowledge.

i. Generation of thermophysical data for various locally available roofing sheets and ceiling material that can provide information and template for professionals in the built environment that will ensure adequate roofing materials in Ibadan.

ii. Provision of appropriate roof configurations that will offer acceptable optimum comfortability roof OCF, in the residential buildings in Ibadan.

iii. Provision of validation of statistical models to predict temperature of roofing material, temperature of ceiling material and the temperature of air space at any given time for different roof combinations.

REFERENCES

Adesogan, S. O. (2018). A Study of Roof Failures in and around Ibadan, Nigeria: Causes, Effects and Remedy. *Current Journal of Applied Science and Technology*, 1-10.

Agboola, O. P., and Zango, M. S. (2014). "Development Of Traditional Architecture In Nigeria: A Case Study Of Hausa House Form". *International Journal of African Society Cultures and Traditions Vol.1, No.1*, 61-74.

Akbari, H., and Konopacki, S. (2015). The impact of reflectivity and emissivity of roofs on building cooling and heating energy use. *Research gate*.

Akshaya, S., Harish, S., Arthy, R., Muthu , D., and Venkatasubramanian , C. (2017). Improving Thermal Performance of a Residential Building, Related to Its Orientations - A Case Study. *Earth and Environmental Science*.

Akshaya, S., Harish, S., Arthy, R., Muthu , D., and Venkatasubramanian , C. (2017). Improving Thermal Performance of a Residential Building, Related to Its Orientations - A Case Study. *IOP Conf. Series* (pp. 80-81). Thanjavur: IOP.

Alam, M., Rahman, S., Halder, P. K., Raquib, A., and Hasan, M. (2016). Lee's and Charlton's Method for Investigation of Thermal Conductivity of Insulating Materials. *Mechanical and Civil Engineering*, 53-60.

Albatayneh, A., Mohaidat, S., Alkhazali, A., Dalalah, Z., and Bdour, M. (2018). The Influence of Building's Orientation on the Overall Thermal Performance. *The Academic Research Community Publication*, 1-7.

Alcivar M, A. A., Ramos J, L. M., and Velez D, E. A. (2022). Influence of the orientation and the angle of inclination in the metal roof. *Linguistics and Culture review, 6 (S3)*, 140-157.

Al-Sanea, S. A. (2002). Thermal performance of building roof elements. *Building and Environment*, 665-675.

Ariyadasa, G., Muthurathne, S., and Adikary, S. (2015). Investigating the Physical, Mechanical and Thermal Properties of Common Roofing Materials in Sri Lanka. *innovations for resilient environment*.

ASHRAE, 5. (2004). Thermal environmental conditions for human occupancy. *America national standards institute, ANSI*, 2-25.

Ayinla, K. A., and Odetoye , A. S. (2015). Climatic Pattern and Design for Indoor Comfort in Ogbomoso, Nigeria. *Environment and Earth Science*, 30-37.

Badejo, S. O. (2002). Manufacturing of building materials from sawdust. *Invited paper presented at National workshop on "An Investors' Forum" jointly*.

Badejo, S. O., and Giwa, S. A. (1985). Volume assessment and economic importance of sawmill wood waste utilization in Nigeria. *Technical Report No. 50. Forestry Research Institution of Nigeria. Ibadan.*

Barozzi , B., Bellazzi , A., Maffè , C., and Pollastro, M. C. (2017). Measurement of Thermal Properties of Growing Media for Green Roofs: Assessment of a Laboratory Procedure and Experimental Results. *Buildings*.

Barry, R. (1999). *The construction of Buildings, vol.1 seventh edition.* Oxford: Blackwell Science ltd.

Bekkouche, S. E., Benouaz, T., Cherier, M. K., Hamdani, M., Yaiche, R. M., and Khanniche, R. (2013). Influence Of Building Orientation On Internal Temperature In Saharian Climates, Building Located In Ghardaia Region (Algeria). *Thermal Science*, 349-364.

Bisam, A.-h., Marjorie, M., and Turki, H. (2017). A Study on the Impact of Changes in the Materials Reflection Coefficient for Achieving Sustainable Urban Desig. *Science direct*, 256-270.

Björk, D. F. (2004). *Green roofs effect on durability of roof membranes.* City of Malmö, Sweden: Publication No 006 ISBN 91-973489-5-3.

Blue scope. (2021). *Building materials, thermal effeciency and reflectivity.* Makati: steel direct.

Calderon, U. F. (2019). Evaluacion del mejoramiento del confort termico con la incorporacion de materiales sostenibles en viviendas en autoconstruccion en Bosa, Bogota. *Revista habitat sustentable, 9(2)*, 30-41.

Chudley, R., and Greeno, R. (2004). *Building construction handbook.* Burlington: Elsevier Butterworth-Heinemann.

Cobo, F. C., and Montoya, F. O. (2021). Tuhouse: high-density sustainable social housing prototype for the tropics. *Sustainable habitat magazine 11 (1)*, 32-43.

Couto, G. M., Dessimoni, A. d., Bianchi, M. L., Perígolo, D. M., and Trugilho, P. F. (2012). Use Of Sawdust Eucalyptus sp. In The Preparation Of Activated Carbons. *Utilização de serragem de Eucalyptus sp. na preparação de carvões ativados*, 69-77.

D'Orazio, M., Di Perna, C., Di Giuseppe, E., and Morodo, M. (2012). Thermal performance of an insulated roof with reflective insulation: Field tests under hot climatic conditions. *Building Physics*, 229–246.

Desjarlais, A. O., Petrie, T. W., and Atchley, J. A. (2008). Evaluating the Energy Performance of Ballasted Roof Systems. *Single Ply Roofing Industry*.

Egbinola, C. N., and Amobichukwu, A. C. (2013). Climate Variation Assessment Based on Rainfall and Temperature in Ibadan, South-Western, Nigeria. *Environment and Earth Science*.

Elewa, R. E., Afolalu, S. A., and Fayomi, O. S. (2019). Overview production process and properties of galvanized roofing sheet. *International conference on engineering for sustainable world* (pp. 1-11). Ota: IOP Publishing.

Eruola, A., Bello, N., Ufeogbune, G., and Makinde, A. (2013). Effect of Climate Variability and Climate Change on Crop Production in Tropical Wet-and Dry Climate. *Italian Journal of Agrometeorology*, 17-22.

Eruola, A., Bello, N., Ufeogbune, G., and Makinde, A. (2015). Effect of Climate Variability and Climate Change on Crop Production in Tropical Wet-and Dry Climate. *Italian Journal of Agrometeorology*, 15-22.

Ettah, E. B., Egbe, J. G., Takim, S. A., Akpan, U. P., and Oyom, E. B. (2016). Investigation of the Thermal Conductivity of Polyvinyl Chloride (Pvc) Ceiling Material Produced In Epz Calabar, For Application Tropical Climate Zones. *IOSR Journal of Polymer and Textile Engineering (IOSR-JPTE)*, 34-38.

FEMA 549. (2006). Roof Coverings and Best Practices. *Local Officials Guide For Coastal Construction*, 1-13.

Fema, P. 5. (2012). *Seismic Performance Assessment of Buildings.* Redwood City, Califonia: Applied Technology Council.

Fuchs, S., Balling, N., and Forster, A. (2015). Calculation of thermal conductivity, thermal diffusivity and specific heat capacity of sedimentary rocks using petrophysical well logs. *Geophysical Journal International*, 1977–2000.

George, N. J., Obianwu, V. I., Akpabio, G. T., and Obot, I. B. (2010). Comparison of Thermal Insulation Efficiency of some Selected Materials used as Ceiling in Building design. *IOSR Journal of Polymer and Textile Engineering* , 253-259.

German, C. (2010). Comparison of Thermal Insulation Materials. *ScienceDirect*, 39-41.

Harimi, M., Harimi, D., Kurian , V. J., and Nurmin , B. (2005). Evaluation Of The Thermal Performance Of Metal Roofing Under Tropical Climatic Conditions. *The 2005 World Sustainable Building Conference*, 27-29.

Humphreys, M. A., and Nicol, J. F. (1998). Understanding the Adaptive Approach to Thermal Comfort. *ASHRAE Transactions 104 (1)*, 991-1004.

Humphreys, M. A., Nicol, J. F., and Raja, I. A. (2007). Field Studies of Indoor Thermal Comfort and the Progress of the Adaptive Approach. *Advances In Building Energy Research*, 55-58.

Imaah, N. O. (2008). "The Natural and Human environments in Nigeria: Their Implications for Architecture. *Journal of Applied Sciences and Environmental Management." Vol.12, No2.*, 73.

ISO, 6. (2007). *Building components and building elements- Thermal resistance and thermal transmittance- Calculation method.* Switzerland: ISO Press.

Jackson , I. O., Isienyi , C. N., Osudiala , S. C., Odofin , T. B., Adeyemi, A. A., Odeleye , A. O., and Amoo , O. V. (2012). Analysis Of Temperature Trends Of Ibadan, Nigeria Over The Period of 1965-2013. *Journal of Forestry Research and Management. Vol.9*, 61-72.

Jayasingbe M, T. R., Attalage, R. A., and Jayawardena, A. I. (2003). Roof orientation, roofing materialss and roof surface colour: their influence on indoor thermal comfort in warm humid climate. *Energy for sustainable development, 7(1),* 16-27.

Jelle , B. P. (2012). Traditional, State-of-the-Art and Future Thermal Building Insulation Materials and Solutions - Properties, Requirements and Possibilities. *Building and Infrastructure*.

Jiboye, A. D., and Ogunshakin, L. (2010). The Place of the Family House in Contemporary Oyo Town, Nigeria. *Journal of Sustainable Development*, 117-122.

Joseph, , O. O., Dirisu, J. O., and Odedeji, A. E. (2021). Corrosion resistance of galvanized roofing sheets in acidic and rainwater environments . *Heliyon, 7*, 1-7.

Kale, Y. (2013). Annual abstract of statistics 2011. *National bureau of statistics*, 2-13.

Kochanowski, K., Oliferuk, W., Płochocki, Z., and Adamowicz, A. (2014). Determination Of Thermal Diffusivity Of Austenitic Steel Using Pulsed Infrared Thermography. A r c h i v e s o f M e t a l l u r g y a n d M a t e r i a l s, 893-897.

Kontoleon, K. J., and Bikas, D. K. (2007). "The Effect of South Wall's Outdoor Absorption Coefficient on Time Lag, Decrement Factor and Temperature Variations,". *Energy and Buildings*, 1011-1018.

Korniyenko, S. (2015). Evaluation of Thermal Performance of Residential Building Envelope. *International Scientific Conference Urban Civil Engineering and Municipal Facilities, SPbUCEMF*, 191-196.

Krüger, E. L., Givoni, B., Cheng, V., and Roriz, M. (2004). "Predicting Indoor Temperatures and Thermal Performance of Test Cells". *35th Congress on Heating, Refrigerating and Air-Conditioning (HVAC &R). Proceedings. Belgrade, Serbia, Vol 1*.

Krüger, E. L., Harimi, D., Harimi, M., Kurian, J., and Ideris, Z. (2005). Assessment of Thermal Performance of Roof System with Galnavized Steel in East Malaysia. *PLEA2005 - The 22nd Conference on Passive and Low Energy Architecture. Beirut, Lebanon.*

Kumar, V., Dixit, U. S., and Zhang, J. (2019). Determining thermal conductivity,specific heat capacity and absorptivity during laser based materials processing. *Journal homepage: www.elsevier.com/locate/measurement-ScienceDirect*, 213-225.

Lawal, A. F., and Ojo, O. J. (2011). Assessment of Thermal Performance of Residential Buildings in Ibadan Land, Nigeria. *Journal of Emerging Trends in Engineering and Applied Sciences (JETEAS) 2 (4)*, 581-586.

Lawal, A., Akinpade, J., and Makinde, A. (2017). Analysis of Climate of Southwestern Nigeria for Building Design. *International Journal of Constructive Research in Civil Engineering*, 1-7.

Luff, M. (1984). Energy Management – How a Brewing Group Does It. *Journal of Building Services and Environmental Engineering.*, 10-15.

Medina, M., Kaiser, E., Lopez, R., Domizio, C., and Santilan, L. (2021). Use of the thermal inertial of concrete for energy savings in buildings. *Technological Ingenuity, 3,* e018-e018.

Melisa, V. G., Walsh, C., and Barros, M. V. (2016). Qualitative-quantitative evaluation of alternative thermal insulation for housing: The case of family farming. *INVI Magazine 31(86),* 89-117.

Michels, C., Lamberts, R., and Guths, S. (2008). "Theoretical/Ex- perimental Comparison of Heat Flux Reduction in Roofs Achieved through the Use of Reflective Thermal Insulators,". *Energy and Buildings*, 438-444.

Mijinyawa, Y., Adesogan , S. O., and Ogunkoya , O. G. (2007). A survey of roof failures in Oyo State of Nigeria. *Building Appraisal* , 52 – 58.

Miller, A. W., Desiarlais, A., Parker, D. S., and Kringer, S. (2004). Cool metal roofing for energy efficiency and sustainability. *CIB World Building Congress, Toronto Canada.*

Miller, W., Keyhani, M., Stovall, T., and Youngquist, A. (2007). Natural Convection Heat Transfer in Roofs with above-sheathing ventilation. *ASHRAE*, 1-14.

Mohammad, A.-H. S. (2005). "Performance characteristics and Practical application of Common Building Thermal Insulation Materials. *Building and Environment*, 253, 266.

Mohelnikova, J. (2006). Determination of Specific Heat of a Building Material. *WSEAS TransactionS on HeaT and Mass TransfeR*, 789-791.

Mohsenin, N. N. (n.d.). Thermal properties of foods and agricultural materials. In N. N. Mohsenin, *Measurement of thermal conductivity* (pp. 86-87). New York: Gordon and breach science.

Morau, D., Libelle, T., and Garde, F. (2012). Performance Evaluation of Green Roof for Thermal Protection of Buildings In Reunion Island. *Conference on Advances in Energy Engineering* (pp. 1008 – 1016). Ile de La Réunion: Elsevier Ltd.

Newton, G. F., Roy, A. A., and Solomon, A. I. (2014). Investigation of the Thermal Insulation Properties of Selected Ceiling Materials used in Makurdi Metropolis (Benue StateNigeria). *American Journal of Engineering Research (AJER)*, 245-250.

Ogah, O. S., and Josiphiah, T. K. (2015). Comparative study of some engineering properties of aluminium roof sheets manufactured in Nigeria and china. *International Journal of engineering and computer science 4 (5),* 2076-2079.

Onyeaju, M. C., Osarolube, E., Chukwuocha, E. O., Ekuma, C. E., and Omasheye, G. J. (2012). Comparison of the Thermal Properties of Asbestos and Polyvinylchloride (PVC) Ceiling Sheets. *Materials Sciences and Applications,* 240-244.

Owonubi, J. J., and Badejo, S. O. (2000). Industrial Scale wood waste conversion into building materials at FRIN. *A paper presented at the 38th annual conference of Science Association of Nigeria 10th – 14th.* Ibadan.

Oyekunle , J. A., Dirisu, J. O., Okokpujie, I. P., and Asere, A. A. (2018). Determination Of Heat Transfer Properties Of Various Pvc And Non-Pvc Ceiling Materials Available In Nigerian Market. *International Journal of Mechanical Engineering and Technology (IJMET)*, 963–973.

Pasco Scientific. (1987). *Thermal conductivity aparatus.* Roseville: Foothills Blvd.

Pavlou, K. (2009, July 10). Thermal comfort in buildings.

Prakash, D., and Ravikumar, P. (2015). Optimisation Of Residential Roof Insulation Layer Thickness Base On Economic Analysis By Grey Relation Method. *Journal of Engineering Science and Technology*, 1589-1599.

Prescott, K. (2001). Thermal Comfort In School Buildings In The Tropics. *Environment Design Guide*, 1-5.

RomagnonI, P., and Peron, F. (2008). Impact of solar radiation on the temperature of thermal insulation materials in roof applications. *PU EUROPE excellence in insulation*.

Romero, R. V., Romero, N. V., and Romero, F. B. (2017). Insulated Metal Sheet Roofing. *Asia PacIfIc HIgher educatIon research*.

Sabino, N. (2016). Understanding thermal movement in residential metal roof systems is key to long-term performance. *Professional roofing magazine, Build it to last*.

Schlavon, S., Hoyt, T., and Piccioli, A. (2014). Web application for thermal comfort visualization and calculation according to ASHRAE Standard 55. *Building Simul*, 321-334.

Stathopoulos, T. (2006). Pedestrian level winds and outdoor human comfort. *Journal of wind engineering and industrial aerodynamics*, 769-780.

Synnefa, A., Santamouris, M., and Akbari, H. (2007). Estimating the effect of using cool coatings on energy loads and thermal comfort in residential buildings in various climatic conditions. *Energy and Building*, 1167-1174.

Thirumaran, K., and Mathew, J. (2017). *Determination of thermal performance of roof.* Trichy, Tamilnadu, India: Department of Architecture, National Institute of Technology.

TIOUGH, D. M. (2005). Recycling Sawdust Waste for Construction Purposes – Solution for Disposal Problems.

Uche, O. A., and Oyedipe, A. K. (2010). Investigation Into The Properties Of Long-Span Aluminium Roofing Materials Used In Construction Industries In Nigeria. *Engineering And Technology*.

Ujam, A. J., Egbuna , S. O., and Idogwu, S. (2014). Performance Characteristics of various Corrugated Roofing Sheets in Nigeria. *International Journal of Computational Engineering Research (IJCER)*, 27-39.

Van Lith, A. P., Entrop, A. G., and Halman, J. M. (2018). Assessment of the thermal performance of holistic flat roof systems of industrial buildings. *Journal of Construction Engineering, Management & Innovation*, 1-17.

Wang, M., He, J., Yu, J., and Pan, N. (2007). “Lattice Boltzmann Modeling of the Effective Thermal Conductivity for Fi- brous Material,”. *International Journal of Thermal Sciences*, 848-855.

Zapałowicz, Z. (2018). Simplified methodology to estimate the emissivity for roof covers. *Web of Conferences* (pp. 70-310). Szczecin: EDP Sciences.

Zbigniew, Z. (2018). Simplified methodology to estimate the emissivity for roof covers. *Web of Conferences* (pp. 70-310). Szczecin: al. Piastów.

Zhang, Y., Long, E., Li, Y., and Li, P. (2017). Solar radiation reflective coating material on building envelopes: Heat transfer analysis and cooling energy saving. *Energy exploration and exploitation*, 1-19.

Zheng, R., Janssens, A., Carmeliet, J., Bogaerts, W., and Hens, H. (2010). Performances of highly insulated compact zinc roofs under a humidmoderate climate – Part I: hygrothermal behavior. *Building Physics*, 178–191.

Appendix A

TABLE A.1

Comparison of thermal properties of the Selected Roofing Materials (SRM)

Samples	h(cm)	Density $P = \frac{m}{v}$	Conductivity $K = \frac{(Ro)(80cal/gm)(}{(A)(\Delta T)}$ x10^{-3} (Calcm/cm^2 sec°C)	Resistivity $r = \frac{1}{k}$	Specific heat capacity C x (10^3)	Diffusivity $\alpha = \frac{k}{c\rho}$
A	0.178	2369	0.232	4.310	3.164	3.095
B	0.224	1812	0.200	5.000	8.887	1.390
C	0.936	641.2	0.360	2.778	3.726	1.570
D	0.052	2544	0.190	5.263	5.847	1.277
E	0.048	2135	0.295	3.390	5.228	2.643
F	0.042	1887	0.182	5.560	4.756	2.028
G	0.053	2163.4	0.257	3.891	7.082	1.680
H	0.057	2012	0.036	27.78	6.832	0.262
I	0.072	1542.4	0.219	4.570	7.309	1.943
J	0.049	1978	0.280	3.571	6.883	2.057
K	0.029	6657	0.193	5.181	2.839	1.021

Source: Laboratory result 2021

TABLE A.2

Temperature variations for sampled roofing sheets

Steady temperature = 34℃

time	temperature variations in ℃											
x 60 sec	ST-A	ST-B	CH-A0.7	CH-A0.55	CH-A0.45	MT-A0.7	MT-A0.55	MT-A0.45	BT-A0.55st	BT-A0.55	SU-A	GAL-A
1	30.5	30	31.9	35	33.5	34.9	34.2	31.6	32.5	34.3	33.1	34.3
2	31.9	30.8	35.2	36.7	36.8	36.1	36.7	34.6	33.5	35.9	35.1	35.7
3	32.7	31.5	36.4	37	37.8	36.5	37.2	36.4	33.7	36.1	35.6	36
4	33.1	32.5	36.6	37	37.6	37.1	37	36.5	34.7	36	35.6	35.9
5	33.3	33.7	36.3	37.4	37.2	39.2	36.5	36.1	35.9	36.5	35.4	36.1
6	33.4	34.4	36	37.1	36.7	40.2	36	35.6	36.2	38	37.7	36.3
7	33.3	34.8	35.5	36.6	36.2	39.9	35.5	35.9	36	39.7	40	36.2
8	33.7	34.9	35.2	37.2	36.5	39.2	35	36.9	35.6	39.8	40.5	35.9
9	34.3	35	35.2	38.6	38.6	38.4	34.7	36.8	35.3	39.2	40.1	35.6
10	34.6	34.8	36.9	38.6	39.1	37.7	34.4	36.3	34.9	38.6	39.5	35.3
11	34.6	34.6	39.3	38	38.8	37.1	34.9	35.8	34.7	38	38.9	35
12	34.5	34.4	40	37.3	38.2	37.1	38.5	36.2	35.3	37.4	38.3	34.8
13	34.3	34.2	39.8	37.5	37.6	37.2	40.1	38	35.3	36.9	37.7	34.5
14	34.1	34.2	39.3	37.9	37	39.3	40	38.1	35.5	36.5	37.2	34.3
15	34.1	34.5	38.7	37.7	36.7	40.3	39.5	37.6	35	37.1	36.8	34.1

Source: Laboratory Results (2021)

APPENDIX B

TABLE B.1

Laboratory conductivity test for st-a sample

Channel Name	Ch1 Tout	Ch2 T-in
0day 00:15:00	34.1	40.6
0day 00:14:00	34.1	37.2
0day 00:13:00	34.3	37.9
0day 00:12:00	34.5	38.7
0day 00:11:00	34.6	39.7
0day 00:10:00	34.6	40.8
0day 00:09:00	34.3	42.5
0day 00:08:00	33.7	44.5
0day 00:07:00	33.3	38.6
0day 00:06:00	33.4	38.0

Source: laboratory analysis

TABLE B.2

Laboratory conductivity test for ST-B sample

Time Channel Name	No.1 Ch1 Tout	No.2 Ch2 T-in
0day 00:15:00	34.5	42.3
0day 00:14:00	34.2	43.0
0day 00:13:00	34.2	38.3
0day 00:12:00	34.4	38.5
0day 00:11:00	34.6	39.3
0day 00:10:00	34.8	40.2
0day 00:09:00	35.0	41.3
0day 00:08:00	34.9	42.4
0day 00:07:00	34.8	43.9
0day 00:06:00	34.4	45.6

TABLE B.3

Laboratory conductivity test for CH-A0.7 sample

Time Channel Name	No.1 Ch1Tout	No.2 Ch2 T-in
0day 00:15:00	34.1	40.6
0day 00:14:00	34.1	37.2
0day 00:13:00	34.3	37.9
0day 00:12:00	34.5	38.7
0day 00:11:00	34.6	39.7
0day 00:10:00	34.6	40.8
0day 00:09:00	34.3	42.5
0day 00:08:00	33.7	44.5
0day 00:07:00	33.3	38.6
0day 00:06:00	33.4	38.0

TABLE B.4

Laboratory conductivity test for CH-A 0.55 sample

Time	No.1	No.2
Channel Name	Ch1Tout	Ch2 T-in
0day 00:15:00	37.7	39.9
0day 00:14:00	37.9	40.8
0day 00:13:00	37.5	41.0
0day 00:12:00	37.3	39.4
0day 00:11:00	38.0	40.4
0day 00:10:00	38.6	41.5
0day 00:09:00	38.6	42.5
0day 00:08:00	37.2	41.9
0day 00:07:00	36.6	38.7
0day 00:06:00	37.1	39.6

TABLE B.5

Laboratory conductivity test for CH-A 0.45 sample

Time	No.1	No.2
Channel Name	**Ch1 Tout**	**Ch2 T-in**
0day 00:15:00	36.7	39.8
0day 00:14:00	37.0	39.7
0day 00:13:00	37.6	40.7
0day 00:12:00	38.2	41.8
0day 00:11:00	38.8	43.2
0day 00:10:00	39.1	44.6
0day 00:09:00	38.6	45.9
0day 00:08:00	36.5	42.4
0day 00:07:00	36.2	39.2
0day 00:06:00	36.7	39.6

TABLE B.6

Laboratory conductivity test for MT-A 0.7 sample

Time	No.1	No.2
Channel Name	Ch1Tout	Ch2 T-in
0day 00:15:00	40.3	44.0
0day 00:14:00	39.3	44.0
0day 00:13:00	37.2	39.4
0day 00:12:00	37.1	39.2
0day 00:11:00	37.1	38.6
0day 00:10:00	37.7	39.5
0day 00:09:00	38.4	40.5
0day 00:08:00	39.2	41.7
0day 00:07:00	39.9	43.0
0day 00:06:00	40.2	44.2

TABLE B.7

Laboratory conductivity test for MT-A 0.55 sample

Time	No.1	No.2
Channel Name	**Ch1 Tout**	**Ch2 T-in**
0day 00:15:00	39.5	41.9
0day 00:14:00	40.0	43.0
0day 00:13:00	40.1	44.0
0day 00:12:00	38.5	43.9
0day 00:11:00	34.9	37.9
0day 00:10:00	34.4	35.6
0day 00:09:00	34.7	35.9
0day 00:08:00	35.0	36.4
0day 00:07:00	35.5	37.1
0day 00:06:00	36.0	37.8

TABLE B.8

Laboratory conductivity test for MT-A 0.45 sample

Time Channel Name	No.1 Ch1 Tout	No.2 Ch2 T-in
0day 00:15:00	37.6	40.6
0day 00:14:00	38.1	41.7
0day 00:13:00	38.0	42.6
0day 00:12:00	36.2	40.6
0day 00:11:00	35.8	38.0
0day 00:10:00	36.3	39.0
0day 00:09:00	36.8	40.0
0day 00:08:00	36.9	40.9
0day 00:07:00	35.9	40.0
0day 00:06:00	35.6	38.2

TABLE B.9

Laboratory conductivity test for BT-A 0.55st sample

Time Channel Name	No.1 Ch1 Tout	No.2 Ch2 T-in
0day 00:15:00	35.0	38.2
0day 00:14:00	35.3	39.0
0day 00:13:00	35.5	39.9
0day 00:12:00	35.3	40.7
0day 00:11:00	34.7	38.3
0day 00:10:00	34.9	37.8
0day 00:09:00	35.3	38.6
0day 00:08:00	35.6	39.6
0day 00:07:00	36.0	40.6
0day 00:06:00	36.2	41.8

TABLE B.10

Laboratory conductivity test for BT-A 0.55 sample

Time Channel Name	No.1 Ch1Tout	No.2 Ch2 T-in
0day 00:15:00	37.1	40.2
0day 00:14:00	36.5	38.4
0day 00:13:00	36.9	38.3
0day 00:12:00	37.4	39.1
0day 00:11:00	38.0	39.9
0day 00:10:00	38.6	40.9
0day 00:09:00	39.2	42.0
0day 00:08:00	39.8	43.3
0day 00:07:00	39.7	44.5
0day 00:06:00	38.0	43.9

TABLE B.11

Laboratory conductivity test for SU-A 0.55 sample

Time Channel Name	No.1 Ch1 Tout	No.2 Ch2 T-in
0day 00:15:00	36.8	38.7
0day 00:14:00	37.2	38.9
0day 00:13:00	37.7	39.7
0day 00:12:00	38.3	40.6
0day 00:11:00	38.9	41.6
0day 00:10:00	39.5	42.7
0day 00:09:00	40.1	44.0
0day 00:08:00	40.5	45.3
0day 00:07:00	40.0	46.3
0day 00:06:00	37.7	45.7

TABLE B.12

Laboratory conductivity test for GAL-A sample

Time Channel Name	No.1 Ch1 Tout	No.2 Ch2T-in
0day 00:15:00	34.1	35.2
0day 00:14:00	34.3	35.5
0day 00:13:00	34.5	35.9
0day 00:12:00	34.8	36.4
0day 00:11:00	35.0	36.8
0day 00:10:00	35.3	37.3
0day 00:09:00	35.6	37.8
0day 00:08:00	35.9	38.5
0day 00:07:00	36.2	39.3
0day 00:06:00	36.3	39.9

APPENDIX C

TABLE C.1

Laboratory conductivity test for PVC sample

Time Channel Name	No.1 Ch1 Tout	No.2 Ch2 T-in
0day 00:15:00	35.3	39.7
0day 00:14:00	35.8	40.6
0day 00:13:00	36.3	41.7
0day 00:12:00	36.9	43.0
0day 00:11:00	37.5	44.6
0day 00:10:00	38.0	46.3
0day 00:09:00	38.4	48.3
0day 00:08:00	38.3	50.5
0day 00:07:00	37.4	53.0
0day 00:06:00	35.0	55.3

TABLE C.2

Laboratory conductivity test for ASB sample

Time Channel Name	No.1 Ch1 Tout	No.2 Ch2 T-in
0day 00:15:00	34.4	38.0
0day 00:14:00	34.5	38.6
0day 00:13:00	34.8	39.2
0day 00:12:00	34.9	39.8
0day 00:11:00	34.8	40.4
0day 00:10:00	34.7	40.9
0day 00:09:00	34.1	39.7
0day 00:08:00	34.0	37.4
0day 00:07:00	34.0	37.7
0day 00:06:00	33.9	37.9

TABLE C.3

Laboratory conductivity test for PVC sample

Time Channel Name	No.1 Ch1 Tout	No.2 Ch2 T-in
0day 00:15:00	33.0	37.7
0day 00:14:00	32.9	38.4
0day 00:13:00	32.8	39.1
0day 00:12:00	32.6	39.9
0day 00:11:00	32.4	41.0
0day 00:10:00	32.1	42.1
0day 00:09:00	32.0	38.6
0day 00:08:00	31.9	36.7
0day 00:07:00	31.7	37.2
0day 00:06:00	31.5	38.0

TABLE C.4

Laboratory conductivity test for PVC sample

Time Channel Name	No.1 Ch1 Tout	No.2 Ch2 T-in
0day 00:15:00	36.1	40.6
0day 00:14:00	35.5	41.1
0day 00:13:00	35.1	39.3
0day 00:12:00	35.1	37.9
0day 00:11:00	35.0	38.4
0day 00:10:00	34.8	38.7
0day 00:09:00	34.5	38.0
0day 00:08:00	34.3	38.1
0day 00:07:00	33.9	37.7
0day 00:06:00	33.6	37.4

TABLE C.5

Temperature variations for the ceiling samples

Regulated temperature = 34℃

TIME	TEMPERATURE VARIATIONS IN ℃			
X 60 SEC	PVC-A	ASB-A	POP-A	GYP-A
1	30.8	33.5	30.2	30.6
2	32.1	33.9	30.4	31.8
3	32.8	34	30.6	32.6
4	32.9	33.9	30.9	33.0
5	33.1	33.8	31.3	33.3
6	33.0	33.9	31.5	33.6
7	37.4	34	31.7	33.9
8	38.3	34	31.9	34.3
9	38.4	34.1	32	34.5
10	38	34.7	32.1	34.8
11	37.5	34.8	32.4	35
12	36.9	34.9	32.6	35.1
13	36.3	34.8	32.8	35.1
14	35.8	34.5	32.9	35.5
15	35.3	34.4	33	36.1

Source: Laboratory Variations

APPENDIX D

TABLE D.1

Indoor and outdoor temperatures for the sample materials

Test	Measured Thickness	Indoor temp. ℃	indoor temp. ℃	indoor temp. ℃	Indoor temp. ℃	indoor temp. ℃	outdoor temp. ℃	outdoor temp. ℃	outdoor temp. ℃	outdoor temp. ℃	outdoor temp. ℃
Materials	(mm)	Dec.19	Mar. 20	July. 20	July. 20	July. 20	Dec. 19	Mar.20	July. 20	July. 20	July. 20
ST-A	1.88	31.62	30.72	27.6	27.1	27.5	41.25	32.3	30.1	31.1	30.2
CH-A 0.7	0.52	31.55	31.46	28.6	26.9	27.9	40.54	33.2	30.2	30.8	30.4
CH-A 0.55	0.4	32.15	31.43	27.5	27.1	28.3	43.28	32.14	30.9	31.9	30.6
CH-A 0.45	0.22	31.44	32.36	27.4	27.7	28.7	44	32.2	30.5	31.2	30.9
MT-A 0.7	0.67	30.68	31.34	28	26.9	27.9	40.03	32	30.3	30.7	30.5
MT-A 0.55	0.43	31.58	30.25	28.2	26.9	28	37.72	31.14	30.6	31.8	30.2
MT-A 0.45	0.33	30.65	30.45	28.6	27.6	28.3	38.71	31.2	31.1	31.9	31.4
BT- A 0.55 ST	0.41	30.73	31.96	29.9	27.6	28.7	38.41	33.1	31.4	31.5	31.2
BT- A 0.55	0.39	31.79	31.58	28	27.2	28	38.02	30.2	31.4	32	31.7
BT- A 0.45	0.43	32.09	31.8	28.1	27.2	27.9	43.99	32.3	31.2	32.6	31.9
GAL-A	0.37	31.78	26.33	28.2	27.5	28.5	37.99	31.3	31.7	32.9	32
PVC-A 5	5.2	30.86	31.7	28.2	27	27.9	34.87	30.03	30.9	30.8	30.5
ASB -A	3.9	32.14	29.16	27.7	26.7	27.7	38.97	30.2	30.1	31.2	30.7

POP -A 8	5.2	31.66	25.97	28.2	26.5	27.6	35.98	30	30.6	31.6	31
GYP -A 8	6.34	31.25	26.74	27.5	26.3	27.6	38.48	31.14	30.5	31	30.8

TABLE D.2

The average monthly temperature absorbed by sampled roofing materials

MONTHLY	PERIOD	duplicate	Amb	ST-A	CH-A 0.7	CH-A 0.55	CH-A 0.45	MT-A 0.7	MT-A 0.55	MT-A 0.45	BT-A 0.55st	BT-A 0.45	SU - A 0.55	GAL-A
October	8am	1	26.7	36.5	37.8	37	39.2	37.4	32.6	36.2	38	35.5	36.6	34.7
		2	25.5	25.9	27.6	27.6	26.8	27.2	26.7	26.8	28.6	27.9	27.6	28.3
		3	27.3	32.5	32.4	32.7	33.2	32.2	30.9	32.2	35.1	33.1	32.6	33.5
	12pm	1	38.7	33.3	33.6	33.7	34.3	34.1	32.9	32.5	35.4	34.5	34.8	35.1
		2	29.3	48.2	50.1	51.3	57.5	49.8	51.3	45.2	54.3	51.5	50.8	51.4
		3	29.6	48.3	47.7	45.4	54.1	53.5	50.6	45.5	51.7	48.4	48.2	43.3
	3pm	1	28.6	35.1	35	34	45.3	39.8	39.3	39.7	38.6	37.9	37.3	35.8
		2	30.5	52.4	50.1	46.7	48.4	43.1	42.6	45.7	51.2	48.2	46.9	43.8
		3	31.2	49.2	48.3	45.7	44.6	41.7	37.2	41.7	47.5	45.6	44.1	41.9
	6pm	1	27.8	28	28.2	29	28.3	28.4	28.4	29.2	27.9	28.1	28.1	29
		2	29.8	32.4	31.9	31.9	32	31.8	31.6	31.9	32.5	32	32	32.2
		3	29.5	29.8	29.5	29.7	29.5	29.6	29.8	29.5	29.3	29.3	29.4	30.2
	9pm	1	24.6	24.8	24.8	25.7	24.4	24.6	25.3	26.1	24.3	24.6	26.5	25.1
		2	27.9	27.3	27.6	28.8	27.7	28	28.2	28.8	27.9	27.9	28	28.6
		3	27.9	27.5	27.9	28	27.7	27.8	28.3	28.6	27.8	27.8	28.1	28.5
Nov	8am	1	26.3	28.4	28.8	29.4	29.1	29	29.3	29.8	28.9	29	29.1	29.7
		2	27.8	38.6	38.6	36.9	35.9	33.9	32.6	33.2	37.9	34.8	33	32.8
		3	27.2	29.6	30.1	30.3	29.7	29.4	29.4	29.8	31.8	30.4	30.1	31.1
	12pm	1	29.9	43.3	42.9	42.2	40.2	40.5	38.9	37.1	40.1	39	38.5	39.1
		2	30.7	58.8	56.5	58.3	56.4	56	54.3	47.8	54.5	51.4	49.4	50.3
		3	31.4	52.6	50.6	49.4	53.2	52.7	52.2	45.2	53.2	50.4	49.8	44.5
	3pm	1	30.5	35.8	35.8	34.7	37.1	36.4	35.6	34.7	37.7	35.4	35.9	36
		2	31.8	52.1	46.1	43	43.1	42.2	41.9	43.7	49.1	46.1	43.8	41
		3	32.5	43.6	42.5	40	38.6	37.1	36.7	39.7	41.6	38.7	37.7	36.6
	6pm	1	29.4	30	30.2	30.3	30.3	30.3	30.2	30.3	29.8	29.8	29.8	30.8
		2	31.2	30.3	30.2	30.6	30.5	30.5	30.5	30.6	30.4	30.3	30.4	30.9
		3	30.8	30.9	30.7	30.7	31	30.9	30.8	31	30.9	30.7	30.7	31.2
	9pm	1	25.7	25.3	25.9	27.6	26	26	26.3	27.9	26.3	25.9	26	27
		2	28.6	28.6	28.6	29.2	28.7	28.9	29.4	29.1	28.6	28.6	29.7	30.1

		3	28.6	28	28.4	28.8	28.1	28	28.8	29.2	28	28.6	28.2	29.3
Dec	8am	1	26.5	28.7	29.5	30.2	30.1	30.1	30	30.8	31.5	31	31	31.6
		2	26.4	30	29.7	29.8	29.2	29.9	28.9	28.8	28.6	28	28.1	28.5
		3	24.5	26.6	27	27.6	27.2	26.7	27.9	27.7	27.4	27.3	27.3	29.1
	12pm	1	28.4	34.1	35.4	34.9	37.3	35.4	34.5	33.7	38.4	37.2	36.6	35.4
		2	30.9	44.4	42.8	43.4	40.7	40.7	37	34	47.9	44.6	44.9	43.4
		3	32.7	47.1	43.5	45	47.4	46.4	44.6	40.2	46.9	44.6	40.9	42.2
	3pm	1	31.7	39.2	38.7	37.5	37.3	36.5	35.7	36.4	39.1	37.4	36.2	36
		2	32	42.1	35.9	35.7	36.6	36	35	36.3	40.1	36.8	35.1	34.7
		3	32.4	40.7	41.2	40.5	42.2	40.5	39.8	38.6	43.3	41	39.8	38.1
	6pm	1	30.6	30.9	30.8	31.2	30.6	30.7	30.8	31.2	29.9	29.8	29.9	30.3
		2	30.9	31.6	31.4	31.4	31.3	31.2	31.2	31.4	31	30.9	30.8	31.1
		3	31	31.5	31.4	31.4	31.1	31.1	31	31.4	31.2	31	30.9	31.2
	9pm	1	25.1	24	24.3	25.3	24.3	24.2	24.5	26.1	24.4	24.4	24.6	25.3
		2	29.1	27.8	28	28.7	28.8	27.9	28.7	28.9	28.2	28.2	27.9	29.5
		3	28.5	26.6	27.3	28.4	27.3	27.3	27.9	28.2	27.1	27.5	27.6	29.3

TABLE D.3

The average monthly temperature absorbed by sample ceiling materials

MONTHLY	PERIOD	Duplicate	Amb-in	PVC	ASB	POP	GYP
October	8am	1	28	28.8	28.4	28.6	28.5
		2	25.4	26.1	26	26.1	26.1
		3	27.4	28	27.7	27.9	27.9
	12pm	1	27.7	28.3	29.3	28.6	28.7
		2	30.6	31.5	30.7	32.2	31.2
		3	29.4	29.8	29.8	30.1	29.9
	3pm	1	27.9	28.7	28.8	29.4	29.3
		2	29.8	30.2	29.9	30.8	30.6
		3	30.1	30.4	30.4	30.9	30.8
	6pm	1	27	27.7	27.6	28.1	28.1
		2	28.3	28.7	28.7	28.9	28.8
		3	27.9	29	29.1	29.8	28.8
	9pm	1	24.3	24.8	25.4	25.3	25.6
		2	28.2	28	28.1	28	27.9
		3	28.1	28.6	28.9	28.6	28.4
Nov	8am	1	27.3	27.7	27.4	27.8	27.4
		2	29.6	29.8	29.5	29.8	29.6
		3	28.1	28.1	28	28	27.9
	12pm	1	30.2	30.2	30	30.3	30
		2	29.2	29.9	29.6	29.9	29.8
		3	29	30.2	30	30.3	30.2
	3pm	1	29.7	29.9	29.6	29.9	29.8
		2	29.9	31.4	31.2	31.4	31.3

		3	29.8	30.9	30.7	31	30.9
	6pm	1	28.7	29.1	29	29	29.1
		2	29.1	30.1	29.6	29.9	29.8
		3	29	30.1	30	30.1	30
	9pm	1	26.9	27.2	28.3	27.2	26.9
		2	29.5	29.4	29.6	29.4	29.4
		3	29	29.5	29.4	29.5	29.3
Dec	8am	1	27.3	27.7	28	27.9	28
		2	25.8	27.5	27	27.4	27.3
		3	26.4	26.6	26.1	26.2	25.8
	12pm	1	28.9	29.3	29.7	29.3	29.4
		2	29.3	29.5	29.4	29.6	29.8
		3	28.6	29.2	28.8	29.4	29.6
	3pm	1	30.4	30	30.3	30.9	30.9
		2	30.2	30.2	30	30.1	30.1
		3	30.6	31.4	31.3	31.3	31.3
	6pm	1	29.8	30	29.9	30	29.8
		2	29.4	29.7	29.5	29.5	29.5
		3	29.7	29.9	30	30	30
	9pm	1	24.6	25.8	26	26.7	27
		2	28.7	29	28.9	28.9	28.9
		3	28.6	29.3	29.6	29.2	29.1

APPENDIX E

TABLE E.1

Comparison of hourly heat absorption by the sampled roofing sheets in October 2020

Period	AMB	ST-A	CH-0.7	CH-0.55	CH-0.45	MT-0.7	MT-0.55	MT-0.45	BT-0.55st	BT-0.55	BT-0.45	GAL
8:30	25.5	25.9	27.6	27.6	26.8	27.2	26.7	26.8	28.6	27.9	27.6	28.3
11:30	29.3	48.2	50.1	51.3	57.6	49.8	51.3	45.2	54.3	51.5	50.8	51.4
3:30	30.5	52.4	50.1	46.7	48.4	42.1	42.6	45.7	51.2	48.2	46.9	43.8
5:30	29.8	32.4	31.9	31.9	32	31.8	31.6	31.9	32.5	32	32	32.2
8:30	27.9	27.3	27.6	28.8	27.7	28	28.2	28.8	27.9	27.9	28	28.6

Source: Field Survey (2020)

TABLE E.2

Comparison of hourly heat absorption for the sampled ceilings in October 2020

PERIOD	AMB	PVC-A	ASB-A	POP-A	GYP-A
8:30	28	28.8	28.4	28.6	28.5
11:30	27.7	28.3	29.3	28.6	28.7
3:30	27.9	28.7	28.8	29.4	29.3
5:30	27	27.7	27.6	28.1	28.1
8:30	24.3	24.8	25.4	25.3	25.6

Source: Field survey (2020)

APPENDIX E

The equation represents the polynomial relational equation for the ambient heat accumulated. The Figure 4 shown the heat movement trend for the internal ambient space.

$y = 0.001x^4 - 0.0525x^3 + 0.8685x^2 - 4.8611x + 31.8$
$R^2 = 1$

SOLUTION

$$= \int_9^{12}(0.001x^4 - 0.0525x^3 + 0.8685x^2 + 4.8611x + 31.8)\text{dx}$$

$$= \left[\frac{0.001x^5}{5} - \frac{0.0525x^4}{4} + \frac{0.86585x^3}{3} - \frac{4.8611x^2}{2} + 31.8x\right]_9^{21}$$

$$= \left[\frac{0.001(21)^5}{5} - \frac{0.0525(21)^4}{4} + \frac{0.86585(21)^3}{3} - \frac{4.8611(21)^2}{2} + 31.8(21)\right]_9^{21} -$$

$$\left[\frac{0.001(9)^5}{5} - \frac{0.0525(9)^4}{4} + \frac{0.86585(9)^3}{3} - \frac{4.8611(9)^2}{2} + 31.8(9)\right]_9^{21}$$

$$= (816.8202 - 2552.563125 + 2672.87895 - 107187255 + 667.8) - (11.8098 - 86.113125 + 210.401 - 196.87455 + 286.2)$$

$$= 533.063475 - 255.423675$$

$$= 307.6398$$

$q_{amb} = 307.64j$

The figure 4 represented both the external and internal quantity of heat absorbed for the month of October.

The quantity of ambient heat y_{amb} absorbed for the month of October was represented by equation 4.

$$y = 0.01x^4 - 0.0525x^3 + 0.8685x^2 - 4.8611x + 31.8$$

And the quantity of heat absorbed by polyvinylchloride y_{pvc} was given by equation 4

$$y = 0.00005x^4 + 0.0102x^3 - 0.4551x^2 + 7.175 - 7.2$$

Also, the quantity of heat absorbed by asbestos ceiling y_{asb} for this month was also given by equation 4

$$y = -0.0003x^4 + 0.0244x^3 - 0.8032x^2 + 10.797x - 20.8$$

Similarly, the quantity of heat also absorbed by plaster of paris y_{pop} was expressed in equation 4

$$y = 0.0002x^4 - 0.048x^3 - 0.1741x^2 + 5.056x - 2.1$$

While the quantity of heat in gypsum equation was given by equation 4

$$y = 0.001x^4 - 0.0543x^3 + 0.9407x^2 - 5.7278x + 35.7$$

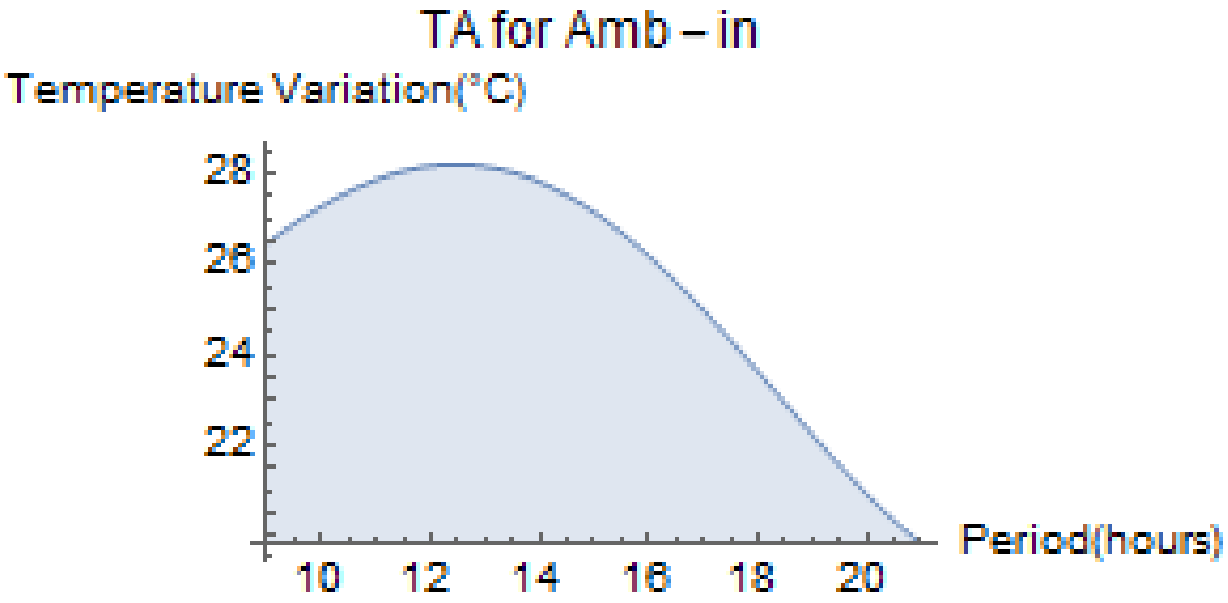

FIGURE E1: Thermal Absorptivity at Ambient in October

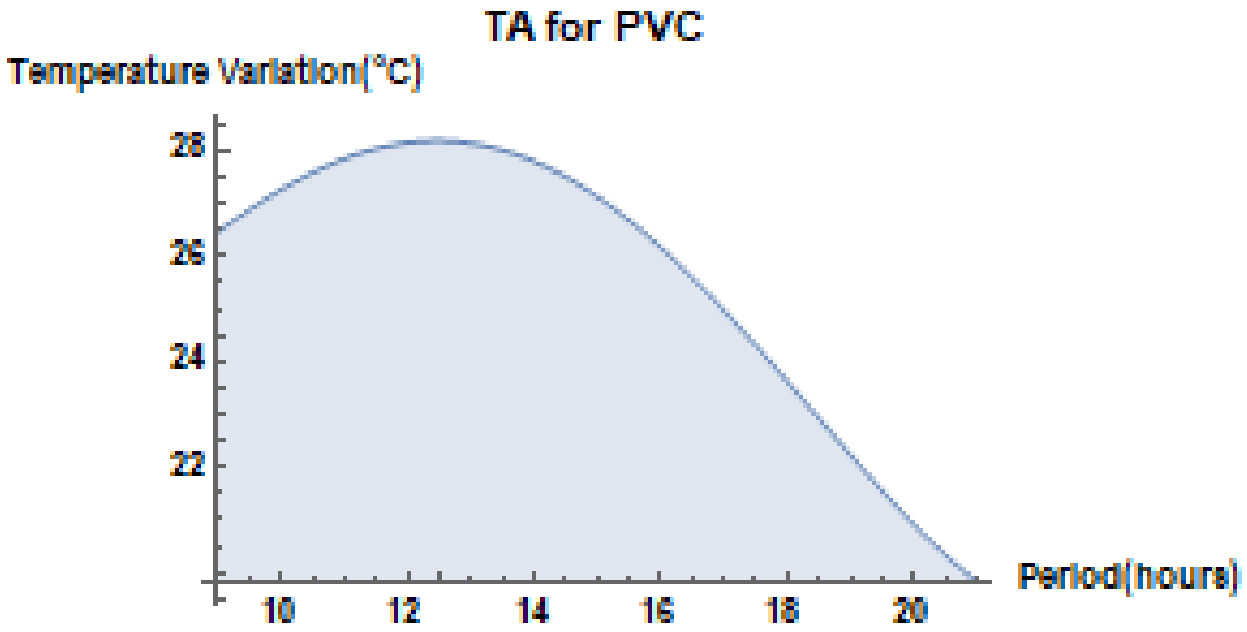

FIGURE E2: Thermal Absorptivity for PVC in October

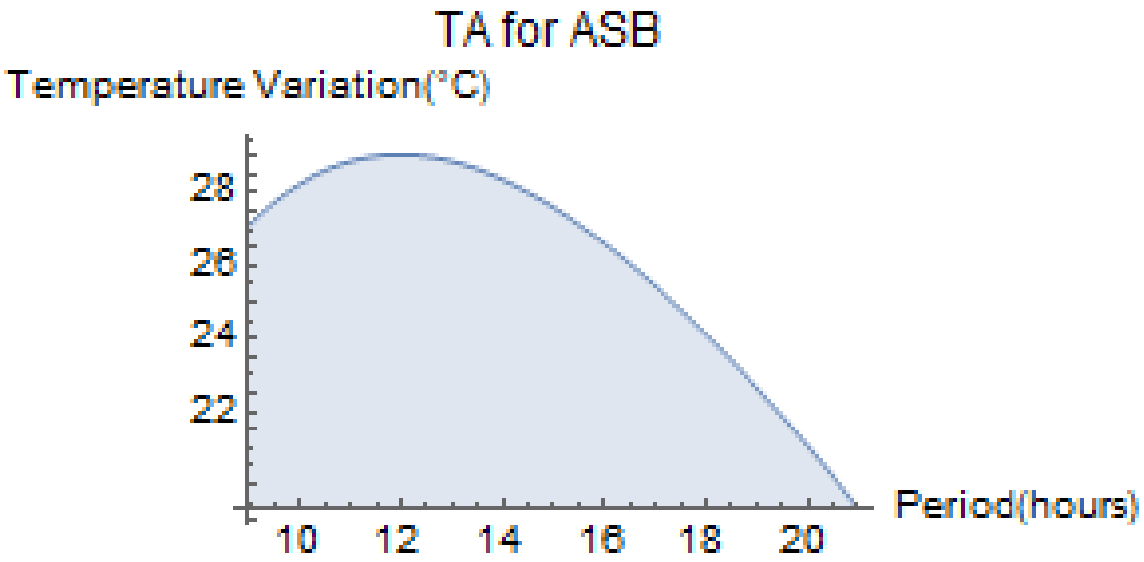

FIGURE E3: Thermal Absorptivity for Asbestos in October

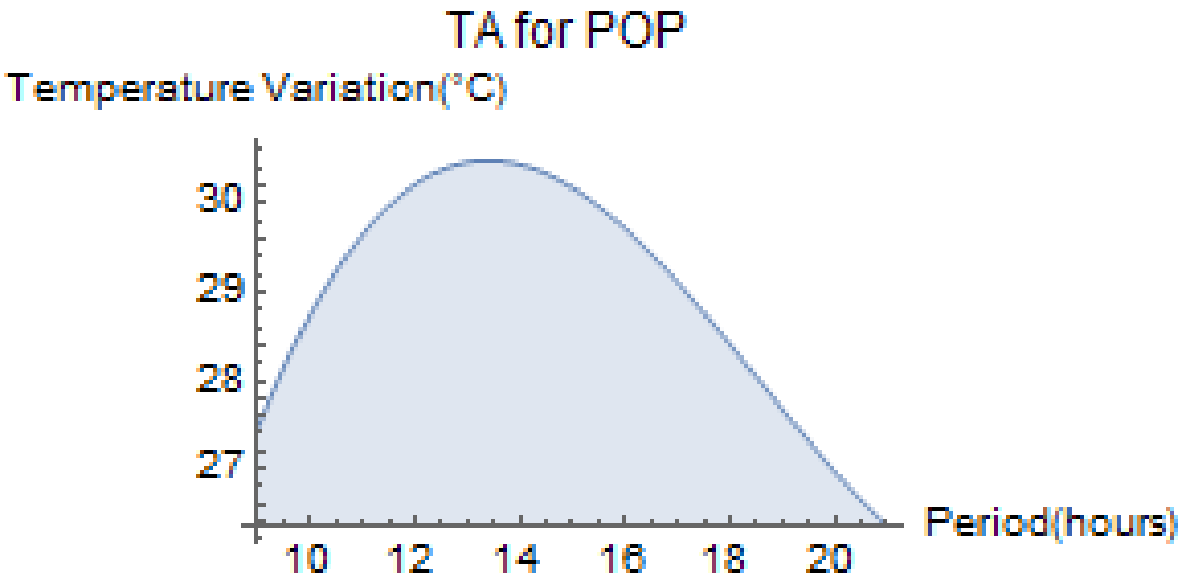

FIGURE E4: Thermal Absorptivity for Plaster of Paris in October

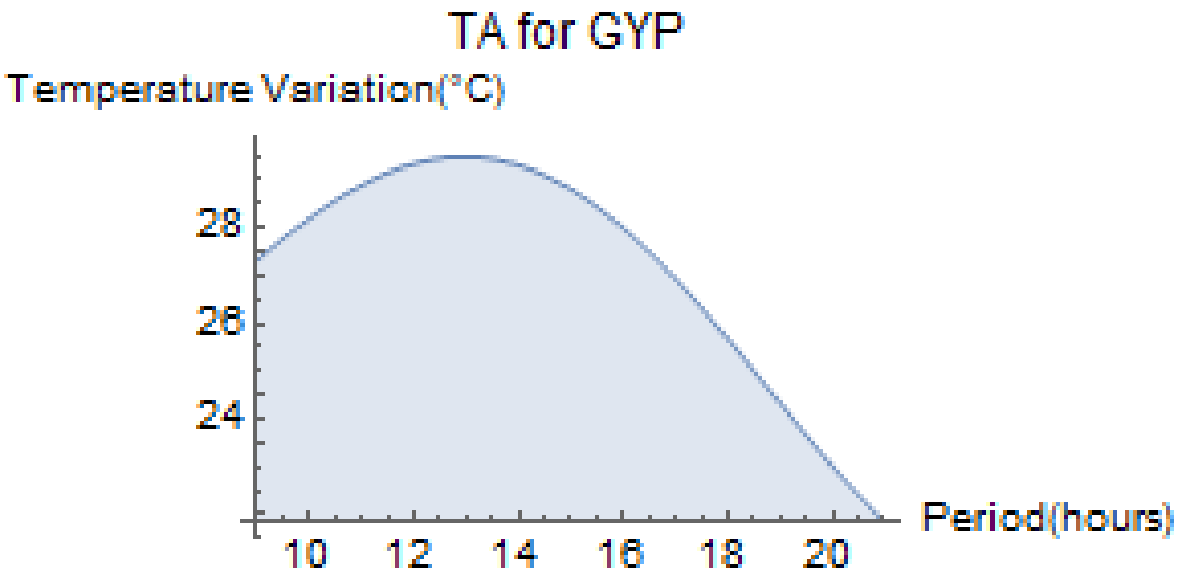

FIGURE E4: Thermal Absorptivity for Gypsum in October

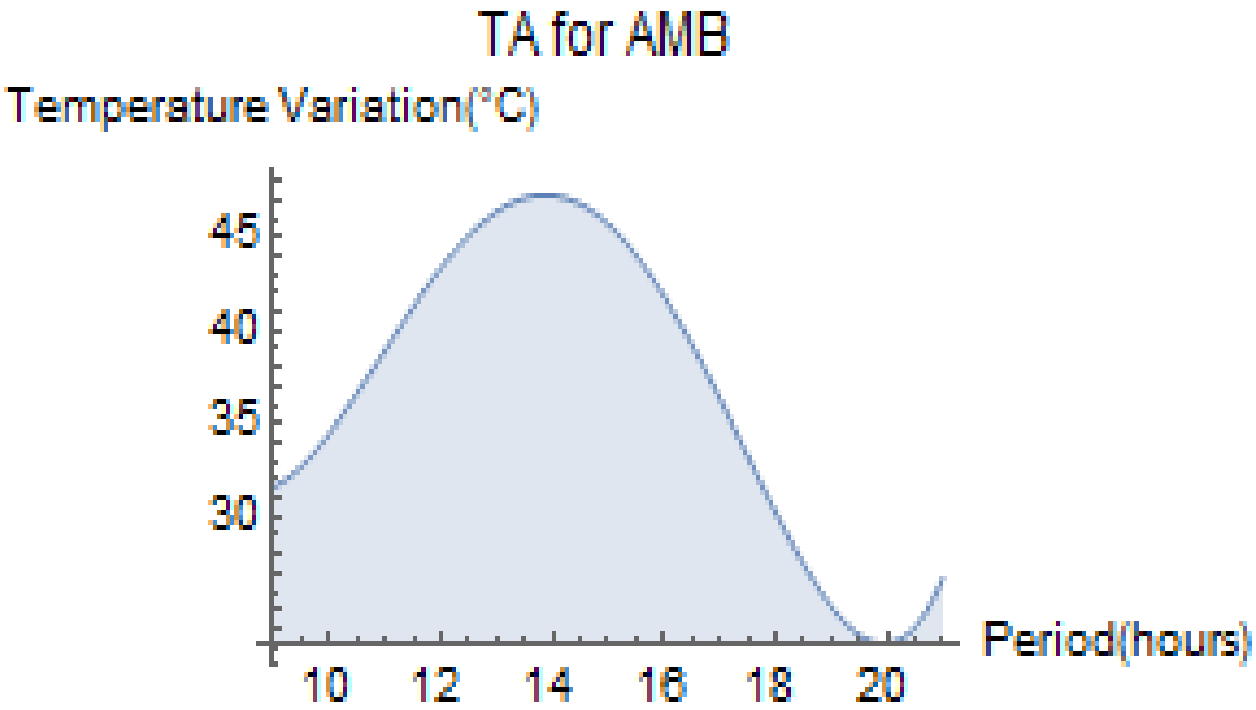

FIGURE E5: Thermal Absorptivity at Ambient in October

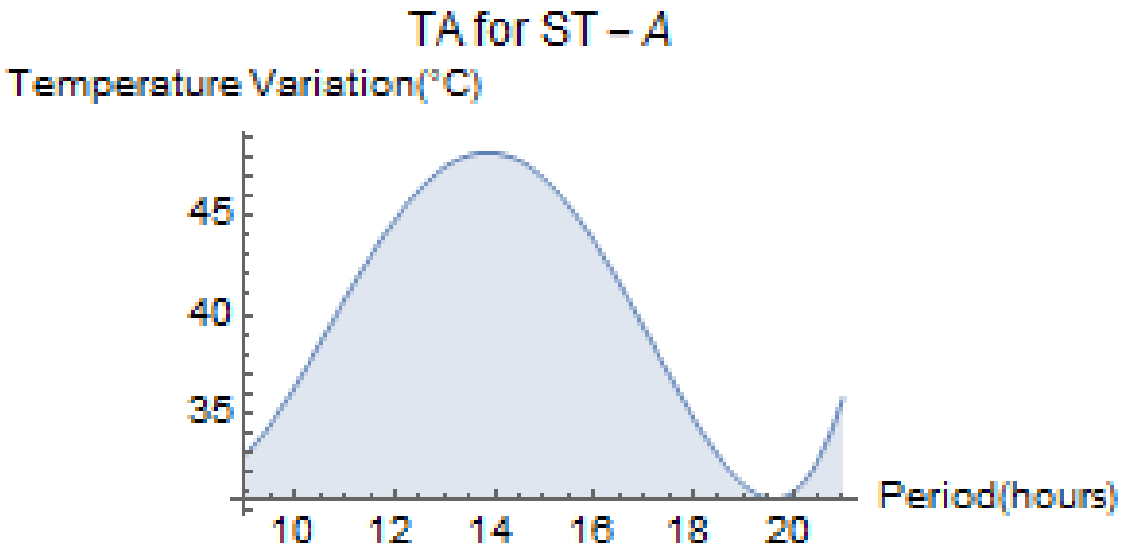

FIGURE E6: Thermal Absorptivity for SCS in October

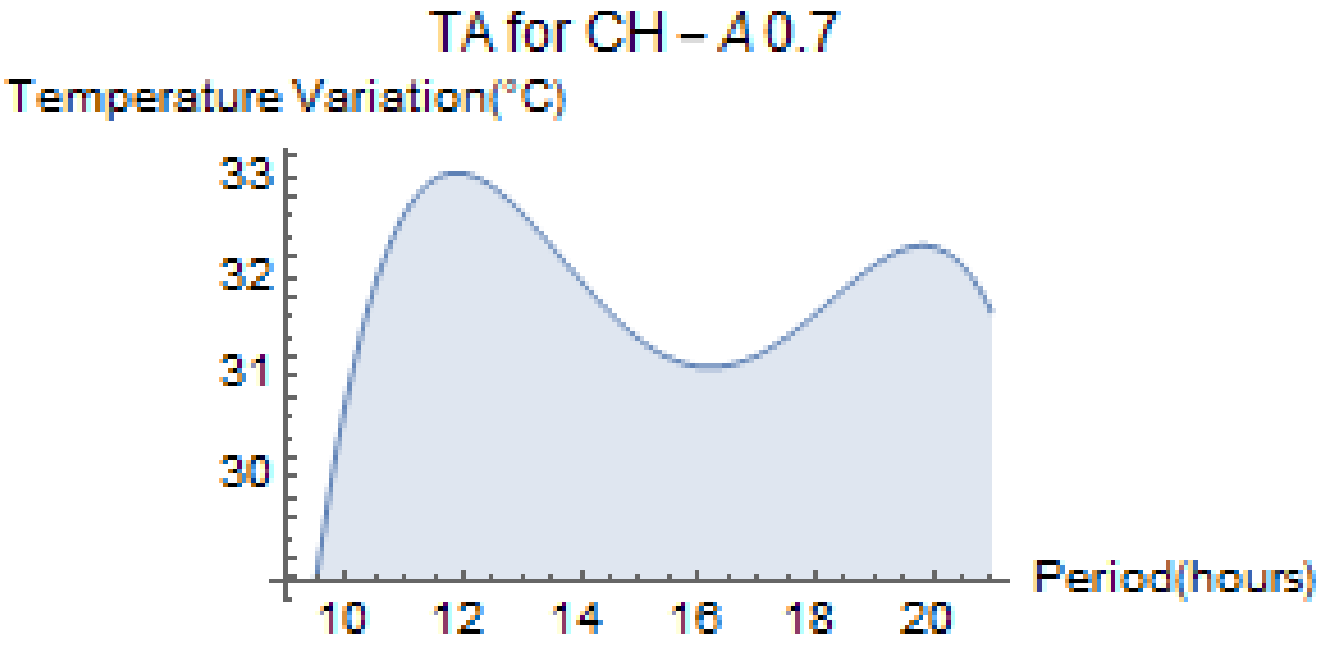

FIGURE E7: Thermal Absorptivity for ARS in October

TABLE E3

Average temperature absorbed by roofing samples for the month of November 2020

PERIOD	AMB	ST-A	CH-0.7	CH-0.55	CH-0.45	MT-0.7	MT-0.55	MT-0.45	BT-0.55st	BT-0.55	BT-0.45	GAL
8:30	27.2	29.6	30.1	30.3	29.7	29.4	29.4	29.8	31.8	30.4	30.1	31.1
11:30	31.4	52.6	50.6	49.4	53.2	52.7	52.2	45.2	53.2	50.4	49.8	44.5
3:30	32.5	43.6	42.5	40	38.6	37.1	36.7	39.7	41.6	38.7	37.7	36.6
5:30	30.8	30.9	30.7	30.7	31	30.9	30.8	31	30.9	30.7	30.7	31.2
8:30	28.6	28	28.4	28.8	28.1	28	28.8	29.2	28	28.6	28.2	29.3

Source: Field Survey (2020)

TABLE E4

Average temperature absorbed by Ceiling samples for November 2020

PERIOD	AMB	PVC	ASB	POP	GYP
8:30	28.1	28.1	28	28	27.9
11:30	29	30.2	30	30.3	30.2
3:30	29.8	30.9	30.7	31	30.9
5:30	29	30.1	30	30.1	30
8:30	29	29.5	29.4	29.5	29.3

Source: Field Survey (2020)

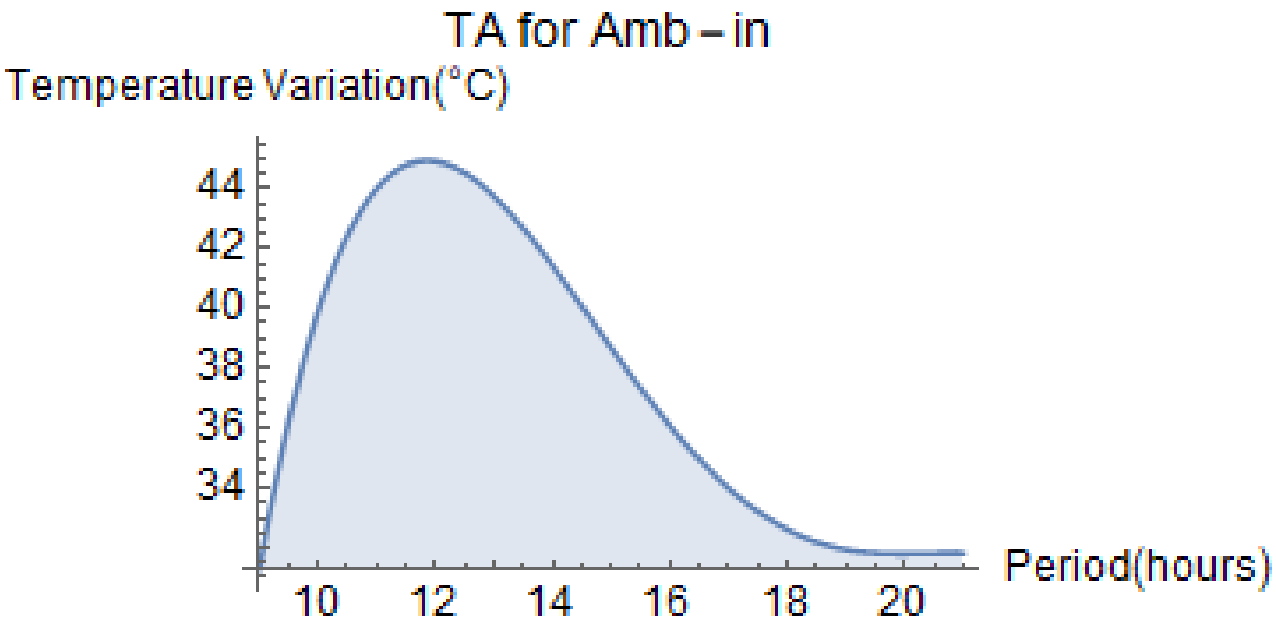

FIGURE E8: Thermal Absorptivity at ambient in November

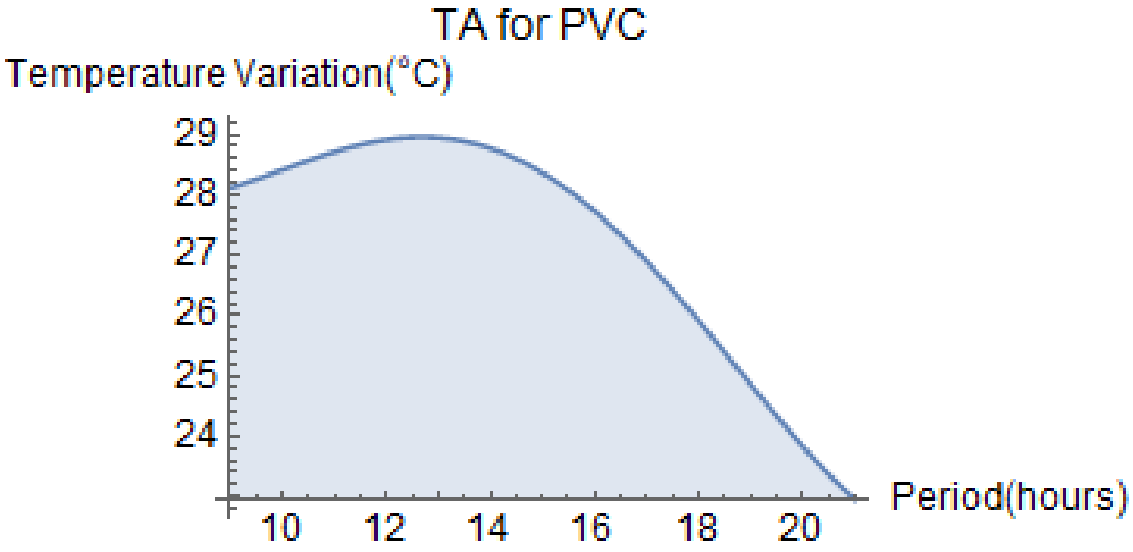

FIGURE E9: Thermal Absorptivity for PVC in November

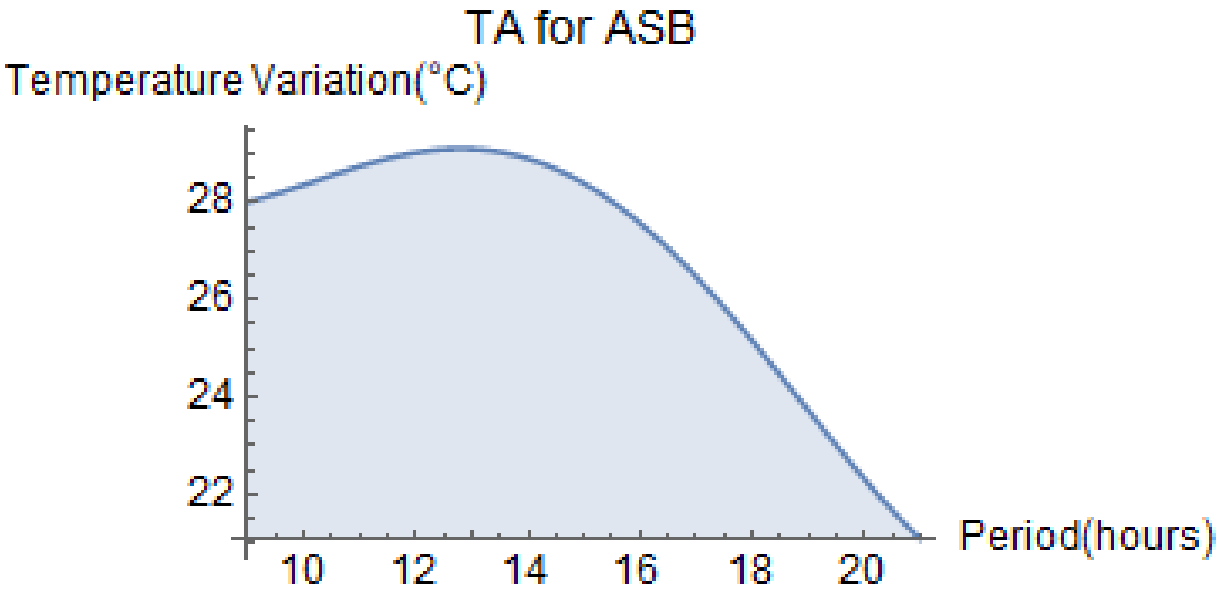

FIGURE E10: Thermal Absorptivity for ASB in November

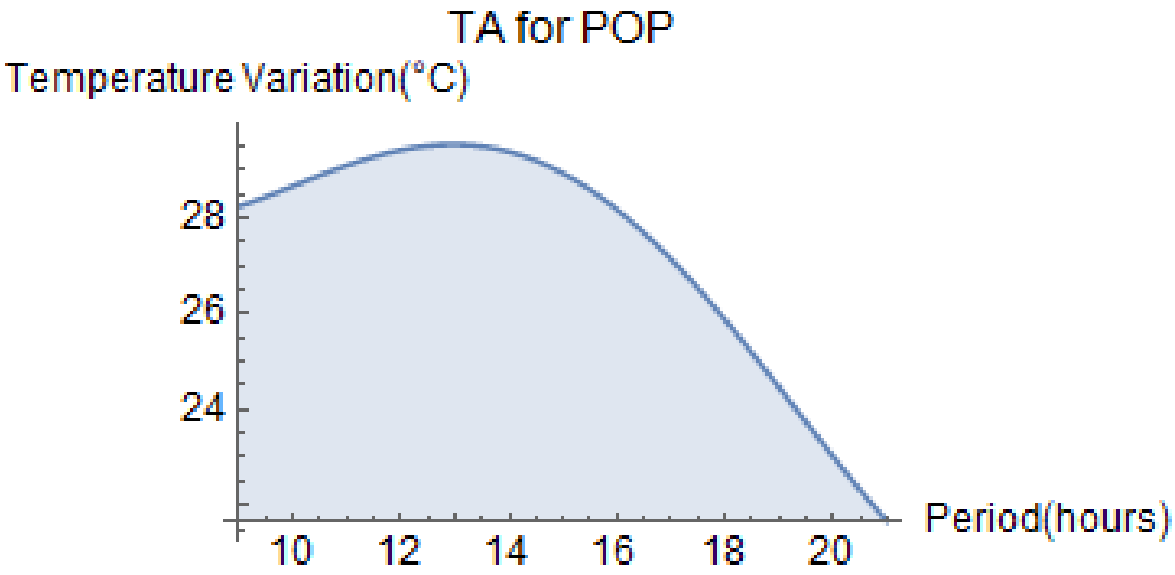

FIGURE 11: Thermal Absorptivity for POP in November

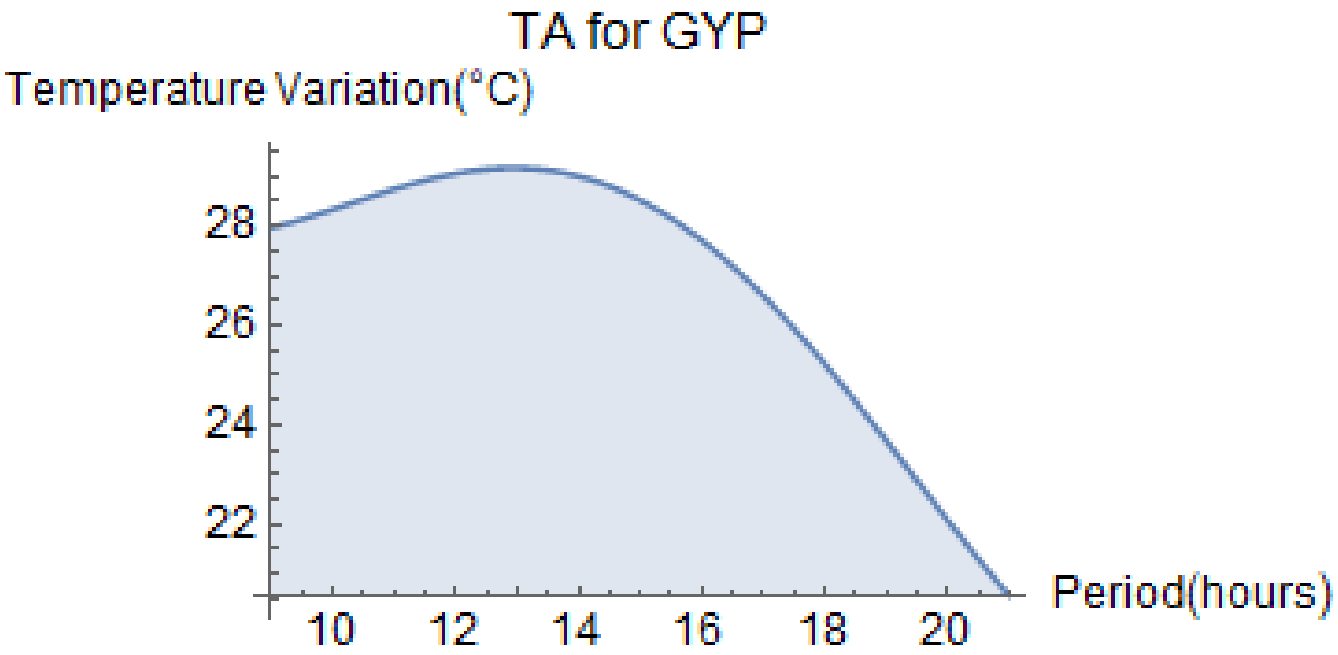

FIGURE E12: Thermal Absorptivity for GYP in November

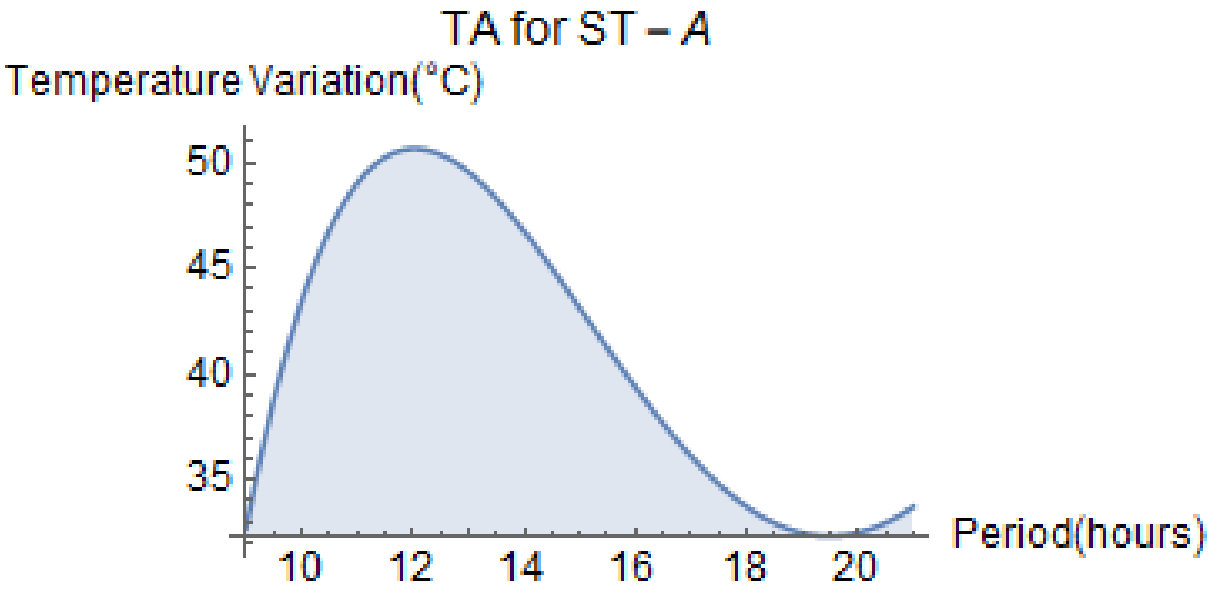

FIGURE E13: Thermal Absorptivity for SCS in November

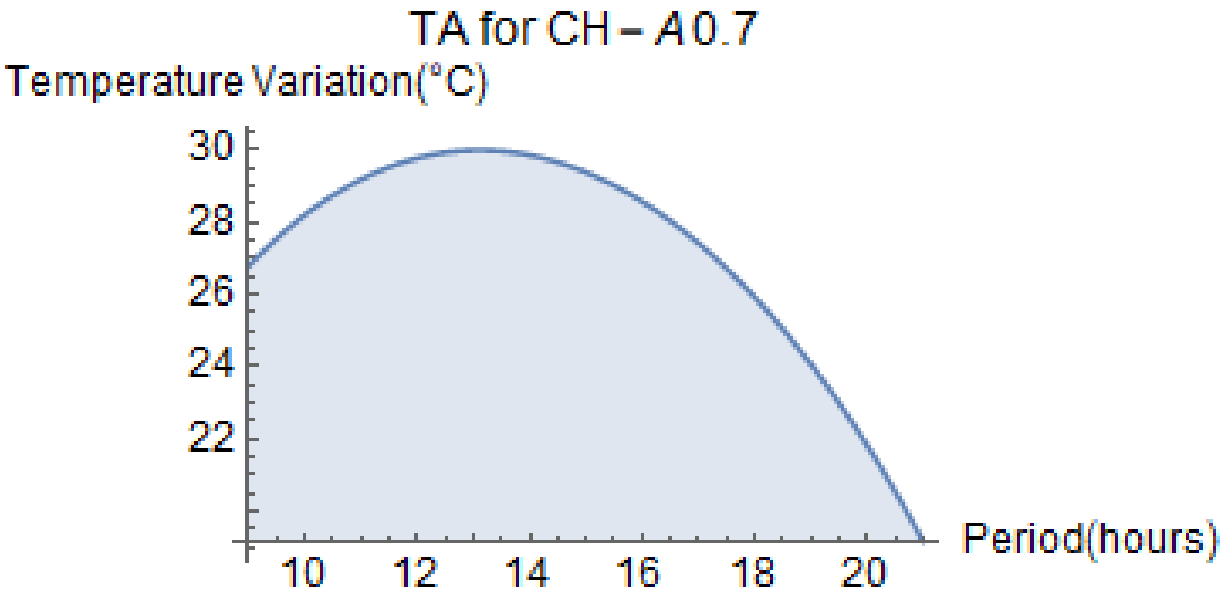

FIGURE E14: Thermal Absorptivity for ARS in November

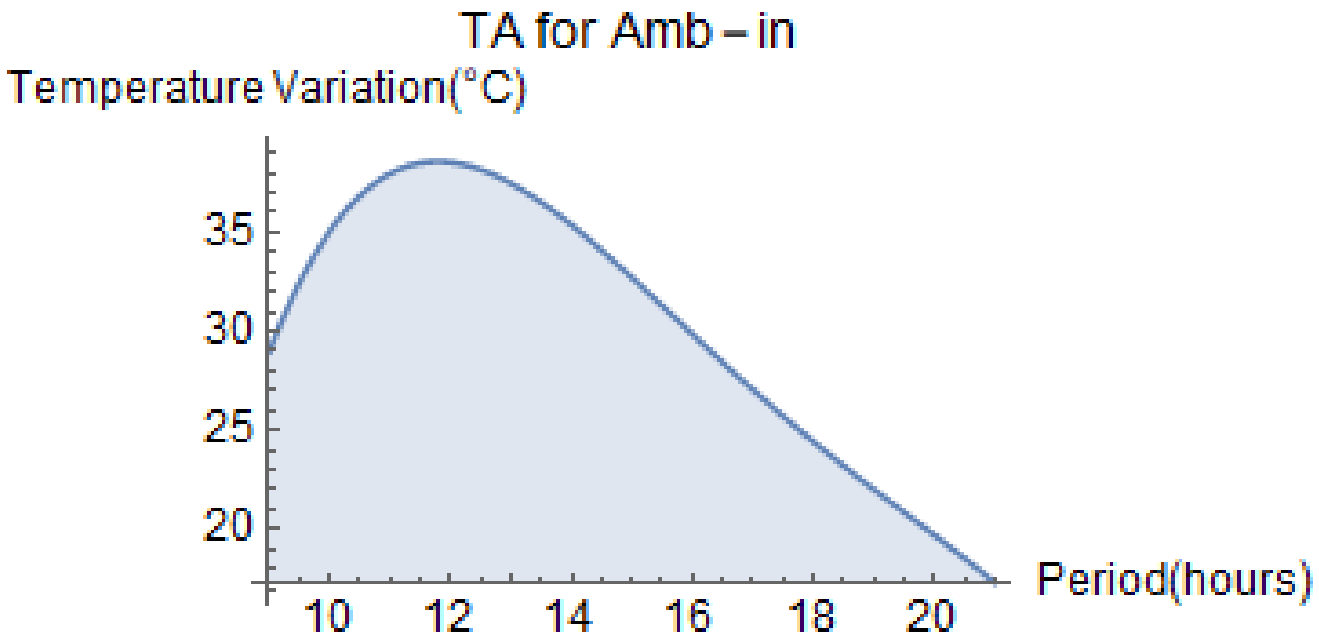

FIGURE E15: Thermal Absorptivity at ambient in December

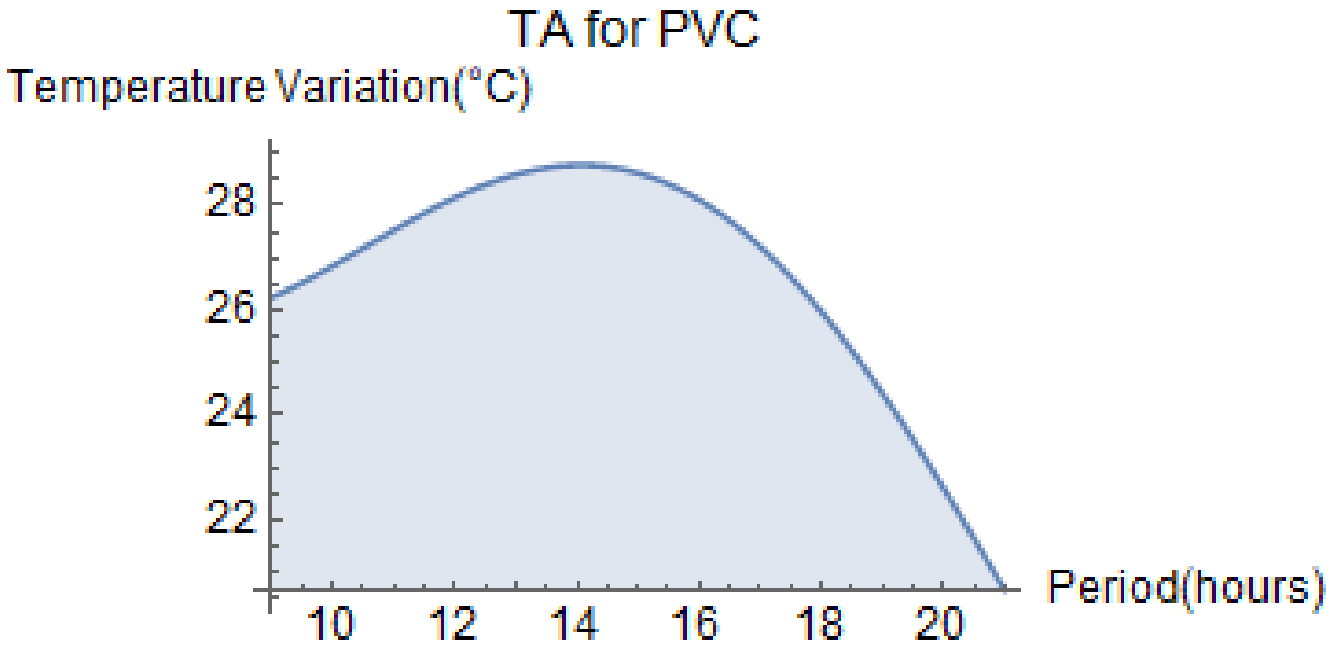

FIGURE E16: Thermal Absorptivity for PVC in December

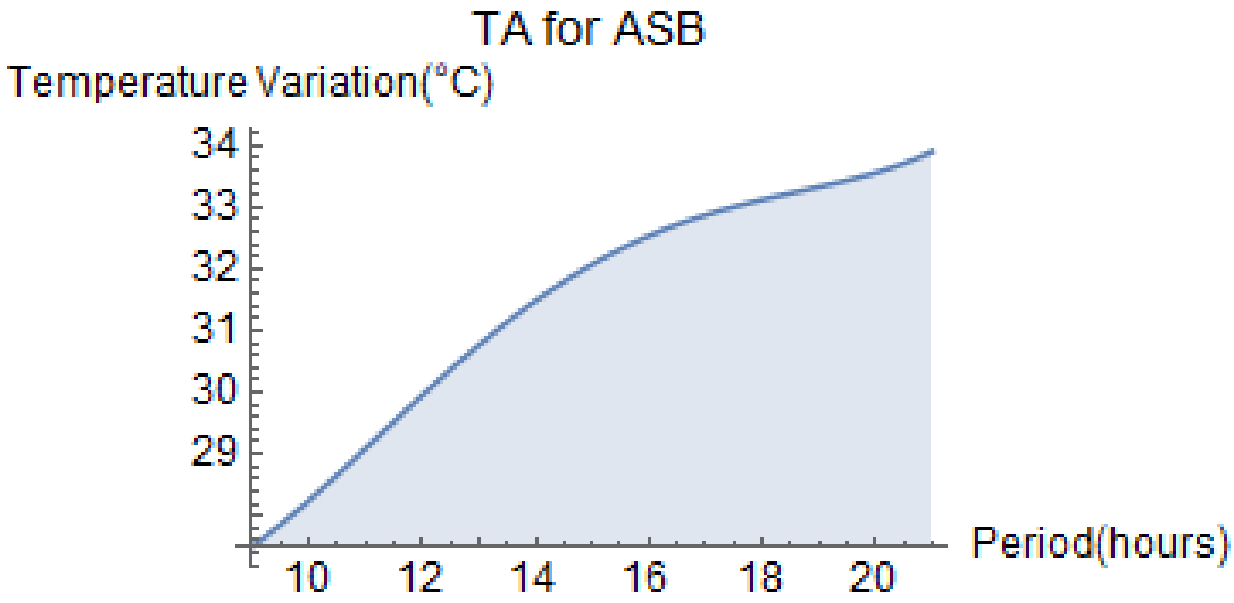

FIGURE E17: Thermal Absorptivity for ASB in December

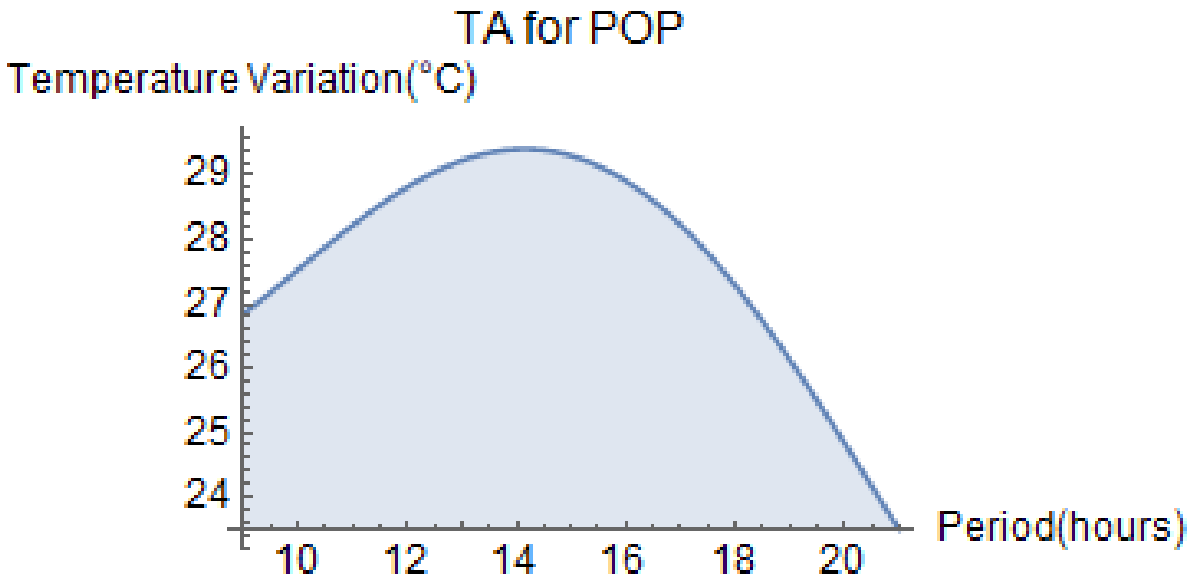

FIGURE E18: Thermal Absorptivity for POP in December

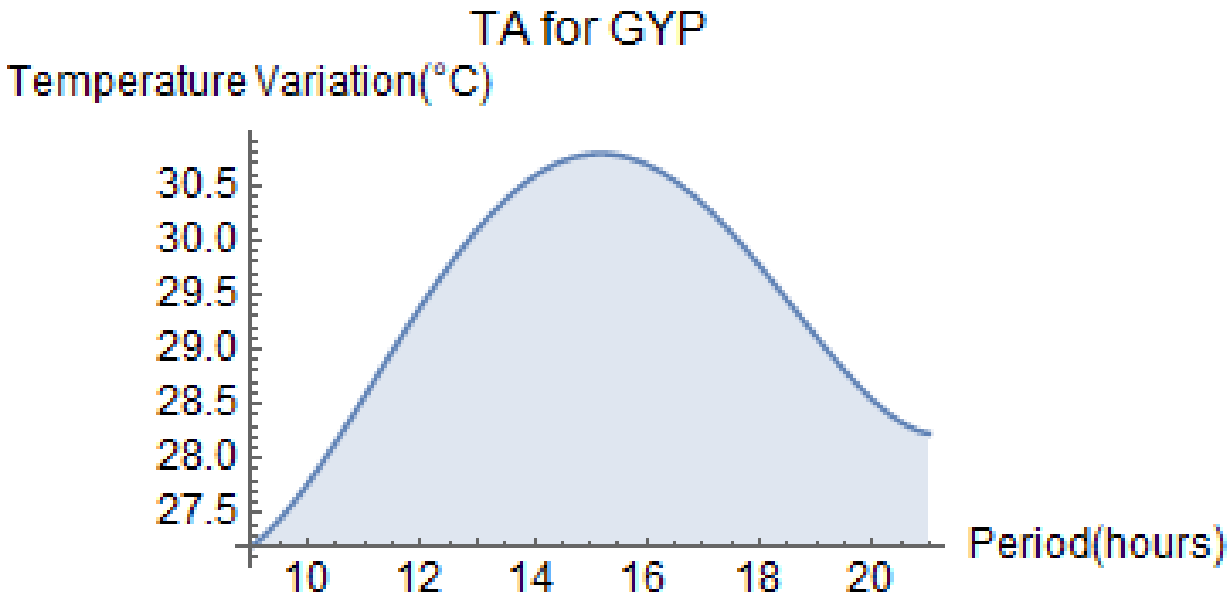

FIGURE E19: Thermal Absorptivity for GYP in December

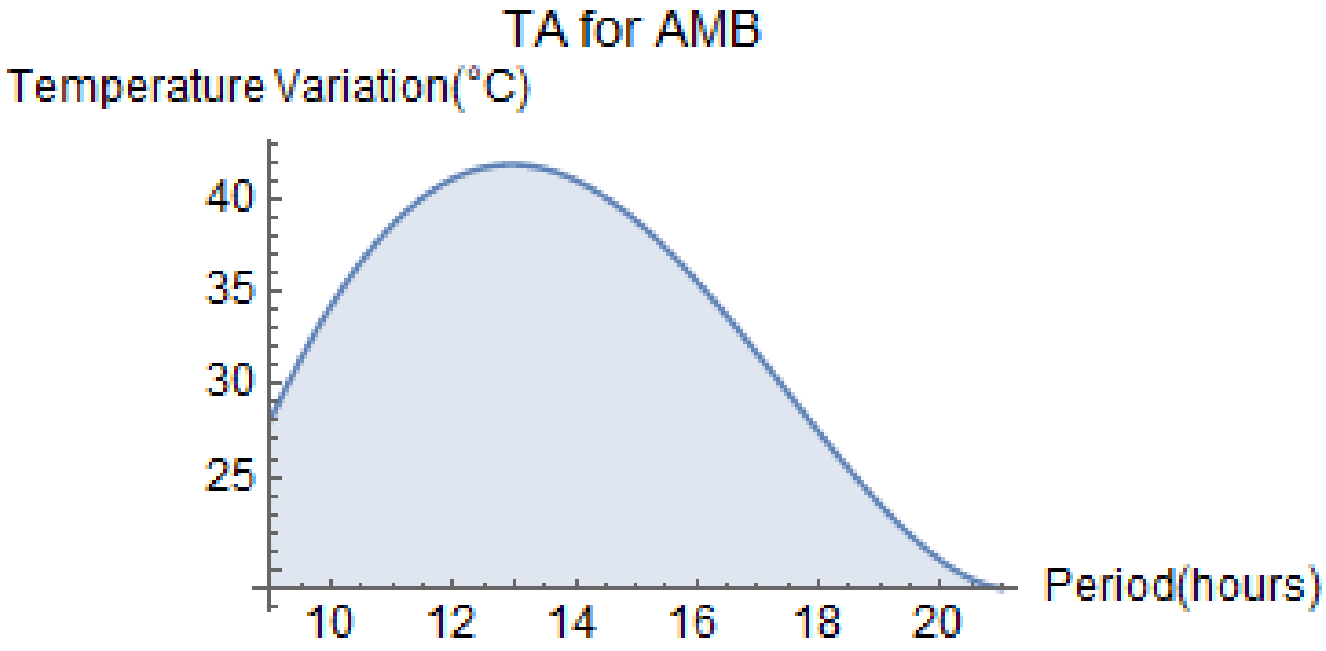

FIGURE E20: Thermal Absorptivity at ambient in December

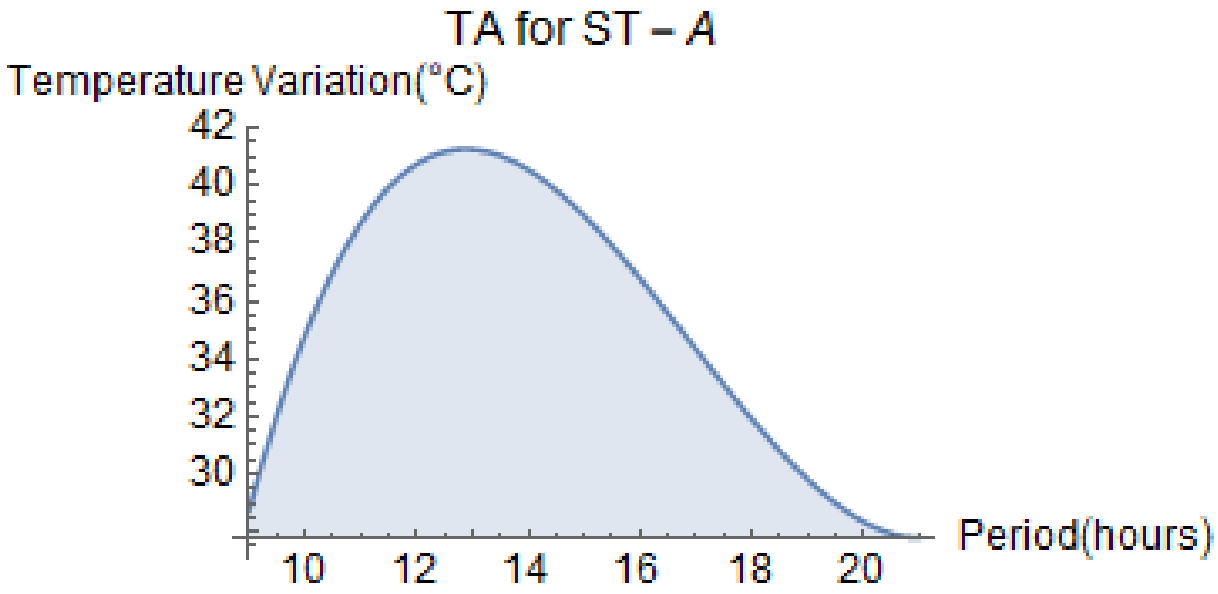

FIGURE E21: Thermal Absorptivity for SCS in December

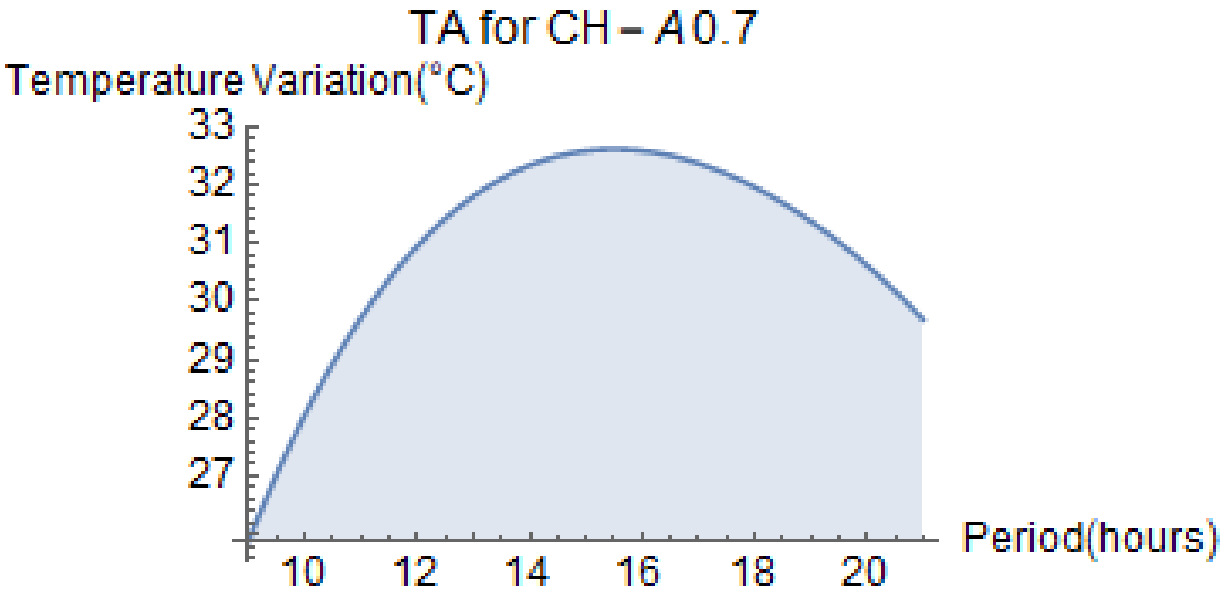

FIGURE E22: Thermal Absorptivity for ARS in December

TABLE E5

Average monthly thermal absorptivity for stone coated and aluminum roofing sheets

	Monthly absorptivity in joule		
Sample materials	**October**	**November**	**December**
Amb-in	441.75	503.75	398.62
PLAR	392.66	395.16	398.09
SCS	478.71	491.04	425.18
ARS	380.55	327.73	372.51

TABLE E6

Average monthly thermal absorptivity for the selected ceiling materials (SCM)

	Monthly absorptivity in Joule		
Sample materials	**October**	**November**	**December**
Amb	307.64	451.60	364.33
Pvc	309.50	326.98	320.52
Asb	314.40	322.50	377.81
Pop	348.66	328.83	333.31
Gyp	326.74	322.55	353.43
Pcb	310.45	426.65	320.60

APPENDIX F

Table F1:

Hourly temperature variations in model 1

Period in hour	Temperature variations in °C			
	T.pop	T.air space	T.str	T.amb
9:00:00	27.7	27.5	32.1	29.2
9:30:00	28.3	28.2	33.4	29
10:00:00	28.9	29.2	28.4	30.3
10:30:00	29.3	29.6	28.6	30.3
11:00:00	29.7	29.8	37.7	30.2
11:30:00	30.6	31.1	43.1	31.5
12:00:00	30.7	30.6	37.4	30.1
12:30:00	31.3	32.1	44.7	32.7
1:00:00	33	32.9	44.4	32.3
1:30:00	32.8	33.7	48.6	34
2:00:00	32.9	32.9	40.5	32.6
2:30:00	31.3	31.1	31.4	29.6
3:00:00	29.3	27.2	24.8	24.5
3:30:00	29.3	28.8	34.7	26.6
4:00:00	29.3	28.9	29.2	26.2
4:30:00	29	28.5	27.7	26.1
5:00:00	28.6	27.8	26.4	25.9

Source: Field survey 2021

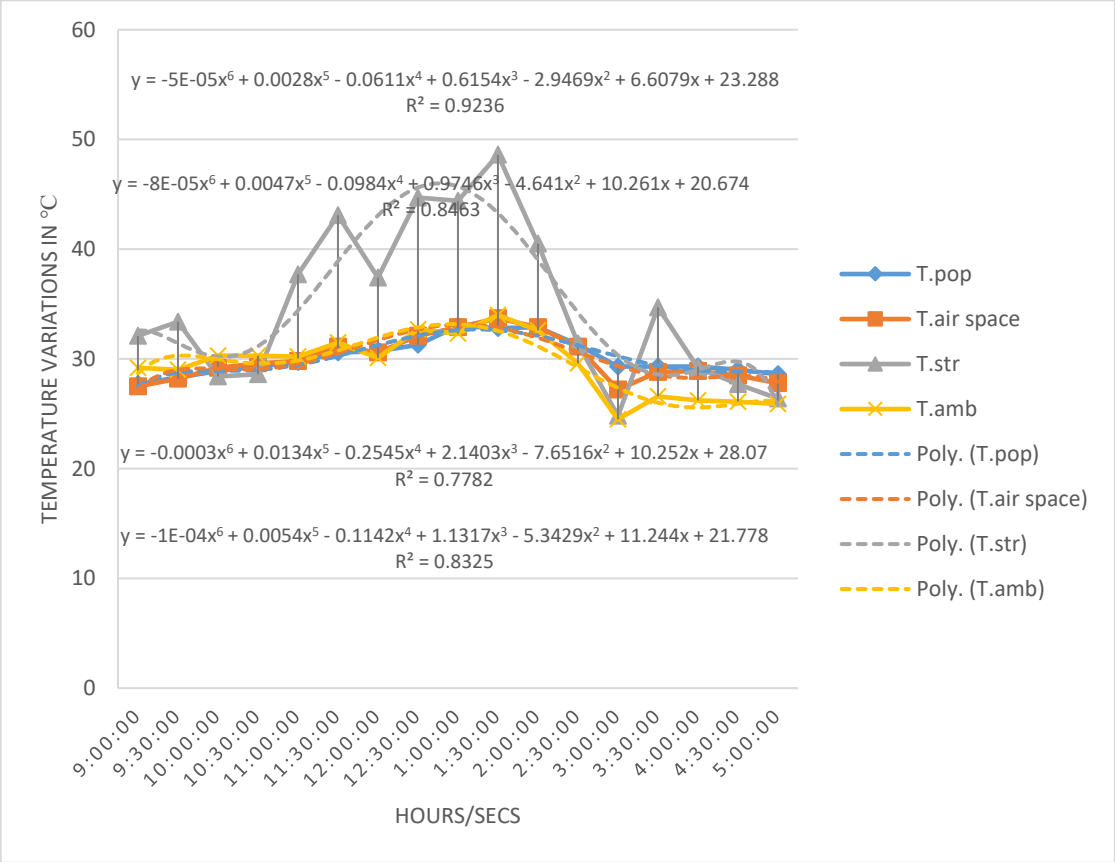

Figure F.1: Period of optimal comfort during the Day

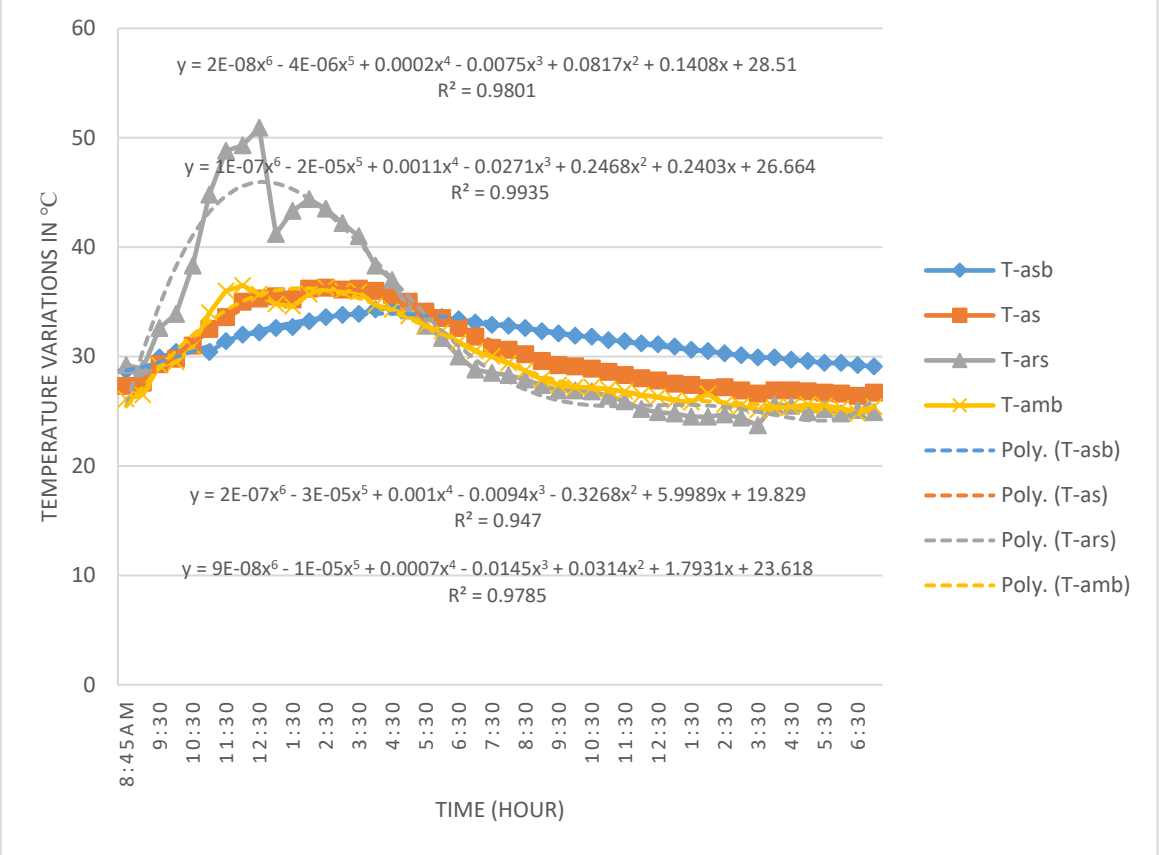

Figure F2: Period of optimal comfort during the Day